University of St Andrews

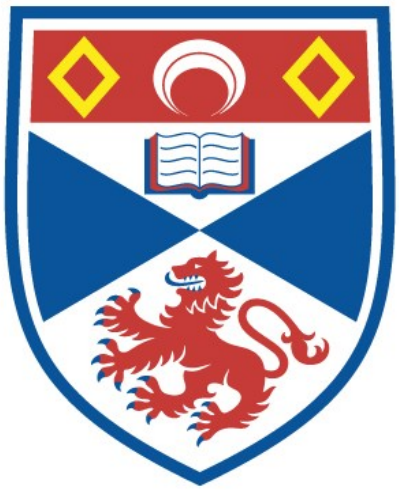

Full metadata for this thesis is available in
St Andrews Research Repository
at:
http://research-repository.st-andrews.ac.uk/

This thesis is protected by original copyright

LOW TEMPERATURE GALVANOMAGNETIC PROPERTIES OF INDIUM PHOSPHIDE

A Thesis

presented by

Iqbal Fayad Mohammad

to the

University of St Andrews

in application for the

Degree of Master of Science

TH 9928

"To the Country

To my father, husband, sisters and brothers and

to the memory of my mother."

CERTIFICATE

I certify that Iqbal Fayad Mohammad has carried out research work in the School of Physical Sciences in the University of St Andrews under my direction, that she has fulfilled the conditions of Ordinance No 12, and that she is qualified to submit the accompanying thesis in application for the Degree of Master of Science.

Research Supervisor

DECLARATION

I hereby certify that this thesis has been composed by me, that it is a record of my work and that it has not previously been presented for a higher degree.

The research was carried out in the School of Physical Sciences in the University of St Andrews, under the supervision of Dr D M Finlayson.

Iqbal Fayad Mohammad

CONTENTS

ACKNOWLEDGEMENTS

I wish to express my sincere thanks to my supervisor Dr D M Finlayson for his guidance, encouragement and advice which greatly enhanced my understanding. My thanks are also due to Professor Stradling the Head of the Department.

I would also like to express my thanks to Mr Gavine for his help in supplying liquid helium and also to Mr Barman for supplying liquid nitrogen.

My thanks are due to my loving husband for all his care, support and encouragement throughout my study.

ABSTRACT

Measurements have been made of the resistivity ρ, Hall coefficient R_H and Hall mobility μ_H as a function of temperature, T over the range 1.37 - 300^{o}K of n-type samples of InP with N_D-N_A concentrations of 1.4 x 10^{22} - 3.8 x 10^{24} m^{-3}. Compensation ratios have been determined from the theory of ionised impurity scattering. The magnetoresistance has been measured as a function of the magnetic field up to 12 tesla at different temperatures; at low magnetic fields negative magnetoresistance has been observed for the temperature range 1 - 4^{o}K in samples exhibiting metallic conductivity. A square root dependence agrees with the Kawabata theory; at higher fields a positive magnetoresistance is found. In samples identified by Hall and resistivity measurements as non-metallic the magneto resistance is always positive.

INTRODUCTION

The electrical properties of n-type InP at low temperatures have been studied for more than twenty years; Kovalevskaya et al (1967) have measured electrical properties of n-type InP from liquid helium temperatures to room temperature and more recently, Blood et al (1974) measured the resistivity and Hall coefficient (R_H) and the mobility (μ).

These measurements are in qualitative agreement with the theoretical understanding of transport phenomena in III-V compounds.

Magnetoresistance has been studied by Galvanov et al (1969). Standard theory predicts for semiconductors a positive magnetoresistance increasing quadratically with magnetic field. However, in a wide variety of semiconductors a negative magnetoresistance has been observed at low temperatures.

Mott (1949) has suggested that, as the number of impurities in a semiconductor is increased, at a certain concentration, a transition from non-metallic to metallic behaviour is to be expected. This concept has been elaborated by Mott in a number of papers and recent books (Mott and Davis 1971, Mott 1974). It is in the region of the metal-non-metal (MNM) transition that a negative magnetoresistance is most frequently observed. Toyozawa (1962) suggested that, even if the bulk of the material is in the metallic state, the local impurity density may be low enough to provide small regions in which localized spins can exist. Into these regions the mobile electrons can tunnel and interact with the localized spins. As the number of impurities is increased, such small relatively isolated regions become scarce and the moments and hence the negative magnetoresistance will vanish. However, according to Toyozawa (1962) the negative magnetoresistance component should be proportional to B^2. A theory of negative magnetoresistance has been proposed recently by Kawabata (1980) for heavily doped

semiconductors in the metallic region. He started with the simple electron gas model with randomly distributed scattering centres and derived an expression for the magnetic field dependent conductivity.

Lee and Ramakrishnan (1982) considered the spin Zeeman effect on magnetoresistance and obtained a positive magnetoresistance at high fields.

CHAPTER I

GENERAL SEMICONDUCTOR BACKGROUND

1.1 Metals, Insulators and Semiconductors

To explain metals, insulators and semiconductors in terms of the band theory of solids, Wilson (1931) introduced a model which predicted at absolute zero temperature a sharp distinction between crystalline materials showing metallic conduction, on the one hand, and insulating behaviour on the other. Insulators according to this model are materials where all energy bands are completely occupied or completely empty.

Since for every occupied state with wave function ψ of the form $\psi = \exp(ikx)U(x,y,z)$, there is also an occupied state for which $\psi = \exp(-ikx)\overset{*}{U}(x,y,z)$, no current can flow.

A metal, on the other hand, is a material in which one or more energy bands are partly full. In such materials at zero temperature states are full up to a limiting energy E_f (the Fermi energy) and states with higher energies are empty.

For a perfect crystal the conductivity should tend to infinity as $T \to 0$. The density of states for a metal with one electron per atom, two electrons per atom and for an insulator is shown in Fig(1.1).

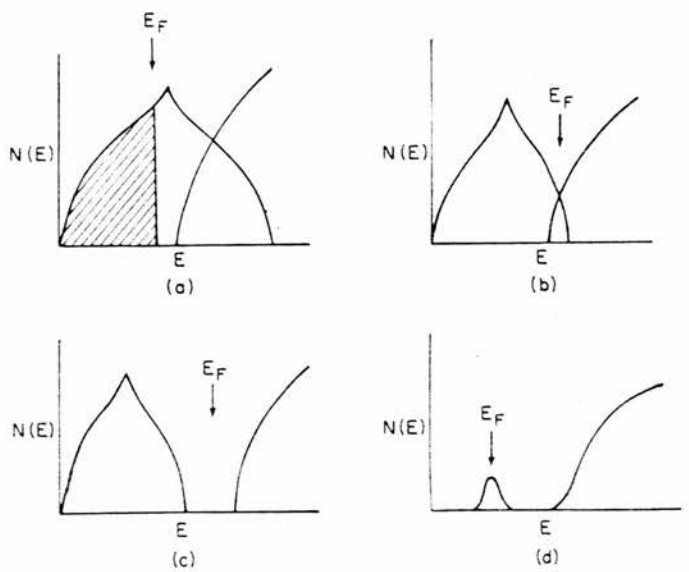

Electron density of states $N(E)$ in a cubic material; E_F denotes the Fermi energy. (*a*) Normal metal, (*b*) semimetal, (*c*) insulator, (*d*) n-type degenerate semiconductor.

Fig. (1.1)

For an insulator Δw is the energy gap between the full band (known as the valence band) and the empty band (the conduction band); at a finite temperature the number of electrons and holes (current carriers) will be proportional to the factor $\exp(-\frac{1}{2}\Delta w/kT)$. For a crystalline insulator $N(E_f)$ must vanish.

1.2 Hall Effect

The Hall field is the electric field developed across the faces of a conductor, in the direction j x B, when a current j flows across a magnetic field B.

$$R_H = \frac{r}{ne} \tag{1.1}$$

The quantity R_H is called the Hall coefficient. The dimensionless quantity r is called the Hall factor. It depends on the combination of scattering processes effective under the prevailing conditions. The Hall factor is usually fairly near to unity. Thus r = 1 when all electrons move at the same speed, as is true for a degenerate electron gas where they all move with the Fermi velocity. The quantity $r = (\frac{3\pi}{8}) = 1.18$ when the electron gas is non-degenerate and scattering is exclusively by LA phonons. When there is appreciable scattering by ionized flaws, r can exceed 1.9 for an isotropic band; on the other hand, r can be as small as 0.7 if the constant energy surfaces for an electron are perturbed sufficiently from a spherical form.

The Hall coefficient is very useful in the study of conduction processes since it provides the easiest method of determining the electron density. In conjunction with measurements of resistivity it provides a value for the electron mobility, the electron velocity in unit field. Note that the mobility $\mu_H = R_H/\rho$ may differ from the

mobility defined by the relation $\sigma = \frac{1}{\rho} = ne\mu$; the former is often used because of the difficulty in determining precisely the value of the Hall factor r.

1.3 Mobility, Mean Free Paths and Scattering

For a degenerate electron distribution in a semiconductor, the mean free paths and times of interest are those for electrons within one or two $k_B T$ of the Fermi energy; in practice the mobility in a semiconductor sample with very many free electrons usually has a very uninteresting behaviour, with little change of mobility over a wide range of temperature - a flat characteristic.

There is a more interesting diversity in the patterns of mobility-temperature behaviour when electrons in a semiconductor have a non-degenerate (Boltzmann) distribution. That is when the electron density is small enough and/or the temperature is large enough to validate a non-degenerate approach. For this non-degenerate type of situation it is supposed that the mean free path depends upon temperature and on electron energy. The scattering mechanisms discussed below have been studied for example by Harris and Ridley (1971).

1.3.1 Acoustic-phonon scattering

Acoustic phonon due to normal vibration modes of a linear diatomic lattice. The relaxation time for this scattering is given by Kolodziejczak (1967)

$$\tau_{ac} = \frac{\pi C_L \hbar^4}{2^{\frac{1}{2}} m_d^{3/2} \Xi_\alpha^2 K_B T} \gamma^{-\frac{1}{2}} \left(\frac{d\gamma}{dE}\right) \qquad (1.2)$$

where C_L is an average longitudinal elastic constant given by Herring and Vogt (1956) and Ξ_α is the deformation potential for

the direction α; it has been shown that this is approximately isotropic by Gryaznov and Ravich (1970), which enables the mobility to be found

$$U_{ac} = \frac{\pi C_L \hbar^4 e}{2^{\frac{1}{2}} m_e m_d^{3/2} \xi_1^2 (K_B T)^{3/2}} \{\frac{{}^0L_{-2}^1}{{}^0L_0^{3/2}}\} \qquad (1.3)$$

where ξ_1 is the isotropic deformation potential.

1.3.2 Optical phonon scattering

At high temperatures, the relaxation time for this process is given by Kolodziejezak (1967)

$$\tau_{po} = \frac{\hbar^2 \gamma^{\frac{1}{2}}}{(2m_d)^{\frac{1}{2}} e^2 K_B T (\frac{1}{\epsilon_\infty} - \frac{1}{\epsilon_o})} (\frac{d\gamma}{d\varepsilon})^{-1} \qquad (1.4)$$

where ϵ_o and ϵ_∞ are the static and high frequency dielectric constants. The mobility is given by

$$\mu_{po} = \frac{\hbar^2}{e m_e (2m_d K_B T)^{\frac{1}{2}} (\frac{1}{\epsilon_\infty} - \frac{1}{\epsilon_o})} \{\frac{{}^0L_{-2}^2}{{}^0L_0^{3/2}}\} \quad . \qquad (1.5)$$

Then, introducing a combined relaxation time

$$\tau' = \{\tau_{ac}^{-1} + \tau_{po}^{-1}\}^{-1} \quad . \qquad (1.6)$$

1.3.3 Ionized-impurity scattering

This will dominate the scattering process at temperatures below about 100 K. For non-degenerate material the mobility is given by the Brooks Herring formula.

$$\mu = 2^{7/2} \epsilon^2 (K_B T)^{3/2} . (\pi^{3/2} m^{*\frac{1}{2}} e^3 N f(x))^{-1} , \qquad (1.7)$$

where

$$f(x) = \ln(1 + x) - \frac{x}{1+x} \qquad (1.8)$$

where

$$x = 6 m^* \epsilon (K_B T)^2 (\hbar^2 \pi n_o e^2)^{-1} . \qquad (1.9)$$

For arbitrary degeneracy the more complicated formulation of Mansfield (1956) is required, the general equation for the conductivity

due to impurity scattering can be written as

$$\sigma_I = \frac{32\ \epsilon^2 m^*(K_B T)^3\ f_2(j^*)}{Ne^2\ h^3\ f(x)} \tag{1.10}$$

where
$$f(x) = \ln(1+x) - \frac{x}{(1+x)} \tag{1.11}$$

where
$$x = \frac{\bar{\eta}(K_B T)^{\frac{1}{2}}\ \epsilon\ h}{e^2(2m^*)^{\frac{1}{2}} f'_{\frac{1}{2}}(j^*)} \tag{1.12}$$

1.3.4 Carrier-carrier scattering

Collisions between charge carriers will have the effect of changing the distribution of energy and momentum amongst the carriers, while leaving the total energy and momentum of the carrier system unaltered. At sufficiently high carrier densities these collisions will dominate over other scattering mechanisms, and the distribution function will tend to a drifted Fermi-Dirac (or Maxwellian) centred about a momentum displacement $\hbar K_D$, i.e.

$$f^*(K) = f_o(K) - K_D \cdot \frac{df_o}{dK} + \ldots. \tag{1.13}$$

to first order in the drift momentum. Following Keyes (1958), introduce a constant relaxation time τ_e with which the distribution function f(K) decays into f*(K); this then enables a simple solution of the Boltzmann equation with a relaxation time τ'. The mobility in the presence of carrier-carrier scattering is

$$\mu = \frac{e}{m_e} \frac{\langle \frac{\tau'}{\tau'+\tau_e} \left(\frac{d\gamma}{dE}\right)^{-1} \rangle}{\langle \frac{1}{\tau'+\tau_e} \left(\frac{d\gamma}{dE}\right)^{-1} \rangle} \frac{O_L 3/2}{O_L 3/2} \left\{\frac{-1}{O_0}\right\} . \tag{1.14}$$

When carrier-carrier scattering is negligible, $\tau_e \to \infty$ and equation (1.14) reduces to equation

$$\mu_i = \frac{e}{m_e} \frac{\langle \tau_i (d\gamma/dE)^{-1} \rangle}{\langle 1 \rangle} \tag{1.15}$$

In the opposite extreme of dominant carrier-carrier collisions, $\tau_e \to 0$ so that

$$\mu = \frac{e}{\langle m_e \tau'^{-1} (\frac{d\gamma}{dE})^{-1} \rangle} \left\{ \frac{[O_L 3/2]^2}{O_L^{-1} 3/2 \; O} \right\} \tag{1.16}$$

1.4 Compensation Ratio ($K = \frac{N_A}{N_D}$)

Semiconductors usually exhibit an appreciable degree of compensation and a knowledge of the value of K should be included among the basic electronic characteristics of these materials. Donor and acceptor concentrations can be determined from a method based on the scattering of free carriers by ionized impurities.

As the temperature is lowered below room temperature, initially the mobility controlled by phonon scattering increases and then decreases at low temperature where impurity scattering becomes dominant. By selecting a temperature well below the maximum to ensure dominance of ionized-impurity scattering, we can get the concentration of ionized impurities from the general equation for the conductivity due to impurity scattering, then we can get N_A from the equation $N = n + 2N_A$ where N is the number of scattering centres and n is the electron density, the donor density can then be obtained from the equation $N_D = n_{sat} + N_A$, then we can get the compensation ratio $K = \frac{N_A}{N_D}$.

1.5 Magnetoresistance

The change of resistance in a magnetic field is called the magnetoresistance effect, discovered by W Thomson (1856). If ρ_o is the resistivity with no applied magnetic field and ρ is the resistivity in the presence of magnetic field, the magnetoresistance

coefficient M is defined as the change in resistivity per unit of no magnetic field resistivity.

When a magnetic field is applied to a sample the electrons are deflected by the Lorentz force until a Hall field E_H is set up so that $E_H e = Bev$.

If all electrons move with the same velocity v as in an ideal metal then after the initial transient, they are no longer deflected and the resistance is independent of the magnetic field. When we have distribution of velocities as in a semiconductor , this always gives a decrease in current or positive magnetoresistance. This is all that is expected of simple theory. Almost all semiconductors show negative magnetoresistance in some range of temperature and/or concentration. Until recently this has been usually explained in terms of the spin scattering theory of Toyozawa (1962) who suggested that the negative magnetoresistance component should be proportional to B^2.

However the source of the magnetic scatterings has remained obscure and the proportionality to B^2 seldom observed. A new theory of negative magnetoresistance was produced in (1980) and this will be discussed later in section (2.3.6).

CHAPTER II

LOCALIZATION AND THE METAL NON-METAL TRANSITION

2.1 Impurity Band

A metallic impurity band is a system of continuous levels along which an electron can move as in the usual energy bands in the crystal.

So the Hall effect for electrons at the impurity levels is given by the same simple formula as that for electrons in the conduction band: $R_H = \frac{r}{ne}$ ($r \simeq 1$). This result allows us to deal with the impurity conduction in the same way as with the band conduction. Non-metallic impurity conduction occurs when an electron occupying an isolated donor has a wave function localized about the impurity and an energy slightly below the conduction band minimum.

Because there is a small finite overlap of the wave function of an electron on one donor with neighbouring donors, a conduction process is possible in certain circumstances in which the electron moves between centres by tunnel effect without activation into the conduction band. The electrons of high mobility in the conduction band completely dominate the conductivity at higher temperatures. However, although the mobility of an electron moving in the impurity levels is (very) small since it depends on interaction between widely spaced impurities, at low temperatures impurity conduction will dominate due to the absence of electrons in the conduction band.

The circumstance in which non-metallic impurity conduction is possible is the presence of 'compensation' by which we mean the presence of minority centres, acceptor in an n-type conductor. These acceptor electrons form a certain proportion of the donors Fig (2.1).

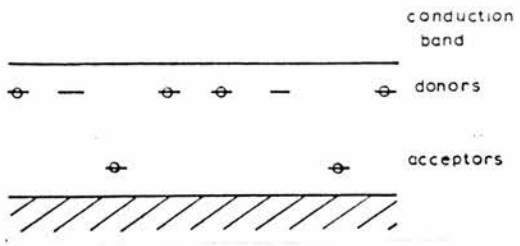

Fig (2.1)

Without compensation, impurity conduction is not possible, unless the overlap between the centres is very large; this occurs above a critical concentration N_c. Such impurity conduction was first observed by Busch and Labhart (1946) in silicon carbide.

A feature of impurity conduction, is its sensitivity to the impurity concentration, when the impurity concentration is small. The curves plotting $\ln\rho$ against $\frac{1}{T}$ exhibit a finite slope in the temperature range where non-metallic impurity conduction predominates, suggesting that the charge transfer between impurity centres must be thermally activated.

Above the critical concentration N_c, the resistivity becomes independent of temperature; the conductivity is then apparently metallic and carriers move freely without thermal activation.

At low temperatures where non-metallic impurity conduction is dominant three mechanisms operating in different concentration ranges, have been identified by Mott and Twose (1961).

The first mechanism occurs at low concentration, where the conductivity tends to zero with temperature i.e. not "metallic". To move an electron from one localized state to the next, a finite amount of energy is necessary. This only comes from phonons which make transition by the tunnel effect to another centre possible, Miller and Abrahams (1960).

The second mechanism occurs at intermediate concentration where the observed activation energy (now called ε_2) becomes very sensitive to the mean donor separation. From experiments on Ge, Davis and Compton (1965) believe this process is due to thermal excitation of electrons from the donor ground state to the band arising from the interaction between the states of negatively charged donors (the D^- band).

The third mechanism occurs at high donor concentration where the ground state wave functions overlap sufficiently to form an 'impurity band' which also merges with D^- band.

The energy ε_2 disappears and the carrier concentration becomes temperature independent as in a metal. The activation to the conduction band is not observed at intermediate temperatures because at these concentrations the band associated with the donor ground state and excited states all overlap to produce a quasi-continuum of states extending to the conduction band, Stillman et al (1971).

2.2 Metals Non-Metal Transition

2.2.1 Localized states

At low temperatures a range of energies may exist in which N(E) is finite but states are localized, and the mobility of an electron with such an energy is zero at T = 0. $\sigma(\varepsilon)(0)$ vanishes for these energies. The vanishing of $\sigma(\varepsilon)(0)$ then can serve as a definition of localization for electrons with energy E.

2.2.2 Anderson localization

Anderson (1958) was first to show that in certain random fields localization of the one-electron wave function can occur if the random component is strong enough. This is illustrated in Fig (2.2). A crystalline three-dimensional potential energy function $v(x,y,z)$ is shown in (a).

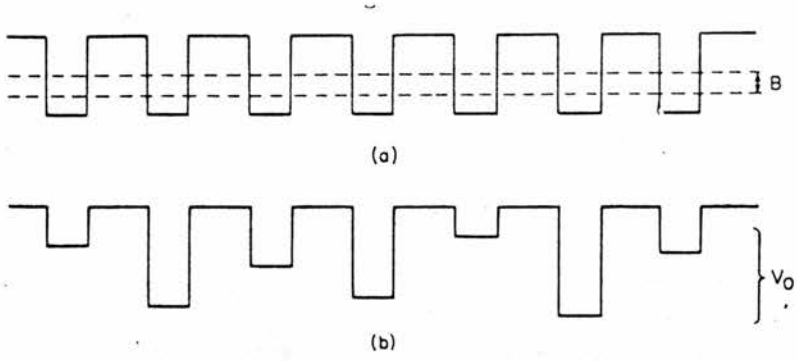

Random potential energy introduced by Anderson; (*a*) $V_0=0$, (*b*) V_0/B large.

Fig (2.2)

A random potential within limits $\pm \frac{1}{2}v_o$ is then introduced. If v_o is small, the mean free path can be calculated from the Born approximation. According to Anderson, there exists a critical value v_o above which at zero temperature diffusion is impossible. The wave functions are then said to be 'localized'. If one has a Fermi gas of electrons and the wave functions for the Fermi energy E_F are localised, then $\sigma(E_F)$ is zero, and thus no current can pass at the absolute zero of temperature. When the temperature is slightly raised, conduction is by thermally activated hopping.

Anderson (1970) has called a degenerate electron gas with localization in a random field of this kind a 'Fermi glass'.

Mott (1966) was first to point out that, since states are likely to become localized in the tail of a band, a critical energy E_c ('the mobility edge') exists separating localized from non-localized states, Fig (2.3).

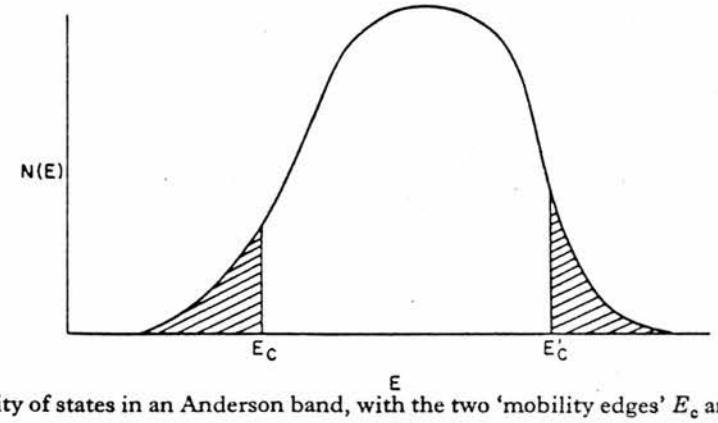

Density of states in an Anderson band, with the two 'mobility edges' E_c and E_c'.

Fig (2.3)

The simplest definition of E_c in terms of the behaviour of the conductivity $\sigma(\varepsilon)$ is as follows.

$$\sigma(E) = 0, \quad E<E_c$$

$$\sigma(E) > 0, \quad E>E_c$$

If, by changing the composition of a material or a magnetic field, the Fermi energy E_f can be made to cross the value E_c, a transition is expected from a metallic state, with a finite value of $\sigma(E_f)$, to a non-metallic state for which $\sigma(E_f)$ vanishes. This is called the 'Anderson transition'.

As the Fermi energy E_f crosses E_c, a sharp transition will occur. Near E_c where states are localized, the envelope of the wave function in Fig (2.4) is expected.

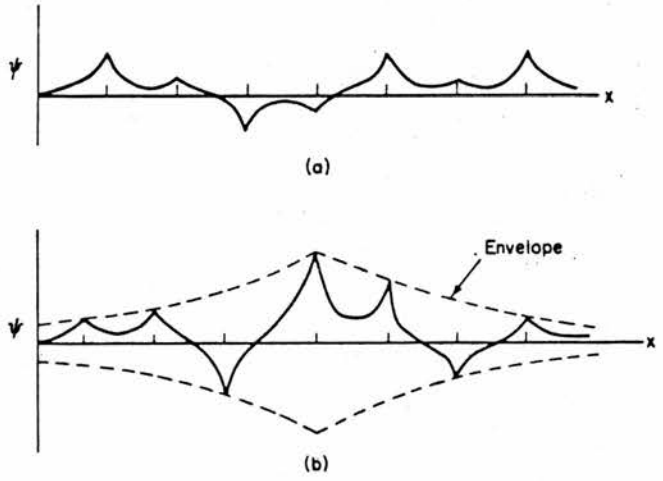

Wave function ψ of an electron when $L \sim a$. (*a*) Extended states, (*b*) weakly localized states.

Fig (2.4)

As $E_f - E_c$ tends to zero, the orbitals of the localized states spread and fill all space, overlapping one another strongly.

If wave functions are localized, so that $\langle \sigma(E) \rangle = 0$, conduction at low temperature is by thermally activated hopping. Every time an electron moves, it hops from one localized state to another, of which

the wave function overlaps that of the first state. Since the two states have quantized energies, the electron must exchange energy with a phonon each time it moves. The hopping processes in which the electron obtains energy from a phonon are rate-determining. Hopping of this kind was first described by Miller and Abrahams (1960) in their theory of impurity conduction. They supposed that an electron on one occupied site would normally jump to a nearest site with energy $\Delta E = |E_f - E_c|$.

2.2.3 Anderson localization on the metallic side of the MNM transition

On the metallic side of MNM transition, the activation energy does not disappear if the compensation **K** is large. Mott and Davis (1968) suggested that this is because the states in the tail of the impurity band, or even of the conduction band, remain localized, and that for large values of **K** the Fermi energy lies in this region. An increase in **K** should also increase the random field and therefore the range of energies in which states are localized. When **K** is not very large, a_E ought not be differ greatly from a , where a_E is the distance between localized states and a is the distance between atoms.

2.2.4 The metal-non-metal transition in doped semiconductors

One of the best-known examples of a metal-insulator transition due to correlation is that which occurs in doped semiconductors at low temperatures when the concentration of donors or acceptors is changed.

In an n-type semiconductor, for a low concentration of donors, the donors will have negligible interaction with one another; each one is a paramagnetic centre, and requiring an energy which is denoted by ε_1 for excitation of the electron into the conduction band. Using the hydrogen model,

$$\varepsilon_1 = \frac{m^* e^4}{2\hbar \epsilon}$$

and the radius a_H of the orbit is given by

$$a_H = \frac{\hbar^2 \epsilon}{m^* e^2}$$

m^* is the effective mass and ϵ the dielectric constant. It is the large value of a_H of order 30Å, which suggests that the lattice is very little distorted by the electron. As the concentration of donors increases, three phenomena occur. One is impurity conduction, which is a conduction mechanism at low temperatures first identified by Hung and Gleissman (1950).

As concentration increases, an activation energy ε_2 appears; this is the energy required to excite an electron not into the conduction band but onto distant donor which is already occupied. It can then move from one occupied donor to another.

We refer to such an electron as moving in the upper Hubbard band. Fig (2.5) shows the plot of the three quantities, due to Davis and Compton, (1965) for a small value of compensation as a function of the mean distance **a** between donors. ε_1 drops as the concentration increases because the effective dielectric constant increases. ε_2 it will be seen, drops continuously to zero; the metal-insulator transition occurs when ε_2 vanishes. Moreover a linear drop in ε_2 as the two Hubbard bands moves together and overlap is what we should expect from the model. The 'tail' shown near the metal-insulator transition is due to another process, hopping between Anderson-localized states, essentially the same as that responsible for ε_3.

At one time (Mott and Twose 1961) it was thought that at the metal-insulator transition, the impurity band was separate from the conduction band Fig (2.6) and merged with it for concentrations about ten times higher.

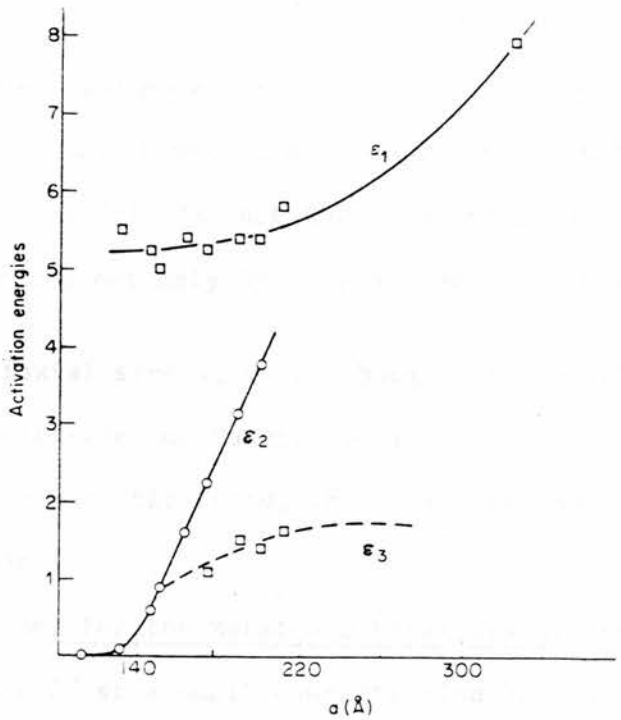

Variations of the activations energies ϵ_1, ϵ_2 and ϵ_3 in meV as a function of the distance between donors in n-type germanium (Davis and Compton 1965). For ϵ_3 the dotted line shows conduction by the mechanism of Miller and Abrahams (1960).

Fig (2.5)

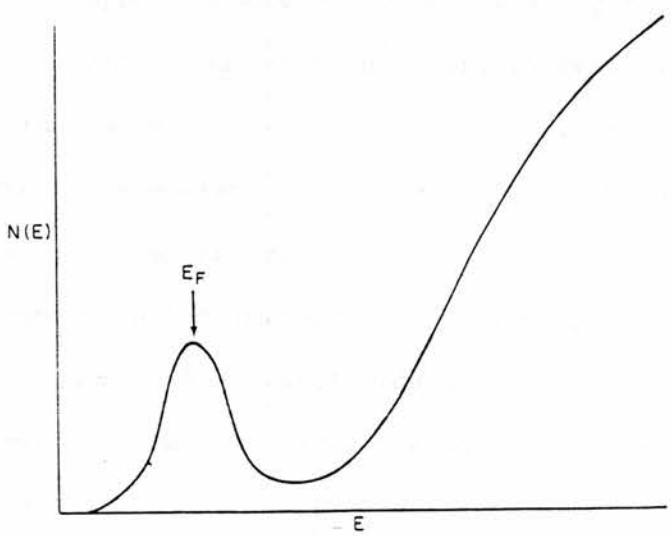

Sketch of an impurity band separated from a conduction band, as first suggested by Mott and Twose (1961).

Fig (2.6)

Therefore the metal-non metal transition in these systems occurred entirely within the impurity band, and should not be discussed in terms of two band model or a model of localized state just below a conduction band. However, more recently Mott has shown ("Metal-Insulator Transition") that the transition can be observed in doped semiconductors not only by varying the concentration, but also by:

a. uniaxial stress, which changes the radius of the orbit (Fritzsche and Cuevas 1960)

b. by a magnetic field, which has the same effect (Stroud et al 1968).

2.2.5 A Model for the Metal-Non Metal Transition in Doped Semiconductors

Consider first a small concentration of donors, far from the metal insulator transition. Fig (2.7) shows density of states in the two Hubbard bands; the lower one represents the spectrum of a 'hole' when an electron is removed from one of the donors for strong compensation; it will have the activation energy ε_3 for impurity conduction. The upper Hubbard band, representing the energies of an extra electron moving from donor to donor; there will be Anderson localization in its tail and E_c separates localized from extended states; we should expect the energy ε_2 to be given by $E_c - E_f$ at high temperatures and $E_A - E_F$ at low temperatures.

As the concentration increases, the overlap will become larger and so the two Hubbard bands will widen. In compensated samples, also, the term $e^2/\epsilon R$, which may be the more important influence on the width of the Hubbard bands, will also increase because R decreases. Thus ε_2, which can still be defined as $|E_c - E_f|$, will decrease. As the concentration increases still further, the two Hubbard bands

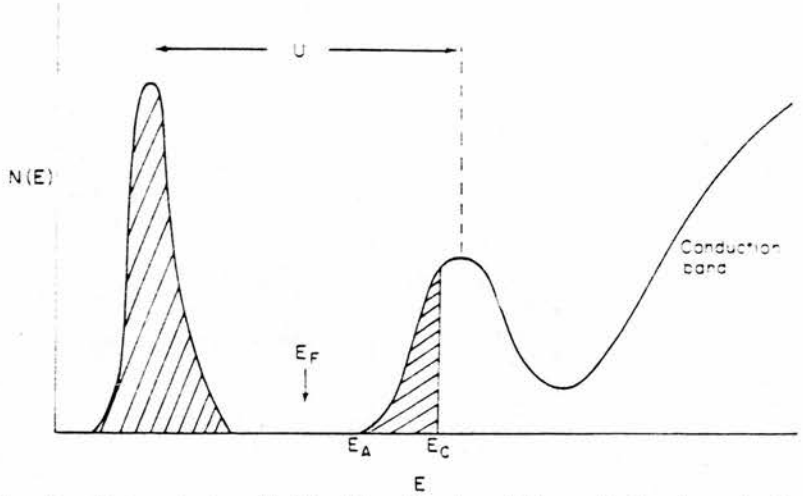

Density of states in two Hubbard bands, when U has split the impurity band of fig. 2.7. Anderson-localized states are shaded. E_F is the Fermi energy E_c the mobility edge.

Fig (2.7)

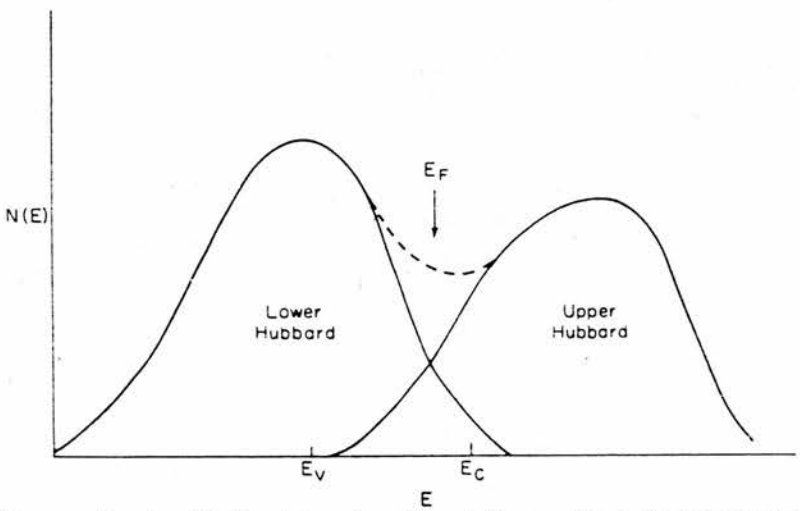

Two overlapping Hubbard bands. E_v and E_c are shown for the two bands separately.

Fig (2.8)

will overlap as in Fig (2.8). But this does not mean that a metal-non metal transition takes place. The tail of the bands where the states are Anderson-localized will overlap first, and, although $N(E_F)$ is then finite, states at the Fermi energy are localized. The metal-insulator transition occurs when states at E_F are no longer localized.

This means that, in doped semiconductors, the metal insulator (Mott) transition has all the properties of an Anderson transition.

When the two bands overlap as in Fig (2.8) but states at E_F are still localized, the system has various properties of interest (Mott 1972b).

a. At sufficiently low temperatures, we always expect a variable range hopping conduction so that

$$\sigma = \text{constant} \quad \exp \frac{-Q}{T^{\frac{1}{4}}}$$

b. If we continue to define ε_2 as

$$\varepsilon_2 = |E_c - E_F|$$

ε_2 is the activation energy for non-hopping conduction, and must go linearly to zero at the metal-insulator transition. Fig (2.9) shows the kind of behaviour to be expected.

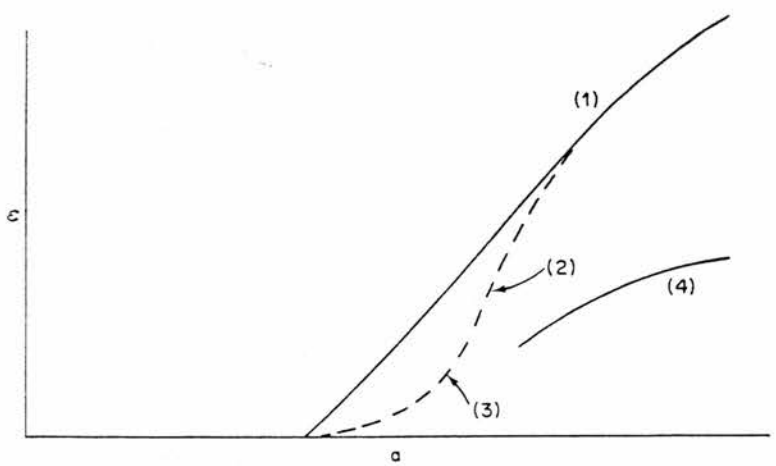

Activation energies: (1) ϵ_2 (excitation to mobility edge). (2) $E_A - E_F$ (before bands overlap). (3) and (4) Hopping by electrons at Fermi level. (3) is when bands overlap, and the process can take place without compensation. (4) is impurity conduction when bands do not overlap. Note that (3) and (4) represent activation energies which are constant only over a finite range of T and then go over to $T^{1/4}$.

Fig (2.9)

2.2.6 Magnetoresistance near the M NM transition

In the metallic state we use extended electrons to contrast with localized electron states for the insulator side of the transition.

In Anderson's (1958) paper he supposed that for a metal with sufficiently strong disorder the electron could localize in suitable regions. In (1961) Mott and Twose argued that a wave could not propagate through a disordered one dimensional system no matter how weak the disorder.

Mott subsequently introduced the concept of a minimum metallic conductivity $\sigma_{min} = 0.025\ e^2/\hbar a$ developed from the Ioffe and Regel (1960) condition that metallic behaviour cannot persist if the mean free path becomes less than the electron wavelength.

During the 1970's Thouless developed a scaling theory of the transition and then in (1979) Abraham's, Anderson, Licciardello, Ramakrishnan showed how to generalize the problem in terms of a dimensionless conductance. Among other things they concluded that in two dimensions there is no metallic conductivity at absolute zero. That is, the electrons are localized no matter how small the disorder. In one dimension the electrons are always localized but in three dimension a transition occurs. Mosfets provide a good approximation to a two dimensional system in which the electron density can be varied by changing gate voltages.

Abrahams et al proposed that in 2D near the σ_{min} value there should be a smooth transition from exponential localization to weak logarithmic behaviour.

However it was pointed out by Altshuler et al (1980) that very similar variation of resistivity with temperature would be expected if many body correlation effects were considered independent of any localization considerations. Thus fundamentally different theories of localization and electron interaction agreed in predicting a logarithmic dependence of resistivity on temperature in a 2D disordered metal.

Almost all semiconductors show negative magneto-resistance in some range of temperature and/or concentration. Until recently this has been usually explained in terms of the spin scattering theory of Toyazawa (1962) but has always presented difficulties both as regards the field dependence and the origin of the impurity spins. Kawaguchi, Kitahara, Kawaji (1978) observed a negative magneto resistance in a 2D system which was not isotropic and was clearly due to orbital rather than spin effects. Hikami, Larkin, Nagaoka (1980) showed that the 2D localization was broken by the application of a magnetic field and so a current flowed or negative magneto resistance would be observed. Kawabata (1980) extended the discussion to three dimension. In three dimensional system although localization does not necessarily occur the conductivity is diminished in the weak localization regime near the MNM transition; the suppression of this effect by the application of a magnetic field results in a negative magnetoresistance. Kawabata started with the simple electron gas model with randomly distributed scattering centres. He derived an expression for the magnetic field dependent conductivity in heavily doped semiconductors. A method of treating the localization in two dimensions was developed by Gorkov et al (1972) with the use of Feynman graph techniques. In order to take account of the effect of electron-phonon and electron-electron interaction. Kawabata considered the conductivity $\sigma(H,T)$ under magnetic field H at temperature T is given by

$$\sigma(H,T) = \sigma_o + \delta\sigma(H,T)$$

where $\sigma_o = ne^2\tau/m^*$ and τ is the relaxation time for impurity (elastic) scattering. The effect of inelastic scattering can be taken into account by introducing τ_ε the energy relaxation time

of electrons ; the temperature dependence of $\delta\sigma$ is determined through τ_ε. τ_ε is proportional to T^{-3} or T^{-2} according to electron-phonon scattering or electron-electron scattering is dominant

$$\delta\,\sigma(H,T) = \frac{-e^2}{\pi^3\hbar L}\sum_{N=0}^{N_o}\frac{1}{\sqrt{N+\frac{1}{2}+\delta}}\tan^{-1}\frac{q_o L}{2\sqrt{N+\frac{1}{2}+\delta}}$$

where $q_o \sim \frac{1}{\lambda}$, $N_o \sim \frac{L^2}{\lambda^2}$, $L = \left(\frac{C\hbar}{eH}\right)^{\frac{1}{2}}$

and $\delta = \frac{3L^2}{4\lambda\lambda_\varepsilon}$

where $\lambda = \left(\frac{2\varepsilon_F}{m^*}\right)^{\frac{1}{2}}\tau$, $\lambda_\varepsilon = \left(\frac{2\varepsilon_F}{m^*}\right)^{\frac{1}{2}}\tau_\varepsilon$

we will consider $\delta\sigma(H,T) \equiv \delta\,\sigma(H,T) - \delta\,\sigma(0,T)$. In the limit $H \to 0$

$$\delta\,\sigma(H,T) = \frac{e^2}{2\pi^2\hbar L}\,F(\delta)$$

where $F(\delta) = \sum_{N=0}^{\infty}\{2\sqrt{N+1+\delta} - \sqrt{N+\delta} - \frac{1}{\sqrt{N+\frac{1}{2}+\delta}}\}$.

we find that $\delta\,\sigma(H,T)$ is independent of the direction of the magnetic field when $\delta << 1$ (case of strong magnetic field or low temperature) the value of $F(\delta) = 0.605$ and hence

$$\delta\,\sigma(H,T) = \frac{e^2}{2\pi^2\hbar L}F(0) = 0.918\sqrt{H}\ .$$

The Kawabata theory dealing with weak localization in 3 dimensional systems therefore yields a negative magnetoresistance. The importance of electron correlation has been emphasised by Altshuler et al (1980) and has been subsequently developed for example by Lee and Ramakrishnan (1982). They considered the spin zeeman effect on magnetoresistance

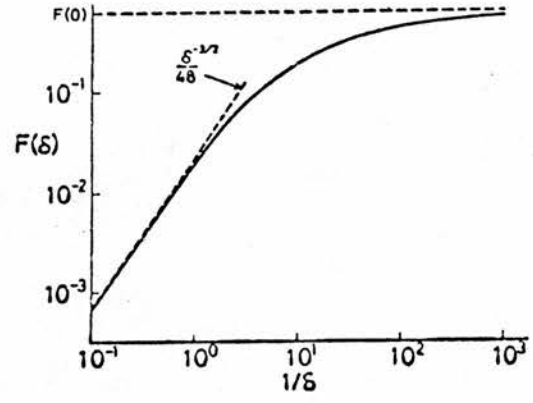

Fig (2.10) Dependence of $F(\delta)$ on δ.

and obtained for the high field

$$\rho = \rho_o - 2\alpha\left(\frac{2}{3} - \frac{F}{2}\right)T^{\frac{1}{2}} + 0.77\ \alpha\ F\left(\frac{|g|\mu_B}{K_B}\right)^{\frac{1}{2}} H^{\frac{1}{2}}$$

where $$\alpha = 1.08 \times 10^{-7}\ \rho_o^{5/2}\left(\frac{n}{T_F}\right)^{\frac{1}{2}}\ k^{-\frac{1}{2}}$$

$$F = \frac{1}{x}\ln(1+x), \quad x = \left(\frac{2k_F}{k}\right)^2 \quad \text{and} \quad k^2 = \frac{6\pi ne^2}{E_f}$$

(Thomas-Fermi)

The high field region occurs when the Zeeman splitting exceed K_BT ie $g\mu_BH = K_BT$. Hence magnetoresistance measurements can provide valuable information on the relative importance of localization and correlation effects near the MNM transition.

CHAPTER III

EXPERIMENTAL TECHNIQUES

3.1 Experimental Details

A number of samples of n-type epitaxial indium phosphide doped with sulphur were prepared by Royal Signal and Radar Establishment with N_D-N_A in the range $1.4 \times 10^{22} - 3.8 \times 10^{24}$ m^{-3} at room temperature. These were used for measurements of the resistivity ρ, Hall coefficient R_H, and mobility μ_H from 1.37 - 300°K using a clover leaf shape as shown in Fig (3.1).

The method is based upon a theorem which holds for a flat sample on which the contacts are sufficiently small and located at the circumference of the sample with no isolated holes. This method was proposed by van der Pauw (1958).

The specific resistivity and Hall effect of flat samples of clover leaf shape can be measured without knowing the current pattern. The contacts A, B, C and D were fixed on the circumference of the samples of InP using indium dots.

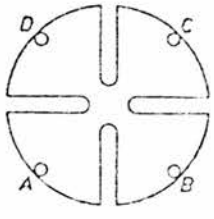

Fig. (3.1)

$R_{AB,CD}$ is the potential difference between the contacts D and C for unit current through the contacts A and B; the current enters the sample through the contact A and leaves it through the contact B. Similarly for the resistance $R_{BC,DA}$; d is the thickness of the sample.

The resistivity ρ can then be determined from the equation (3.1).

$$\rho = \frac{\pi d}{\ln 2} \cdot \frac{(R_{AB,CD} + R_{BC,DA})}{2} f\left(\frac{R_{AB,CD}}{R_{BC,DA}}\right) \qquad (3.1)$$

where f depends on the ratio $\left(\frac{R_{AB,CD}}{R_{BC,DA}}\right)$; in Fig (3.2) a plot is given of f as function of $\frac{R_{AB,CD}}{R_{BC,DA}}$.

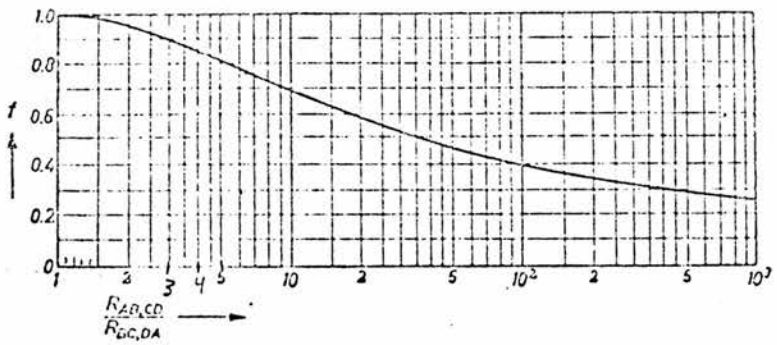

Fig (3.2) The function f used in determining the specific resistivity of the sample plotted as a function of $R_{AB,CD}/R_{BC,DA}$.

The Hall mobility can be determined by measuring the change of the resistance $R_{BD,AC}$ when a magnetic field is applied perpendicular to the sample; the Hall mobility is then given by

$$\mu_H = \frac{d}{B} \cdot \frac{\Delta R_{BD,AC}}{\rho} \qquad (3.2)$$

where B is the magnetic induction and $\Delta R_{BD,AC}$ the change of the resistance $R_{BD,AC}$ due to the magnetic field. The Hall coefficient $R_H = \mu_H \rho$.

The magnetoresistance effect is determined by measuring the change in the potential between the contacts C and D per unit current through the contacts A and B and the change in the potential between the contacts D and A per unit current through the contacts B and C when the magnetic field is applied.

3.2 Contact Preparation and Sample Mounting

van der Pauw clover leaf specimen contacts were prepared in this

laboratory by the following method. The crystal was washed thoroughly with methanol and then with propanol; a piece of indium wire was scraped clean with a razor blade and then very small portions were cut off; these were washed and dried on filter paper and then pressed gently on the surface of the sample by using an iron used only for In soldering; the crystal was placed on the heater strip; the chamber was flushed for a few seconds with reducing gas (nitrogen and hydrogen); the heater was turned on slowly to give a temperature just above the melting point of the contacts (156.6^{o}C). The gas flow was then passed through an acid bath for a few seconds. The dots should appear clean, shiny, and spherical at this stage; the temperature was raised further to the appropriate alloying temperature (approx 350^{o}C), and held there for a few minutes; the temperature was reduced to room temperature and the heater switched off.

The indium dots on the sample were connected to the sample holder contacts by platinum wires of thickness 0.127 mm and length 1 cm. These were soldered to the indium dots using Wood's metal (melting point 64^{o}C) and a soldering iron with a very fine end.

3.4 Digital Voltmeter (DVM) and Digital Multimeter (DMM)

A high precision digital voltmeter type 173B was used to measure a d.c of either polarity. Four basic ranges from 1 V to 1000 V gave an accuracy of 0.01%. These could be extended 50% by the inclusion of automatic over-ranging.

The input impedance is 10 megohms on the 1000 V and 100 V ranges and not less than 1000 megohms on the lower ranges.

An internal calibration reference is derived from an unsaturated cell with voltage stability better than 0.0005% per ^{o}C. To measure current, the digital voltmeter was connected to a standard resistance of 100Ω.

3.3 Electrical Circuitry

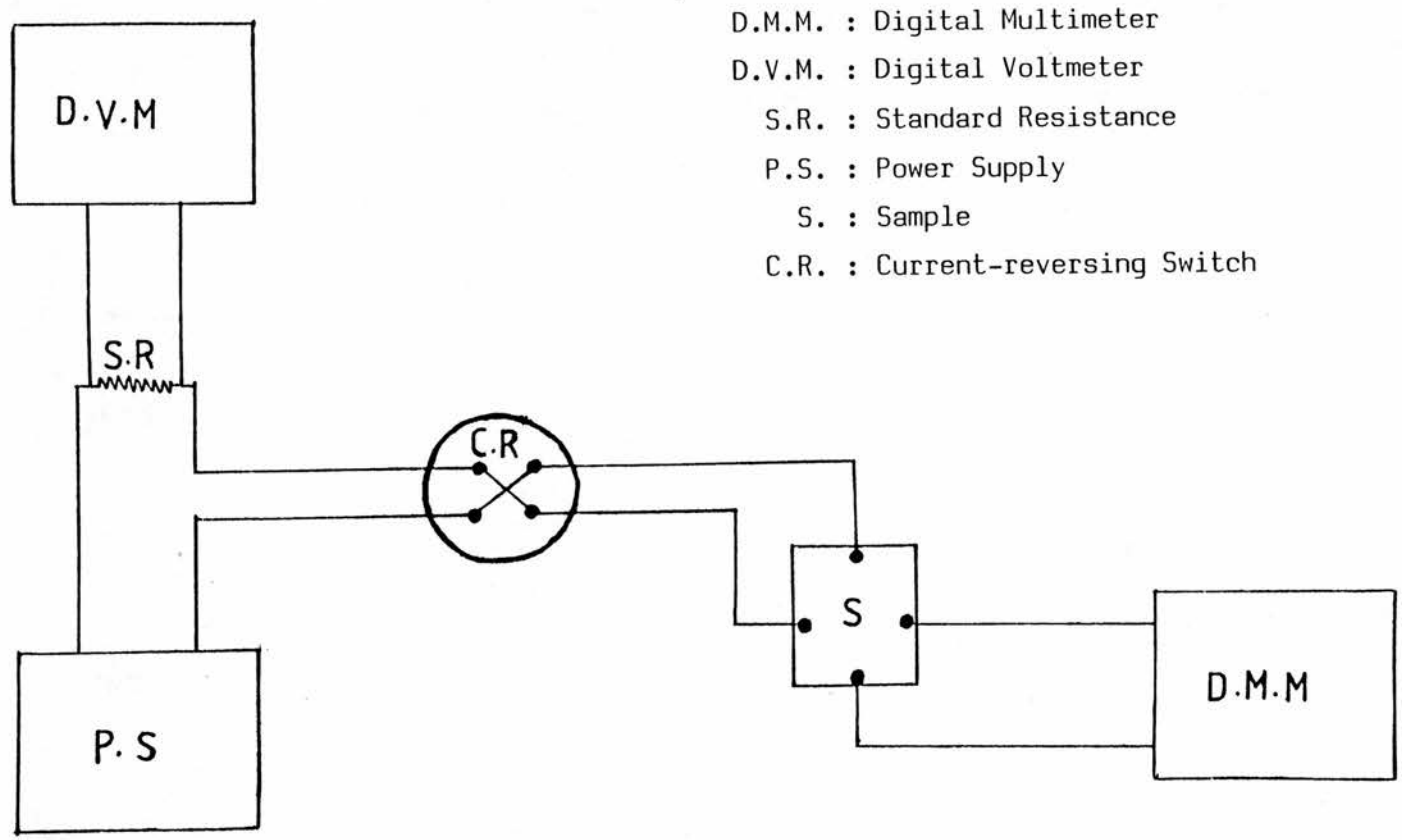

D.M.M. : Digital Multimeter
D.V.M. : Digital Voltmeter
S.R. : Standard Resistance
P.S. : Power Supply
S. : Sample
C.R. : Current-reversing Switch

Fig.3.3

Circuit diagram for measurement up to 7 kG

M.P.S. : Magnet Power Supply
S.G. : Sweep Generator
S.R. : Standard Resistance
M. : Magnet
S. : Sample InP
D.V.M. : Digital Voltmeter
D.M.M. : Digital Multimeter
P.S. : Power Supply

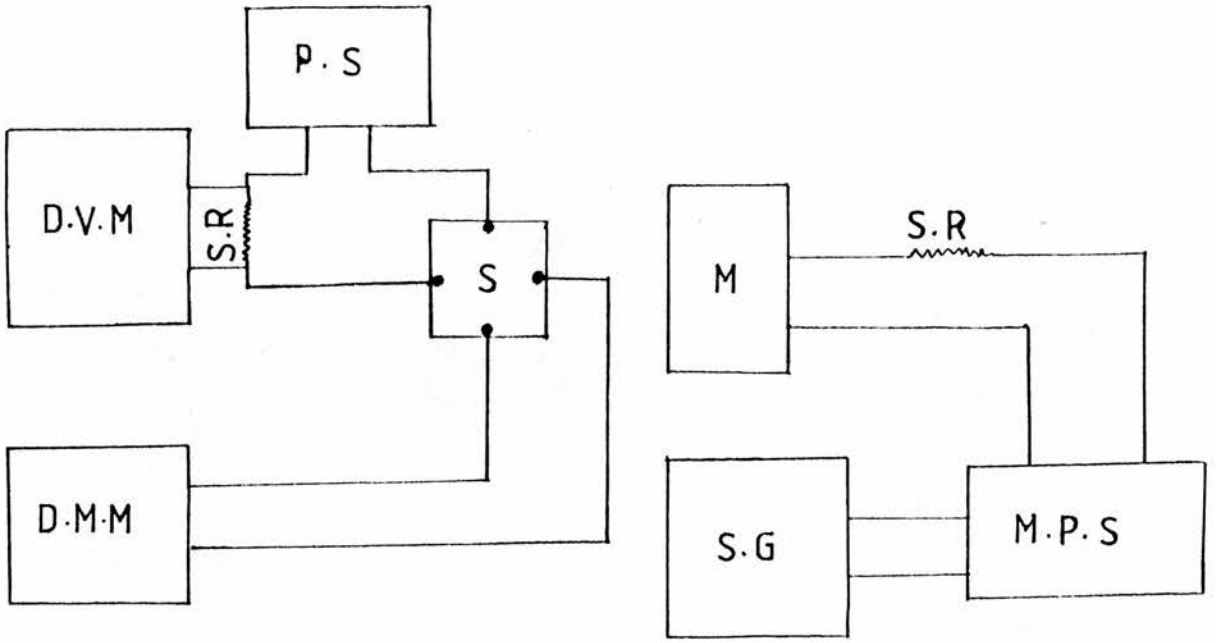

Fig. 3.4

Circuit diagram used for measurement up to 40 kG

For voltage measurement a multimeter model 191 with d.c volts and ohms ranges was used. It provides highly accurate, stable, low noise and fast responding readings from 1 μV to 1200 volts d.c on 5 voltage ranges, and 2 and 4 terminal measurements for 1 milliohm to 20 megohms on 6 resistance ranges.

The 191 is capable of 0.0005% resolution and 1 μV/1 mΩ sensitivity.

The accuracy in measuring the dc voltage in about 0.004 + 1.5 digit from 2V to 200 V and 0.005 + 1.5 digit at 1200 V and 0.005 + 2 digit at 200 mV.

3.5 Cryostat and Magnets

3.5.1 1 tesla iron magnet with glass dewar system

For the measurements between $4^{o}K$ to $300^{o}K$ a simple cryostat in conjunction with an iron magnet for fields up to 0.7 tesla was used. The specimen is mounted inside the central tube. This tube is filled with helium gas at pressure about 1 torr to ensure that the specimen is at a uniform temperature. The tube containing the specimen is surrounded by a can which can be evacuated to a pressure of about 10^{-4} torr.

This is then surrounded by a dewar which is filled with liquid helium.

A second dewar surrounding this was filled with liquid nitrogen to reduce the heat influx to the inner dewar. If the vacuum space of this inner dewar contains a small amount of air, the liquid in the outer dewar will quickly cool the cryostat to liquid nitrogen temperature before the helium is added.

When liquid helium is introduced into the inner dewar the air in its vacuum space is frozen, and the dewar then behaves as a normal "hard" dewar.

To get measurements from $4^{o}K$ to $300^{o}K$ the inner can was thermally

isolated by pumping out the exchange gas surrounding it. A current was then passed through the heater coil raising the temperature of the inner can.

The temperature measurements were made by a GaAs thermometer which fed a voltage into a temperature regulator, the current to the heater was then switched on and off by the controller to keep the temperature steady at a value set on the controller scale. Over the range 4-300^{o}K the temperature can be controlled to within $\pm \frac{1}{2}^{o}$K. The GaAs diode required a constant current of 10μA; the digital read-out on the controller gave readings to 0.5^{o}K but when required higher accuracy could be observed by a direct measurement of the voltage across the diode. The temperature was lowered below 4.2^{o}K by connecting to a fast pump; a simple rubber diaphragm was used to maintain constant any preset vapour pressure; the temperature was measured by a vapour pressure manometer Hg was used for the higher temperatures but butyl phthalate for temperatures below the λ point. A table of vapour pressure versus temperature gave temperature to an accuracy of better than 0.1^{o}K.

helium	^{o}K
Boiling Point	4.216
Lambda Point	2.186

Table (3.1) fixed point

3.5.2 4 and 12.7 tesla Super Conducting Magnets

For measuring the Hall effect and the magnetoresistance at liquid helium temperatures a superconducting coil immersed in liquid helium supplied magnetic fields up to 4 tesla or 12 tesla.

The superconducting coil was driven by power supply controlled by a sweep unit. The current is swept from zero to a value set by the

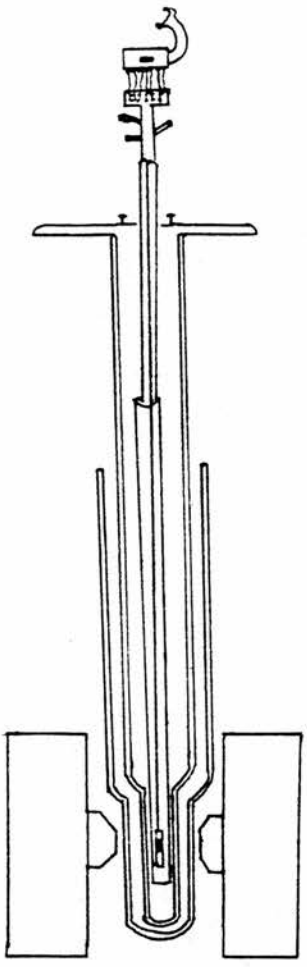

Fig (3.5) Simple Cryostat in Conjunction with an Iron Magnet

current control in the power supply. Sweep times in the range five to ten minutes were used for the 4 tesla magnet. The 12.7 T very high homogeneity superconducting magnet has the capability of being swept up to 90% of full field in three minutes.

Readings were taken in a steady field obtained by setting the switch to hold.

The 4 tesla metal cryostat is illustrated in Fig (3.6). The 12T magnet has a similar cryostat system on a somewhat larger scale.

V.C : Vacuum Chamber

H.T : Helium Transfer

N.T : Nitrogen Transfer

E.L : Electrical Leads

M : Magnet

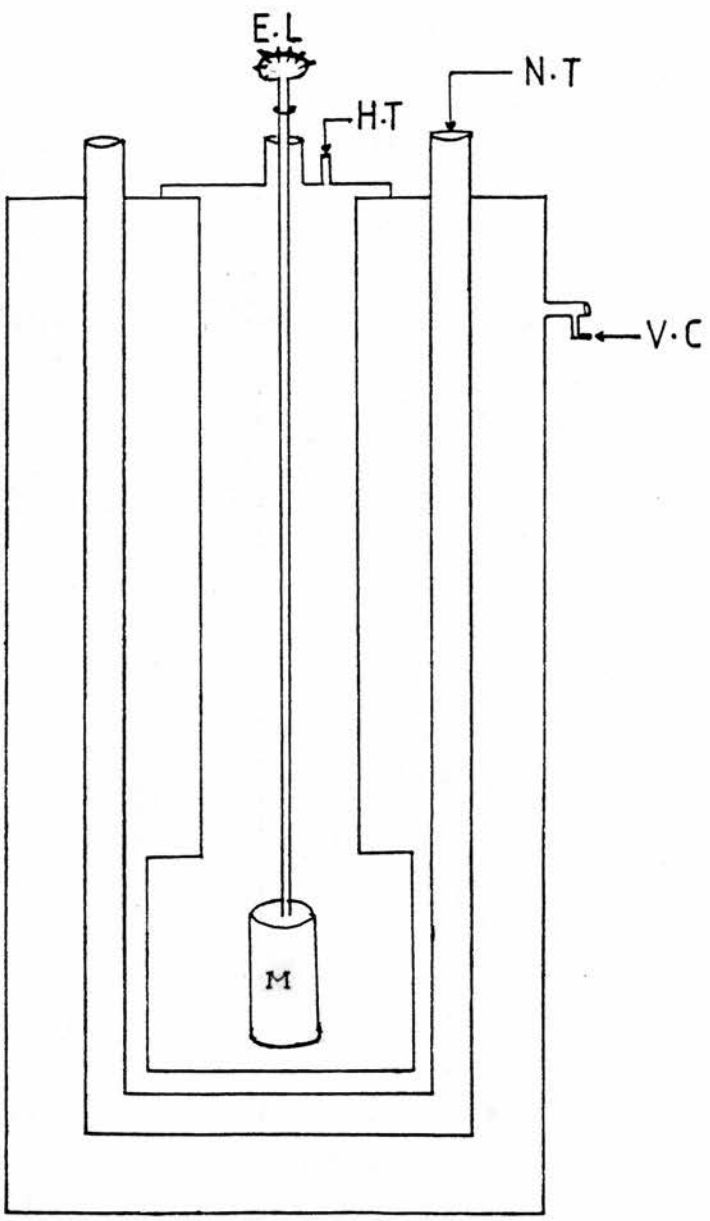

Fig (3.6)

CHAPTER IV

EXPERIMENTAL RESULTS AND DISCUSSION

In order to characterise the samples, measurements of the resistivity and Hall effect were made over a wide range of temperature; the results are shown in Fig (4.1), (4.3) and a summary for eight samples is given in table (4.1).

The resistivity is discussed in Section 4.1. A calculation of n_c and σ_{min}, as well as a discussion of the relation of the conductivity to the electron density in terms of theories by Mott and Kaveh and more recently by Kawabata are given. In Section 4.2 Consideration is given to the Hall maxima and whether these are related to impurity band conduction or to a change in statistics . Section (4.3) includes observations for the Hall mobility curves. In Section (4.4) the compensation ratio **K** is discussed since the values of **K** are important for subsequent interpretation. Section (4.5) includes calculation of the fermi energy, fermi velocity and mean free path at $T = 4^{o}K$ with carrier concentration greater than n_c. Section (4.6) discusses the magnetoresistance results in terms of recent theories of localization and correlation in the weakly localized region.

4.1 Resistivity

Resistivity curves are shown in Fig (4.1). For samples with electron concentration less than N_{crit}, on cooling from $4^{o}K$ to $1.37^{o}K$ the resistivity shows a small increase. For samples with electron concentration greater than N_{crit} the electrical resistivities are constant at the lowest temperature; as the donor concentration is increased the constant region shifts to higher temperature.

The curves also show a rapid drop of the resistivity for temperatures higher than $10^{o}K$ for sample NAG 495 and higher than $20^{o}K$ for sample AGRO 529.

At temperatures greater than 130°K for sample NAG 495 and 180°K for samples AGRO 529 the resistivity again increases.

It will be seen that the transition from metallic (constant low temperature resistivity) to non metallic (increasing resistivity as the temperature is lowered) occurs round about $3 \times 10^{22}\ m^{-3}$ as predicted by Mott theory (1974), where the MNM transition can be estimated from the criterion $n_c = (0.25/a_H)^3$, a_H is the effective Bohr radius given by $\hbar^2\epsilon/m^*e^2$. For a dielectric constant ϵ of 12.4 and effective mass ratio 0.082, we find that

$$a_H = \frac{(1.05 \times 10^{-34})^2\ 12.4/9 \times 10^9}{(0.082 \times 9.1 \times 10^{-31})(1.6 \times 10^{-19})^2} = 8 \times 10^{-9} m$$

$$a_H \approx 80\ \text{Å}$$

giving a MNM transition at a concentration of

$$n_c = \left(\frac{0.25}{8 \times 10^{-9}\ m}\right)^3 = 3.1 \times 10^{22}\ m^{-3}$$

Mott has postulated a minimum metallic conductivity given by $\sigma_{min} = 0.026\ e^2/\hbar d_c$ where d_c, the average distance between impurity centres at n_c, is about $2.5\ a_H$. This gives

$$d_c = 2.5 \times a_H$$
$$= 2.5 \times 8 \times 10^{-9}\ m$$
$$= 2 \times 10^{-8}\ m$$

$$\sigma_{min} = \frac{0.026 \times (1.6 \times 10^{-19})^2}{(1.05 \times 10^{-34})(2 \times 10^{-8})}$$

giving $\sigma_{min} \approx 320\ (\Omega m)^{-1}$.

Following the work of Abrahams et al (1979) several authors have discussed the behaviour of the zero field conductivity in terms of the relation $\sigma = \sigma_o(\frac{n}{n_c} - 1)^s$ where $0.5 \lesssim s \lesssim 1$.

Kaveh and Mott (1982) emphasise the distinction between compensated and uncompensated samples and quote the experiments of Rosenbaum et al (1981) on germanium where it was found that S varied from 0.6 to above 1 as the compensation K changed from 0 to > 0.5.On the other hand a recent communication from Kawabata suggests that S should be about 0.5 for many valley semiconductors and 0.8 to 1 for a one valley system. Although this is not stated explicitly Kawabata's estimate presumably related to uncompensated material.

We have plotted ln σ versus $\ln(\frac{n-n_c}{n_c})$ for the five samples in the weak localization regime ($n > n_c$) and obtain a fairly good straight line with a slope giving S = 0.7 , Fig (4.2). Since we have compensated samples and a one valley system our experimental value will suit either the Kaveh -Mott or the Kawabata interpretation. A wider range of compensation would be necessary to distinguish between the two approaches. From the graph σ_o can be estimated as an intercept having a value of (2×10^3 $(\Omega m)^{-1}$) and $\sigma_o = A\ \sigma_{min}$, where $A \simeq 6$.

4.2 Hall Coefficient R_H

The measurements of the Hall coefficient R_H versus $(\frac{1}{T})$, Fig (4.3), shows the Hall curves with a single maximum. This maximum was observed in samples with $N_D - N_A \lesssim 1.3 \times 10^{23}$ m^{-3} but no maximum was observed for $N_D - N_A = 3.8 \times 10^{24}$ m^{-3}.

When the impurity concentration in the samples was reduced, the amplitude of this maximum increased and shifted toward low temperatures.

At low temperature for samples with $N_D - N_A \gtrsim 4 \times 10^{22}$ m^{-3} we observe a temperature independent R_H.

Some authors (eg Hilsum et al (1961)) explain a decrease of R_H

	T = 300°K			T = 80°K			T = 4°K		
Sample (Symbol)	ρ (Ωm)	$R_H(\frac{m^3}{c})$	$n(m)^{-3}$	ρ (Ωm)	$R_H(\frac{m^3}{c})$	$n(m)^{-3}$	ρ (Ωm)	$R_H(\frac{m^3}{c})$	$n(m)^{-3}$
NAG 602	11.5×10^{-4}	4.42×10^{-4}	1.41×10^{22}	——	——	——	64.95×10^{-4}	9.31×10^{-4}	0.67×10^{22}
NAG 495	8.1×10^{-4}	3.59×10^{-4}	1.7×10^{22}	3.56×10^{-4}	4.877×10^{-4}	1.28×10^{22}	52×10^{-4}	8.6×10^{-4}	0.82×10^{22}
NAG 601	8.35×10^{-4}	3×10^{-4}	2.07×10^{22}	——	——	——	32.8×10^{-4}	6.09×10^{-4}	1.02×10^{22}
NAG 309	4.566×10^{-4}	1.55×10^{-4}	4×10^{22}	3×10^{-4}	2.24×10^{-4}	2.79×10^{22}	25.5×10^{-4}	1.92×10^{-4}	3.25×10^{22}
NAG 311	4.35×10^{-4}	1.49×10^{-4}	4.166×10^{22}	2.746×10^{-4}	2.3×10^{-4}	2.717×10^{22}	22.5×10^{-4}	1.77×10^{-4}	3.53×10^{22}
NAG 506	3.19×10^{-4}	1.13×10^{-4}	5.5×10^{22}	2.637×10^{-4}	1.52×10^{-4}	4.11×10^{22}	9.77×10^{-4}	1.24×10^{-4}	5.03×10^{22}
AGRO 529	1.57×10^{-4}	0.486×10^{-4}	1.3×10^{23}	1.54×10^{-4}	6.48×10^{-5}	9.6×10^{22}	3.03×10^{-4}	0.49×10^{-4}	1.28×10^{23}
NAG 484	0.132×10^{-4}	0.016×10^{-4}	3.8×10^{24}	0.132×10^{-4}	0.016×10^{-4}	3.9×10^{24}	0.135×10^{-4}	0.0163×10^{-4}	3.88×10^{24}

Table [4.1] Summary of Properties of Eight n-type InP Samples

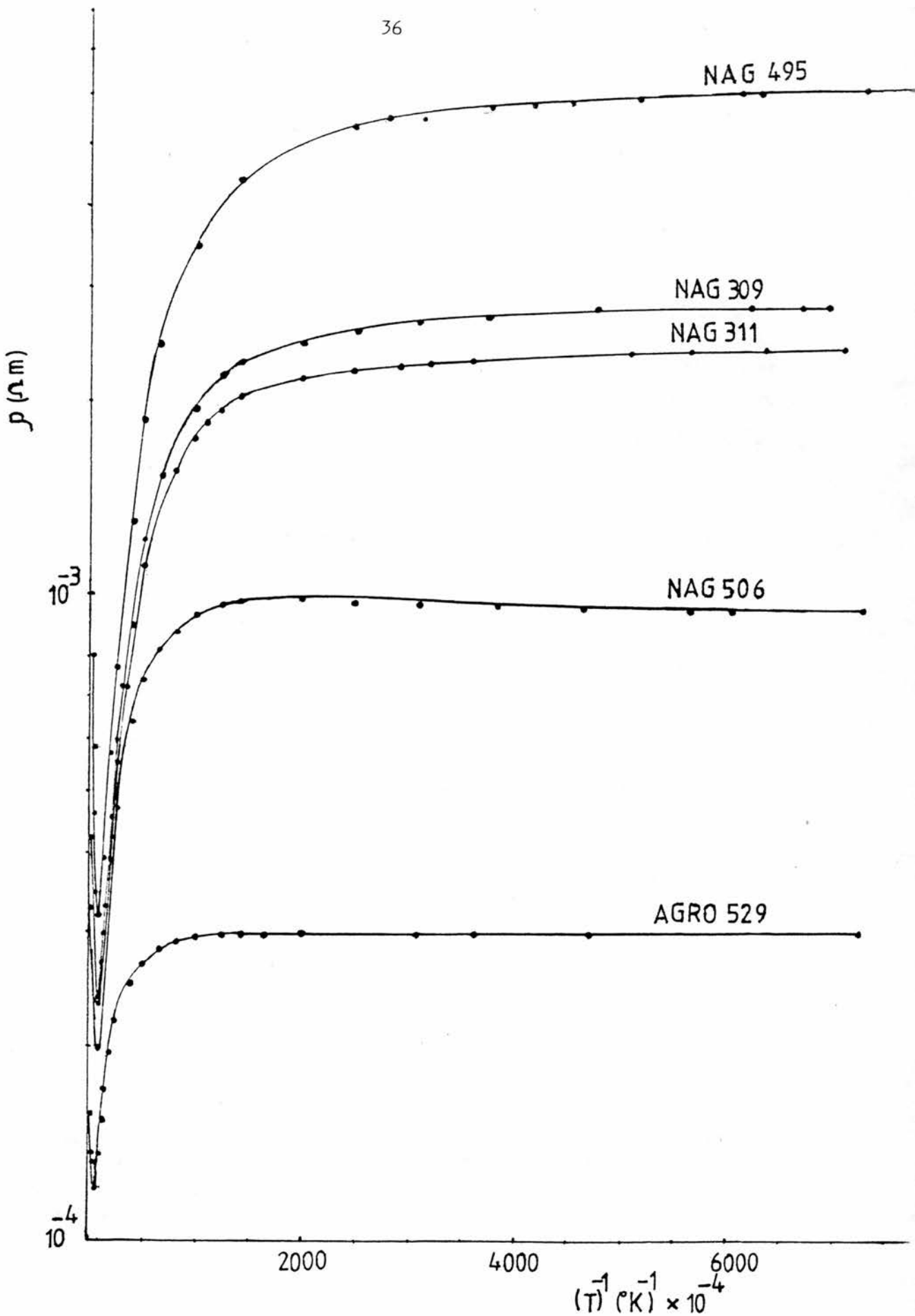
NAG 495
NAG 309
NAG 311
NAG 506
AGRO 529
ρ (Ωm)
10^-3
10^-4
2000
4000
6000
(T)^-1 (°K)^-1 × 10^-4

Fig·4·1

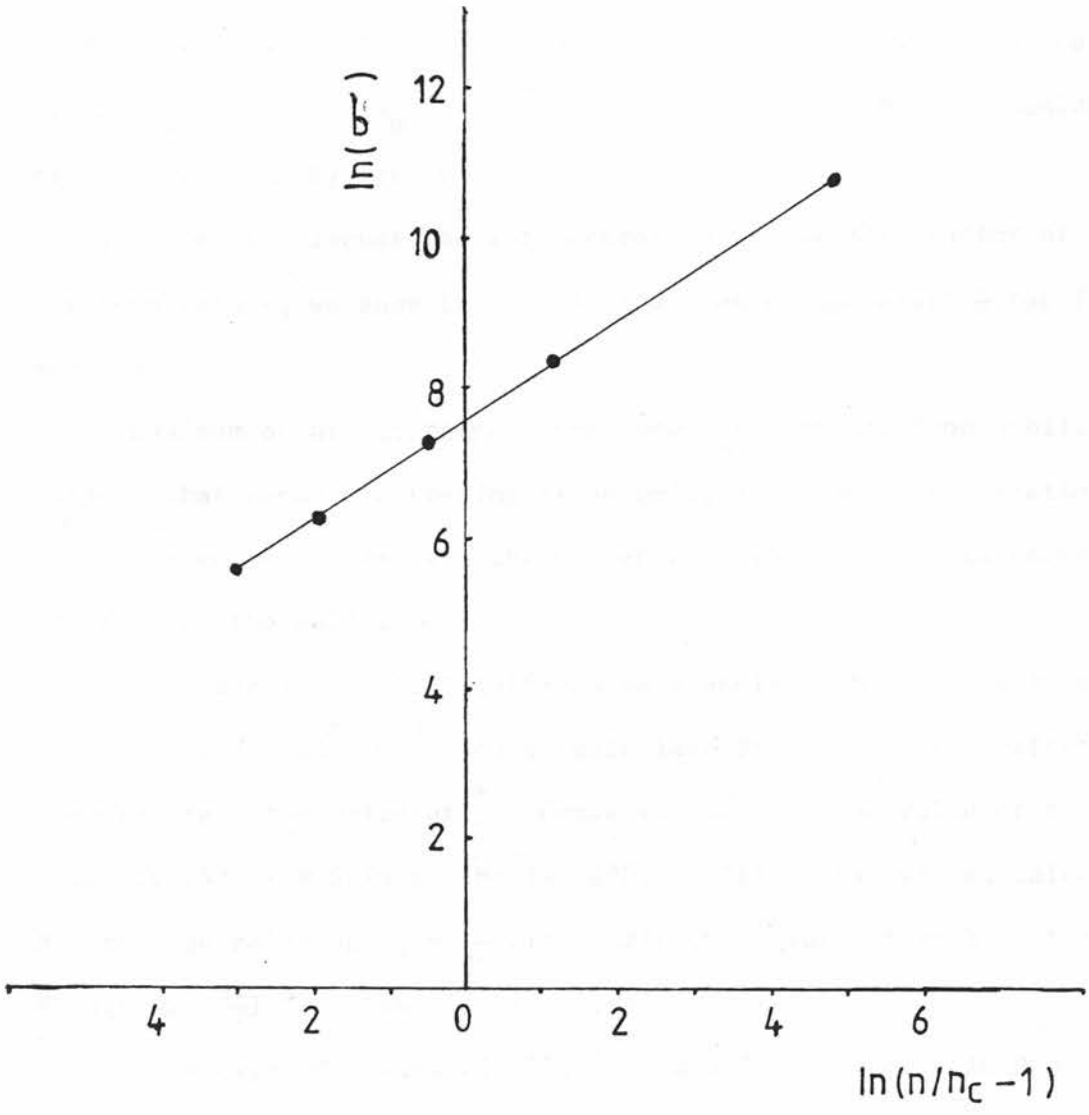

Fig-4-2

with an increase of T in the impurity region as a result of a change of the Hall factor r($R_H = \frac{r}{ne}$), others (eg Agaev (1967) by ionization of shallow impurity levels.

In order to discuss the interpretation of the Hall factor at low temperature, we show in Fig (4.4) a plot of R_H against $\frac{1}{T}$ for five samples.

A maximum occurs at temperatures where we expect, from mobility curves, that phonon scattering is becoming important. Calculations were carried out to explain the presence of that maximum in terms of changing the Hall factor r.

If we take sample AGRO (529) as an example with n constant and equal to $1.27 \times 10^{23}\ m^{-3}$ then we calculate from $nT^{-3/2}$ for different temperatures, the value of $\overset{*}{j}$. Hence we can find the value of r from Fig (4), F M Shipley thesis (1952). After that we can calculate R_H from the relation $R_H = \frac{r}{ne}$ with different values of r; a plot of R_H against $(\frac{1}{T})$ is shown in Fig (4.4).

The calculated values $nT^{-3/2}$, $\overset{*}{j}$, r and R_H for sample AGRO 529 are given in table (4.2) and for the other samples in table (4.3), (4.4), (4.5) and (4.6). It is obvious from this calculation that the presence of the maximum for concentrations greater than the MNM value can be explained entirely in terms of changing statistics. That is, a maximum in the Hall coefficient does not necessarily imply the existence of two separate bands.

Fig (4.5) shows the Hall coefficient of $R_H(T)$ does not depend upon magnetic field at $T = 4^{o}K$ for samples NAG(602), NAG(495), NAG(309), NAG(506) and AGRO 529. A very small change was observed in sample NAG(601).

T(K)	$n(T)^{-3/2} \times 10^{14}$	$\overset{*}{j}$	r	$R_H(m^3/c) \times 10^{-4}$
100	1.27	0.5	1.67	0.822
80	1.77	0.98	1.60	0.787
60	2.73	1.69	1.5	0.738
40	5.02	2.96	1.34	0.66
20	14.2	6.37	1.14	0.56
10	40.2		1.04	0.51
4	159		1.01	0.49
1	1270		1	0.49

Table [4.2] for Sample AGRO 529 of InP

T(K)	$n(T)^{-3/2} \times 10^{13}$	j^*	r	$R_H(m^3/c) \times 10^{-4}$
60	10.67	0.17	1.715	2.16
40	19.6	1.16	1.56	1.96
30	30.186	1.88	1.475	1.56
20	55.45	3.21	1.355	1.71
10	156.85	6.82	1.13	1.42
4	620	15.1	1.04	1.31
1	4960			

Table [4.3] for Sample NAG 506

T(K)	$n(T)^{-3/2}$	$\overset{*}{j}$	r	$R_H(m^3/c) \times 10^{-4}$
100	3.71×10^{13}	-1	1.855	3.13
80	5.18×10^{13}	-0.7	1.87	3.15
60	7.98×10^{13}	-0.15	1.765	2.97
40	1.467×10^{13}	0.67	1.635	2.75
20	4.14×10^{14}	2.495	1.44	2.43
10	1.17×10^{15}	5.55	1.18	1.99
4	4.63×10^{15}	13.55	1.04	1.75
1	3.71×10^{16}			

Table [4.4] for Sample NAG 311

T(K)	$n(T)^{-3/2}$	$\overset{*}{j}$	r	$R_H(m^3/c) \times 10^{-4}$
60	6.72×10^{19}	-0.4	1.8	3.6
40	1.25×10^{20}	0.2	1.74	3.48
20	3.49×10^{20}	2.13	1.45	2.9
10	9.88×10^{20}	4.95	1.21	2.42
4	3.9×10^{21}	12.6	1.045	2.09
1				

Table [4.5] for Sample NAG 309

T(K)	$n(T)^{-3/2}$	$\overset{*}{j}$	r	$R_H(m^3/c) \times 10^{-3}$
60	2×10^{13}	-1.8	1.89	1.27
40	3.68×10^{13}	-1.05	1.855	1.25
20	1×10^{14}	0.17	1.74	1.17
10	2.94×10^{14}	1.84	1.5	1
4	1.16×10^{15}	5.51	1.18	0.793
1				

Table [4.6] for Sample NAG (495)

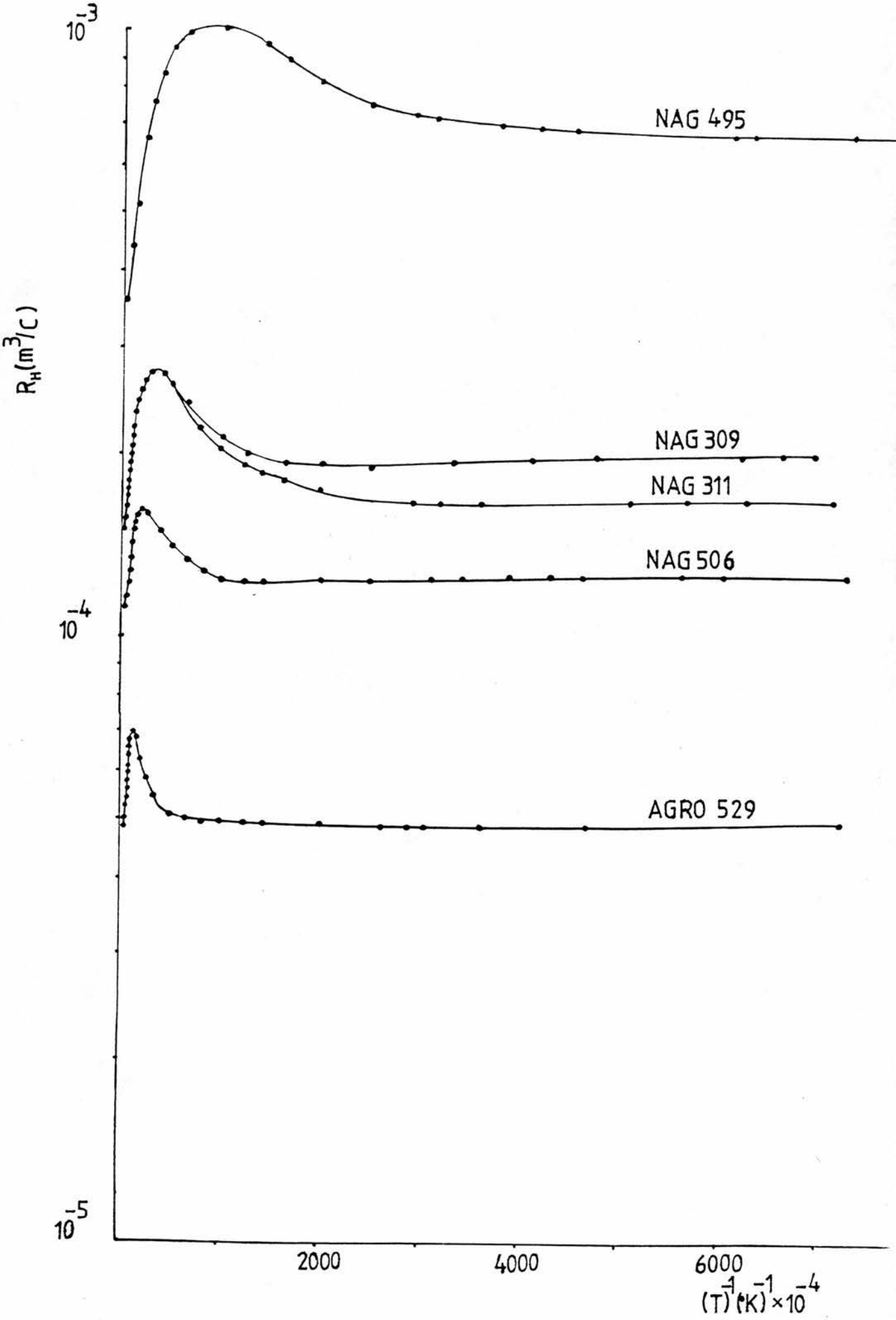
10^{-3}
10^{-4}
10^{-5}
$R_H(m^3/C)$
NAG 495
NAG 309
NAG 311
NAG 506
AGRO 529
2000
4000
6000
$(T)^{-1}(°K)^{-1}\times10^{-4}$

Fig·4·3

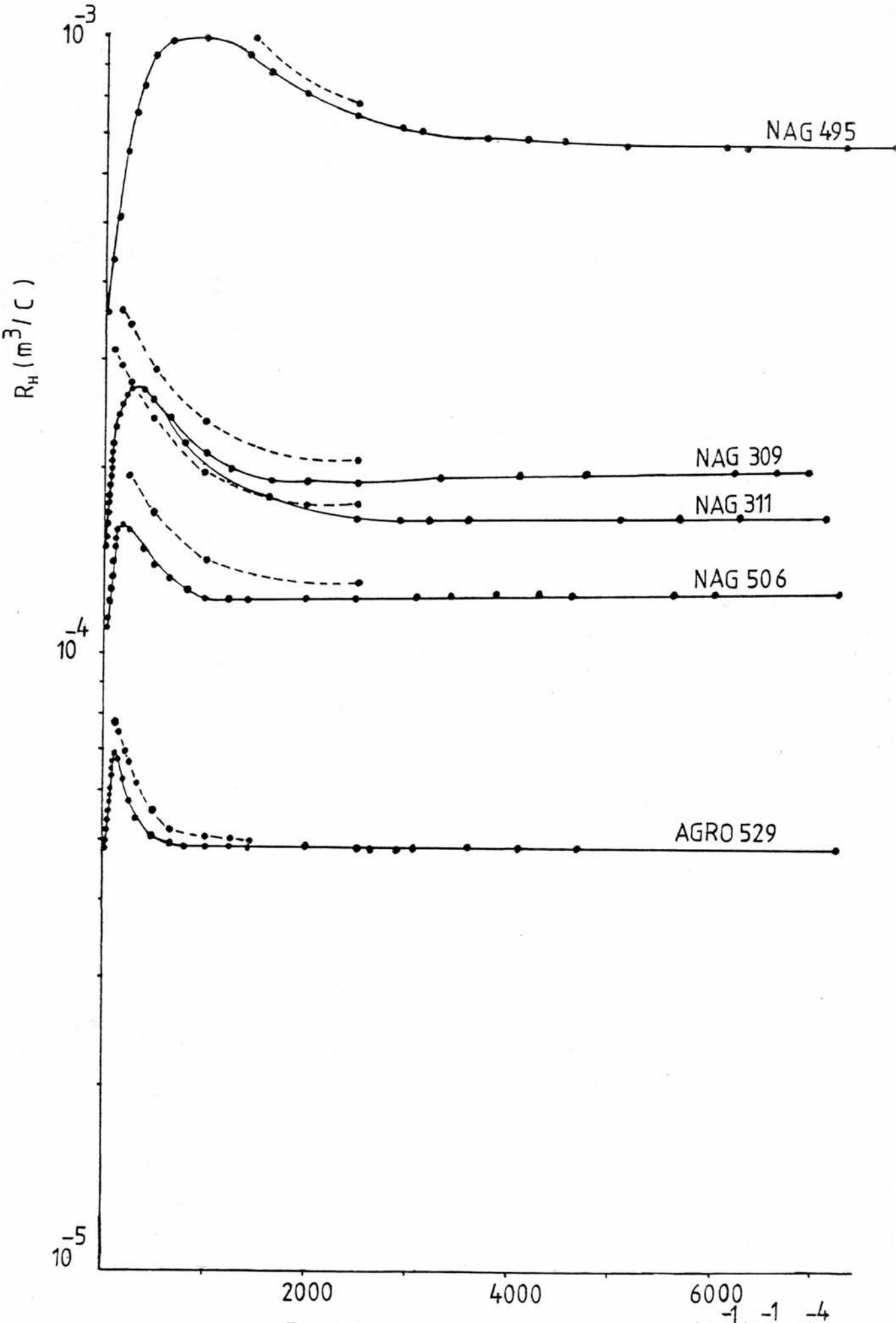
10^{-3}
10^{-4}
10^{-5}
R_H (m^3/C)
NAG 495
NAG 309
NAG 311
NAG 506
AGRO 529
2000
4000
6000
$(T)^{-1}(°K)^{-1} \times 10^{-4}$

Fig.4.4

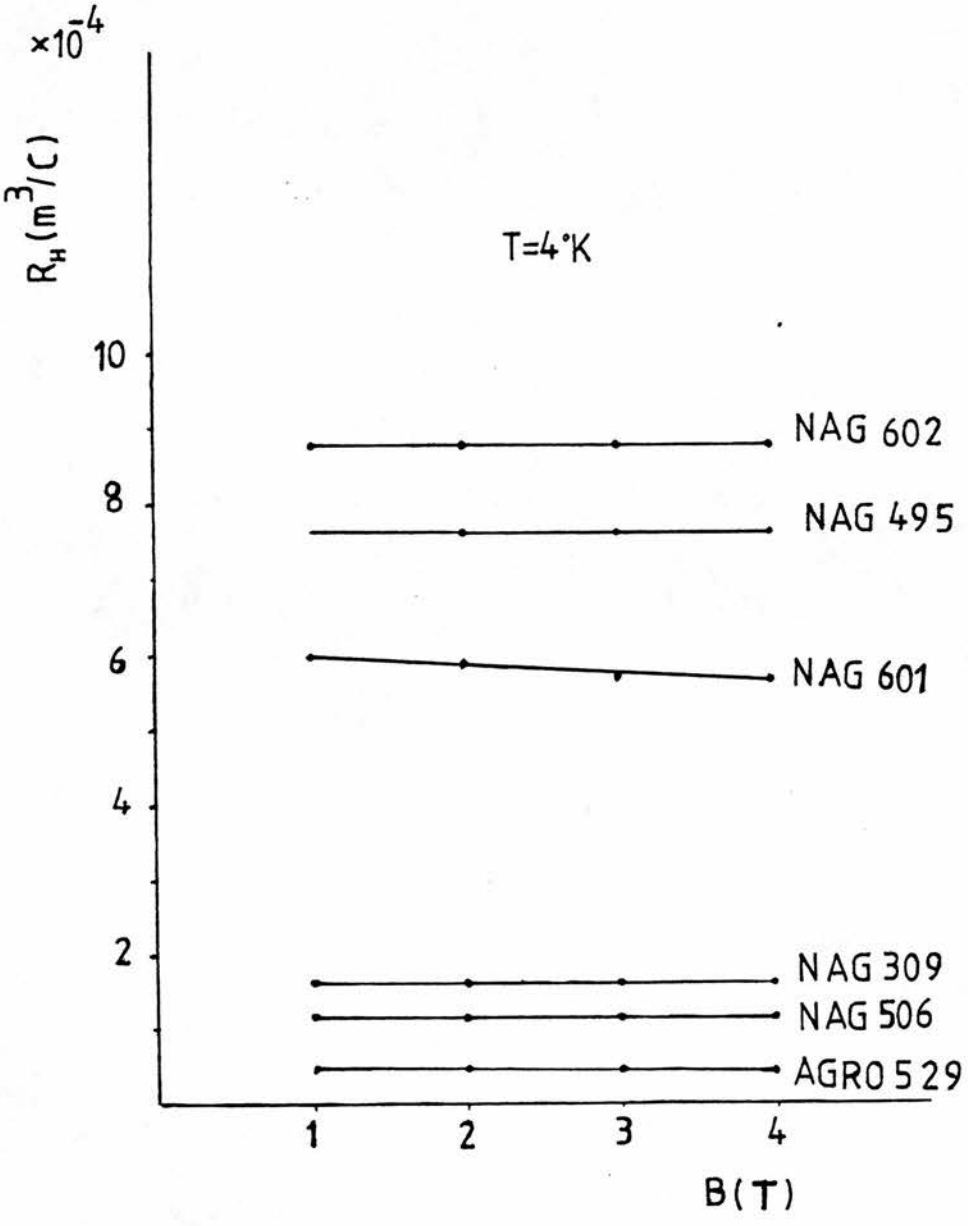
×10⁻⁴
R_H (m³/C)
T=4°K
10
8
6
4
2
NAG 602
NAG 495
NAG 601
NAG 309
NAG 506
AGRO 529
1
2
3
4
B(T)

Fig·4.5

4.3 Hall Mobility

From the curves of the Hall mobility versus T from 1.37°K up to 300°K , Fig (4.6), it will be seen that all the samples had a maximum of mobility in the temperature range 100 - 140°K apart from the very high electron density sample NAG 484 which had a constant mobility. This maximum shifted towards higher temperatures when the impurity concentration was increased. Above the maximum temperature up to 300°K the mobility decreased with temperature roughly as $T^{-3/2}$, and the scattering by phonons increases as the temperature increased.

At low temperatures the dependence is approximately as $T^{3/2}$ and the scattering by ionized impurity scattering is dominant.

The mobility maximum for sample AGRO 529 is less than the mobility maximum for sample NAG 495 and the mobility decreased faster below the maximum for sample NAG 495.

4.4 Compensation Ratio (K)

To calculate the compensation ratio we used Mansfield's theory (1956) applicable at low temperatures where impurity scattering becomes dominant. From the mobility curves Fig (4.6) the maximum ranges from 140°K for sample AGRO 529 to 100°K for sample NAG 495; then selecting a temperature at 40°K well below the maximum to ensure dominance of ionized impurity scattering, we used the general equation for the conductivity due to impurity scattering (4.10). For indium phosphide (InP)

$$\epsilon = \frac{12.4}{9 \times 10^{9}} = 1.38 \times 10^{-9} \quad \text{MKS}$$

$$\overset{*}{m} = 0.082 \times 9.1 \times 10^{-31} \quad \text{Kg}$$

$$k_B = 1.38 \times 10^{-23} \ \text{J.K}^{-1}$$

$$e = 1.6 \times 10^{-19} \ \text{C}$$

$$h = 2\pi \times 1.05 \times 10^{-34} \ \text{J.s}$$

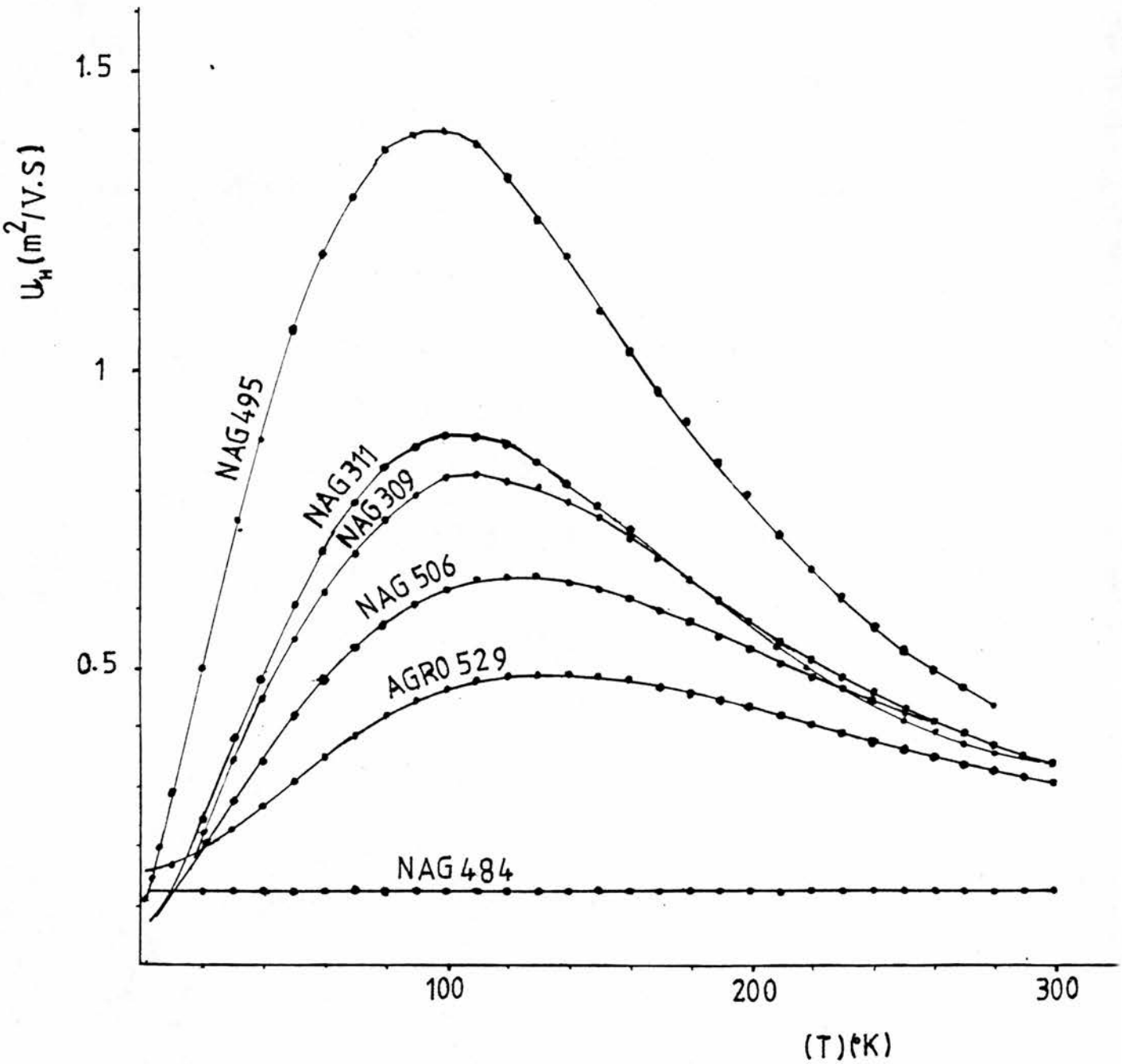
1.5
1
0.5
$\mu_H (m^2/V.S)$
NAG 495
NAG 311
NAG 309
NAG 506
AGRO 529
NAG 484
100
200
300
(T)°K

Fig·4·6

As an example of the calculation at T = $40^{o}K$ for the sample AGRO 529, the values of the resistivity, mobility and the Hall coefficient are calculated from experiment and equal to 2.19×10^{-4} (Ωm), 0.2664 ($m^2/v.s$) and 5.84×10^{-5} m^3/c respectively where $\sigma_I = \frac{1}{\rho} = 45.66\ (\Omega m)^{-1}$, the value of r can be calculated from Fig (4), F M Shipley (1952) and itwas found equal to 1.34, then the values of $f_{\frac{1}{2}}(\overset{*}{j})$, $f_2(\overset{*}{j})$ and $(\overset{*}{j})$ were 1.72, 22.3 and 3.25 respectively was found. $\bar{\eta} = 3.8$ was found from the graph between $\overset{*}{j}$ and $\bar{\eta}$, Mansfield (1956). Then from these values we calculate the total number of ionized impurities (N) from this equation

$$N = \frac{32\ \epsilon^2\ \overset{*}{m}(k_B T)^3 f_2(\overset{*}{j})}{\sigma_I\ e^2\ h^3\ f(x)}$$

where $f(x) = \ln(1 + x) - \frac{x}{(1+x)}$

and $$x = \frac{\bar{\eta}\ (k_B T)^{\frac{1}{2}}\ \epsilon\ h}{e^2 (2\overset{*}{m})^{\frac{1}{2}}\ f_{\frac{1}{2}}(\overset{*}{j})}$$

$$x = \frac{3.8(1.38 \times 10^{-23} \times 40)^{\frac{1}{2}}(1.377 \times 10^{-9})(2\pi \times 1.05 \times 10^{-34})}{(1.6 \times 10^{-19})(2 \times 0.082 \times 9.1 \times 10^{-31})^{\frac{1}{2}} \times 1.72} = \frac{8.11 \times 10^{-53}}{1.7 \times 10^{-53}}$$

$$x = 4.77$$

and $$f(x) = \ln(1+x) - \frac{x}{(1+x)}$$

$$= \ln(1 + 4.77) - \frac{4.77}{(1+4.77)}$$

$$f(x) = 0.926$$

After that

$$N = \frac{32(1.38 \times 10^{-9})^2 (0.082 \times 9.1 \times 10^{-31})(1.38 \times 10^{-23} \times 40)^3 \times 22.3}{45.66\ (1.6 \times 10^{-19})^2\ (2\pi \times 1.05 \times 10^{-34})^3 \times 0.926}$$

$$N = 5.46 \times 10^{23}\ m^{-3}$$

$$r = 1.34 = neR \text{ or } n = \frac{r}{ne} = \frac{1.34}{5.84 \times 10^{-5} \times 1.6 \times 10^{-19}} = 1.43 \times 10^{23}\ m^{-3}$$

$$N_A = \frac{N - n}{2} = \frac{(5.46 - 1.43) \times 10^{23}}{2} = 2.015 \times 10^{23}$$

$$N_D = n_{sat} + N_A = 1.27 \times 10^{23} + 2.015 \times 10^{23} = 3.285 \times 10^{23}$$

$$K = \frac{N_A}{N_D} = \frac{2.015 \times 10^{23}}{3.285 \times 10^{23}} = 0.61.$$

For other samples similar calculations were made, and these are given in table [4.7].

Walukiewicz et al (1980) have made estimates of compensation ratio in InP from room temperature and 77°K, values of mobility and electron density. From their tables a compensation ratio of K = 0.34 is obtained for these samples from the 77°K data, whereas the room temperature data suggest that the sample is almost uncompensated. Accurate determination of the compensation ratio in InP is clearly a matter of some difficulty.

4.5 Fermi Energy, Fermi Velocity and Mean Free Path Calculation

At complete degeneracy the fermi energy $E_F = (3\pi^2 n)^{2/3} \frac{\hbar^2}{2m}$.

For example calculation for the sample AGRO (529)

At T = 4K

$$n = 1.28 \times 10^{23}\ m^{-3}$$

(a) $$E_f = (3\pi^2 \times 1.28 \times 10^{23})^{2/3} \times \frac{(1.05 \times 10^{-34})^2}{(2 \times 0.082 \times 9.1 \times 10^{-31})}$$

$$E_f = 1.523 \times 10^{-21} \text{ joul} = 0.952 \times 10^{-2} \text{ ev.}$$

(b) $$E_f = \tfrac{1}{2} m V_f^2$$

$$V_F = (3\pi^2 n)^{1/3} \frac{\hbar}{m}$$

Sample	$\overset{*}{j}$	$f_2(\overset{*}{j})$	$f_{\frac{1}{2}}(\overset{*}{j})$	$\bar{n}$	ρ (Ωm)	$\mu_H(\frac{m^2}{v.s})$	$R_H(\frac{m^3}{c})$	r	$n_{sat}(m^{-3})$	$N(m^{-3})$	$N_A(m^{-3})$	$N_D(m^{-3})$	$K=\frac{N_A}{N_D}$
AGRO 529	3.25	22.3	1.72	3.8	2.19×10^{-4}	0.2669	5.84×10^{-4}	1.34	1.27×10^{23}	5.4×10^{23}	2.02×10^{23}	3.29×10^{23}	0.613
NAG 506	1.48	6.3	1.09	2.5	4.7×10^{-4}	0.34046	1.6×10^{-4}	1.56	4.96×10^{22}	3.23×10^{23}	1.31×10^{23}	1.81×10^{23}	0.725
NAG 311	0.7	3.4	0.79	2.1	5.66×10^{-4}	0.482	2.73×10^{-4}	1.635	3.7×10^{22}	1.89×10^{23}	0.76×10^{23}	1.13×10^{23}	0.671
NAG 309	0.82	3.8	0.845	2.3	6.13×10^{-4}	o.437	2.68×10^{-4}	1.74	3.13×10^{22}	2.25×10^{23}	0.922×10^{23}	1.24×10^{23}	0.746

Table [4.7] list of the n-type InP Samples at T = 40°K

Samples	$n\ m^{-3}$	$\rho_o(\Omega m)$	$E_f(ev)$	$V_F(m/s)$	$\lambda(m)$	$\tau(s)$
AGRO 529	1.28×10^{23}	3.03×10^{-4}	9.52×10^{-3}	0.219×10^{6}	1.65×10^{-8}	7.529×10^{-14}
NAG 506	5.03×10^{22}	2.77×10^{-4}	6.01×10^{-3}	0.16×10^{6}	0.94×10^{-8}	5.867×10^{-14}
NAG311	3.53×10^{22}	22.5×10^{-4}	7.75×10^{-3}	0.142×10^{6}	0.52×10^{-8}	3.668×10^{-14}
NAG 309	3.25×10^{22}	25.5×10^{-4}	4.5×10^{-3}	0.138×10^{6}	0.485×10^{-8}	3.5×10^{-14}

Table [4.8] T = 4°K

$$= (3\pi^2 \times 1.28 \times 10^{23}\ m^{-3})^{1/3} \times \left(\frac{1.05 \times 10^{-31}\ J.s}{0.082 \times 9.1 \times 10^{-31}\ kg}\right)$$

$$V_f = 2.19 \times 10^5\ m\ s^{-1}$$

c. $\lambda = V_f\ \tau$ where $\tau = \dfrac{\sigma_o m}{ne^2}$, $\rho = 3.03 \times 10^{-4}$ (Ωm)

$$= (2.19 \times 10^5\ m/s)\ \left(\frac{(3300.33)(0.082 \times 9.1 \times 10^{-31})\ kg}{(1.28 \times 10^{23})(1.6 \times 10^{-19})^2}\right.$$

$$\lambda = 1.65 \times 10^{-8}\ m$$

For the other samples similar calculations were made and are given in table [4.8].

4.6 Magnetoresistance

Magnetoresistance curves are shown in Fig 4.7, 4.8, 4.9, 4.10, 4.11, 4.12 and 4.13.

Fig 4.7, 4.8 and 4.9 show a positive magnetoresistance for the three samples with $N_D - N_A \lesssim 3 \times 10^{22}\ m^{-3}$ (i.e. $N_D - N_A$ less than N_C) from $T = 4^oK$ down to 1.37^oK with field up to 7 kG. For the other two samples a small negative magnetoresistance is seen at the lowest temperature at low magnetic fields and positive magnetoresistance at higher magnetic fields.

Fig (4.14) shows a positive magnetoresistance for three samples at $T = 4^oK$ for fields up to 40 kG.

Fig 4.15 shows a positive magnetoresistance versus $\sqrt{B}$ and fig (4.16) shows a positive magnetoresistance versus B^2 with the field up to 40 kg, thus fig (4.16) yields straight lines for the three samples at high fields with a slight bend at lower field. The positive magnetoresistance clearly does not vary as $\sqrt{B}$ but approximates to B^2.

Fig (4.17) shows a positive magnetoresistance with a magnetic field up to 7 tesla at T = $4^{o}K$ for sample NAG 601 and fig (4.18) shows a positive magnetoresistance proportional with B^2 up to 7 tesla.

Fig (4.19) shows the magnetoresistance for our samples at low temperatures between $1.37^{o}K$ and $1.45^{o}K$ with field up to 7 kG, a positive magnetoresistance for the sample NAG 495 and negative for NAG 602 and NAG 601 at low field and positive magnetoresistance at high field, fig (4.20) shows magnetoresistance for the samples with $\sqrt{B}$ and fig (4.21) shows magnetoresistance with B^2.

Fig (4.10), (4.11), (4.12) and (4.13) show a negative magnetoresistance for samples with $N_D - N_A > 3 \times 10^{22}\ m^{-3}$ (i.e. $N_D - N_A$ greater than N_C) at T = $4^{o}K$ and down to $1.37^{o}K$ with a magnetic field up to 7 kG.

In these samples the magnitude of the negative magnetoresistance increases with magnetic field and with decreasing temperature and there is no indication of decrease in the negative value for the field up to 7 kG.

Fig (4.22), (4.23). (4.24) and (4.25) shows magnetoresistance for samples NAG 309, NAG 311, NAG 506 and AGRO 529 respectively with different temperatures. All these samples show a negative magnetoresistance at low temperatures and positive at higher temperatures. Fig (4.26) shows a negative magnetoresistance for samples with field up to 40 kG at T = $4^{o}K$.

For sample AGRO 529 the magnetoresistance increases with increasing magnetic field up to 40 kG but for sample NAG 309 sharp increase with increasing magnetic field up to a certain field is followed by

a decrease with further increase of magnetic field. Sample NAG 506 shows behaviour similar to that of AGRO 529 but has an anamolous and unexplained bump near 30 kG.

Fig (4.27) shows negative magnetoresistance versus $\sqrt{B}$. For the sample AGRO 529 nearly a straight line was observed. Fig (4.28) shows a negative magnetoresistance versus B^2 for the sample AGRO 529. A straight line is observed at higher field;measurements were extended to 12 tesla for sample AGRO 529 shown in fig (4.29), (4.30) and (4.31). This concentration range corresponds to the weakly localized regime and we wish to consider this in greater detail in terms of the theories of Kawabata and of Lee and Ramakrishnan; the data for sample AGRO 529 is used as an example. The magnetic length is given by $L = \sqrt{\frac{\hbar}{Be}}$.

Kawabata expects the negative component of the magnetoresistance to saturate when the magnetic field is increased to a value B_c such that L becomes less than or equal to the mean free path λ.

B_C is determined as follows

$$\lambda = V_f \tau$$

$$V_f = (3\pi^2 n)^{1/3} \frac{\hbar}{m^*}$$

$$\tau = \frac{\sigma_o m}{ne^2}$$

$$\lambda = (3\pi^2 n)^{1/3} \cdot \frac{\hbar}{m^*} \cdot \frac{\sigma_o m^*}{ne^2}$$

$$\lambda = \frac{(3\pi^2)^{1/3}}{n^{2/3}} \cdot \frac{\sigma_o}{e} \cdot L^2 B_c$$

$$\frac{\lambda}{L} = \frac{(3\pi^2)^{1/3}}{n^{2/3}} \cdot \frac{\sigma_o}{e^{3/2}} \cdot \hbar^{\frac{1}{2}} B_c^{\frac{1}{2}}$$

$$\frac{\lambda}{L} = \frac{(3\pi^2)^{1/3}}{(1.6 \times 10^{-19})^{3/2}} \times (1.05 \times 10^{-34})^{\frac{1}{2}} \times \frac{\sigma_o B_C^{\frac{1}{2}}}{n^{2/3}}$$

$$= \frac{3.093}{6.4 \times 10^{-29}} \times 1 \times 10^{-17} \cdot \frac{\sigma_o B^{\frac{1}{2}}}{n^{2/3}}$$

$$\frac{\lambda}{L} = 4.9 \times 10^{11} \frac{B_C^{\frac{1}{2}} \sigma_o}{n^{2/3}} \quad , \quad \lambda = L$$

$$B_C = \left(\frac{\rho_o n^{2/3}}{4.9 \times 10^{11}}\right)^2 = \left(\frac{3.03 \times 10^{-4} (\Omega m)^{-1} \times (1.28 \times 10^{23} \ m^{-3})^{2/3}}{4.9 \times 10^{11}}\right)^2$$

$$B_C = 2.46 \text{ T.}$$

Similar calculation for the other samples are summarized in table [4.9].

$$L = \sqrt{\frac{\hbar}{B_C e}} = \sqrt{\frac{1.05 \times 10^{-34}}{2.5 \times 1.6 \times 10^{-19}}}$$

$$= 1.62 \times 10^{-8} \text{ m}$$

At values of $B > B_C$, since the negative component no longer increases, we expected the positive component to take over and this is observed in fig (4.29) which shows that the magnetoresistance decreases as the field B increases, passes through a minimum value at a field equal to 4.7 tesla and then at higher fields $\frac{\Delta\rho}{\rho_o}$ increases to zero at a field of 7.9 tesla. A normal positive magnetoresistance was observed at higher field. This positive part is perhaps proportional to $\sqrt{B}$ at highest fields available in fig (4.30).

Calculation of δ will be carried out as follows. For the limit $\delta = \left(\frac{3L^2}{4\lambda\lambda_\varepsilon}\right) << 1$, where δ is the correction to the conductivity, then Kawabata obtained the very simple relation $\delta\sigma = 0.92\sqrt{H}$ and we can easily compare our experimental result with theory in this limit.

$$\lambda = \left(\frac{2E_f}{\frac{*}{m}}\right)^{\frac{1}{2}} \tau, \quad \lambda_\varepsilon = \left(\frac{2E_f}{\frac{*}{m}}\right)^{\frac{1}{2}} \tau_\varepsilon .$$

Sample	B_{sat}(Tesla)
AGRO 529	2.4
NAG 506	7.63
NAG 311	24.42
NAG 309	28.08

Table [4.9]

Parameter	Value
m^*/m_o	0.082
ξ_1	6.8 ev
E_G^*	1.4 ev
C_L	12.1×10^{10} N m^{-2}
ϵ_o	12.4
ϵ_∞	9.6
${}^oL_{-1}^{3/2}$	170
${}^oL_o^{3/2}$	170

Table [4.10]

Parameter used in λ_ε Calculation for (InP)

To calculate τ_ε from the acoustic phonon scattering and carrier-carrier scattering, we use relations given by Harris and Ridley (1972). Its value is estimated as follows:

$$\tau_{ac} = \frac{\pi C_L \hbar^4}{2^{\frac{1}{2}} m_d^{3/2} \xi_1^2 K_B T} \nu^{-\frac{1}{2}} \left(\frac{d\nu}{dE}\right)$$

where C_L is an average longitudinal elastic constant and ξ_1 is the deformation potential. The data from table [4.10] Kohn model has been used to calculate ν, the relationship is

$$\nu = E + \frac{E^2}{E_G} \quad .$$

$$E_f = 0.952 \times 10^{-2} \text{ ev}$$

$$\nu = 0.952 \times 10^{-2} \text{ ev} + \frac{(0.952 \times 10^{-2} \text{ ev})^2}{1.42 \text{ ev}}$$

$$\nu = 9.583 \times 10^{-3} \text{ ev} = 1.53 \times 10^{-21} \text{ J}$$

$$\nu^{-\frac{1}{2}} = 2.55 \times 10^{10}$$

$$\left(\frac{d\nu}{dE}\right) = 1 + \frac{2E}{E_G} = 1 + \frac{2 \times 0.952 \times 10^{-2} \text{ ev}}{1.42 \text{ ev}}$$

$$= 1.013$$

$$\left(\frac{d\nu}{dE}\right)^{-1} = 0.987$$

$$\tau_{ac} = \frac{\pi \times 12.1 \times 10^{10} \text{ N m}^{-2} (1.05 \times 10^{-34} \text{ J.s})^4 (2.55 \times 10^{10})(1.013)}{2^{\frac{1}{2}} (0.082 \times 9 \times 10^{-31} \text{K})^{3/2} (6.8 \times 1.6 \times 10^{-19} \text{J})^2 \times (1.38 \times 10^{-23} \text{K}^{-1} \times 4^{\circ}\text{K}}$$

$$\tau_{ac} = 6.366 \times 10^{-10} \text{ s}$$

Assuming that acoustic phonons provide the main inelastic scattering mechanism we have $\tau_\varepsilon = 6.4 \times 10^{-10}$s.

$$\lambda_\varepsilon = V_f \tau_\varepsilon = 0.92 \times 10^{6} \times 6.4 \times 10^{-10}$$

$$= 5.9 \times 10^{-4} \text{ m.}$$

then
$$\delta = \frac{3L^2}{4\lambda\lambda_\varepsilon} = \frac{3 \times (1.62 \times 10^{-8}\text{m})^2}{4 \times 1.65 \times 10^{-8} \times 5.9 \times 10^{-4} \text{ m}}$$

$$= 2 \times 10^{-5} << 1.$$

Kawabata (1980) gives the equation

$$\Delta\sigma\ (B,T) = \frac{e^2}{2\pi^2 \hbar e}\ F(\delta).$$

$F(\delta)$ is the angular average of the statically screened coulomb interaction. For $\delta << 1$. In the limit of very low T, this gives $\Delta\sigma = 0.92\sqrt{H}$. However from fig (2.10) of Kawabata we see that $F(\delta)$ is constant only when $\delta \sim 10^{-3}$, but for larger values we get $\Delta\sigma = 0.92\sqrt{H} - \frac{e^2}{4\pi^2\hbar} \cdot \frac{1}{\sqrt{D\tau_\varepsilon}}$

since $\frac{1}{\tau_\varepsilon} \propto T^3$ for acoustic phonons at low temperature. We see that qualitatively at any rate, that $\Delta\sigma$ must increase as T decreases. This is shown in figures (4.11), (4.12), (4.13) and (4.10) where $\Delta\rho = \frac{1}{\Delta\sigma}$, therefore $\Delta\sigma$ is inversely related to T.

We may note that, since the Kawabata theory approaches the problem from the metallic side of the transition, the agreement with theory will be best for the most heavily doped samples in which a negative magnetoresistance can be observed. It is for this reason that we have paid particular attention to sample AGRO 529.

The positive component of the magnetoresistance was explained by Lee and Ramakrishnan (1982) as due to the splitting of the spin-up and spin-down bands in a magnetic field. The spin splitting produces

a gap $g\mu_B H$ between the lowest unoccupied spin-up electron and the highest occupied spin-down electron. The spin zeeman effect on magnetoresistance obtained for the higher field limit is given by

$$\rho = \rho_o - 2\alpha(\frac{2}{3} - \frac{F}{2})T^{\frac{1}{2}} + 0.77\ \alpha\ F(\frac{|g|\mu_B}{K_B})^{\frac{1}{2}}\ H^{\frac{1}{2}}$$

where $\alpha = 1.08 \times 10^{-7}\ \rho_o^{5/2}\ (\frac{n}{T_F})^{\frac{1}{2}}\ \Omega\ cm.K^{-\frac{1}{2}}$ and where T_f is the Fermi temperatur

$$F = \frac{1}{x} \ln (1 + x)\ ,\quad x = (\frac{2k_F}{K})^2 \quad \text{and} \quad K^2 = \frac{6\pi ne^2}{E_f} \qquad \text{(Thomas-Fermi)}$$

where k and k_f are the screening and Fermi wave vectors, respectively.

The high field region occurs when the zeeman splitting exceeds $K_B T$ i.e. $g\mu_B H = K_B T$where μ_B is the Bohr magneton and equal to $\frac{e\hbar}{2me}$ and has the value 9.27×10^{-21} erg/gauss, and g is the splitting factor. For InP at 4^oK

$$1.26 \times 9.27 \times 10^{-21}\ \text{erg/gauss}\ H = 1.38 \times 10^{-16}\ \text{erg/K}^o \times 4$$

So $H_c = 4.7$ Tesla

So $H_c = 4.7$ Tesla. The calculated value of H_c are in good agreement with the experimental value, (Fig (4.29). To compare the theory of Lee and Ramakrishnan with the experimental result for the positive magnetoresistance can be carried out as follows.

$$\frac{\alpha}{\rho_o} = 1.08 \times 10^{-7}\ \rho_o^{3/2}\ (\frac{n}{T_F})^{\frac{1}{2}}$$

$$T_F = \frac{\hbar^2}{2mK_B}(3\pi^2)^{2/3}\ n^{2/3}$$

So
$$\frac{\alpha}{\rho_o} = \frac{1.08 \times 10^{-7}\ \rho_o^{3/2}\ n^{\frac{1}{2}}\sqrt{2mK_B}}{\hbar(3\pi^2)^{1/3}\ n^{1/3}}$$

For InP for sample AGRO 529 with $n = 1.3 \times 10^{17}\ cm^{-3}$ and $\rho = 3 \times 10^{-2}(\Omega cm)$.

Then we can get $\frac{\alpha}{\rho_o} = 1.08 \times 10^{-7}\ \rho_o^{3/2}\ (\frac{1.3 \times 10^{17}}{53.5})^{\frac{1}{2}}$

$$= 0.027$$

$$x = (\frac{2k_F}{K})^2 = 6.23 \times 10^{-7}\ n^{1/3} = 0.312$$

$$F = \frac{1}{x} \ln (1 + x) = 0.87$$

$$\frac{\rho-\rho_o}{\rho_o} = -2 \times 0.027 \left(\frac{2}{3} - \frac{0.87}{2}\right) T^{\frac{1}{2}} + 0.77 \times 0.027 \times 0.87 \left(\frac{1.26 \times 9.27 \times 10^{-21}}{1.38 \times 10^{-16}}\right)^{\frac{1}{2}} \times H^{\frac{1}{2}}$$

$$= - 0.012\ T^{\frac{1}{2}} + 1.67 \times 10^{-4}\ H^{\frac{1}{2}}$$

For $H = 10$ $T = 10^5$ oer. This gives + 0.053 and an experimental value of $\frac{\Delta\rho}{\rho_o} = 0.11$.

Although the agreement is not exact the theory of Kawabata gives as reasonable explanation of the negative component while the theory of Lee and Ramakrishnan qualitatively explains the positive component.

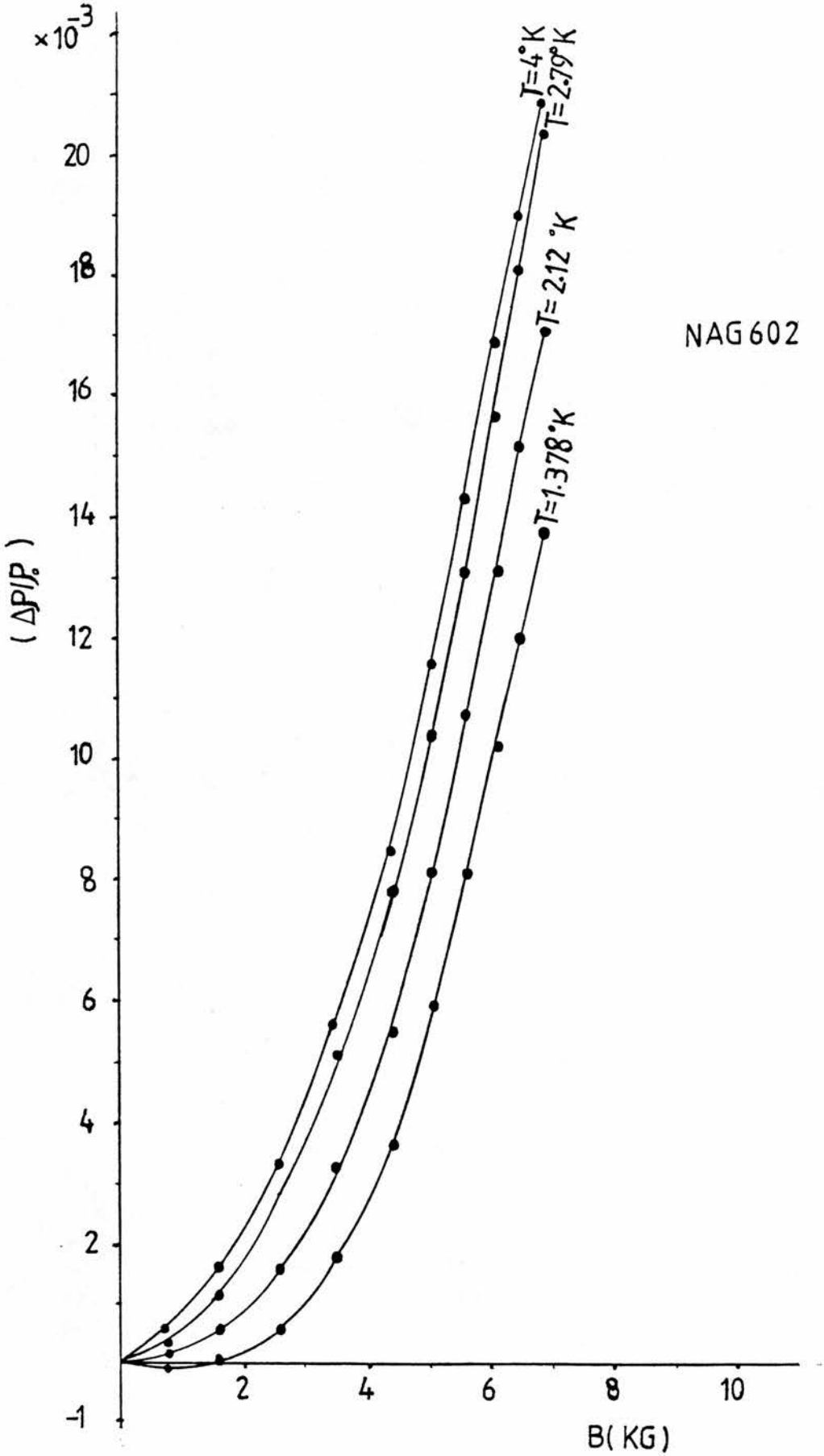
×10⁻³
20
18
16
14
12
10
8
6
4
2
-1
(ΔP/P₀)
T=4°K
T=2.79°K
T=2.12 °K
T=1.378°K
NAG 602
2
4
6
8
10
B(KG)

Fig·4.7

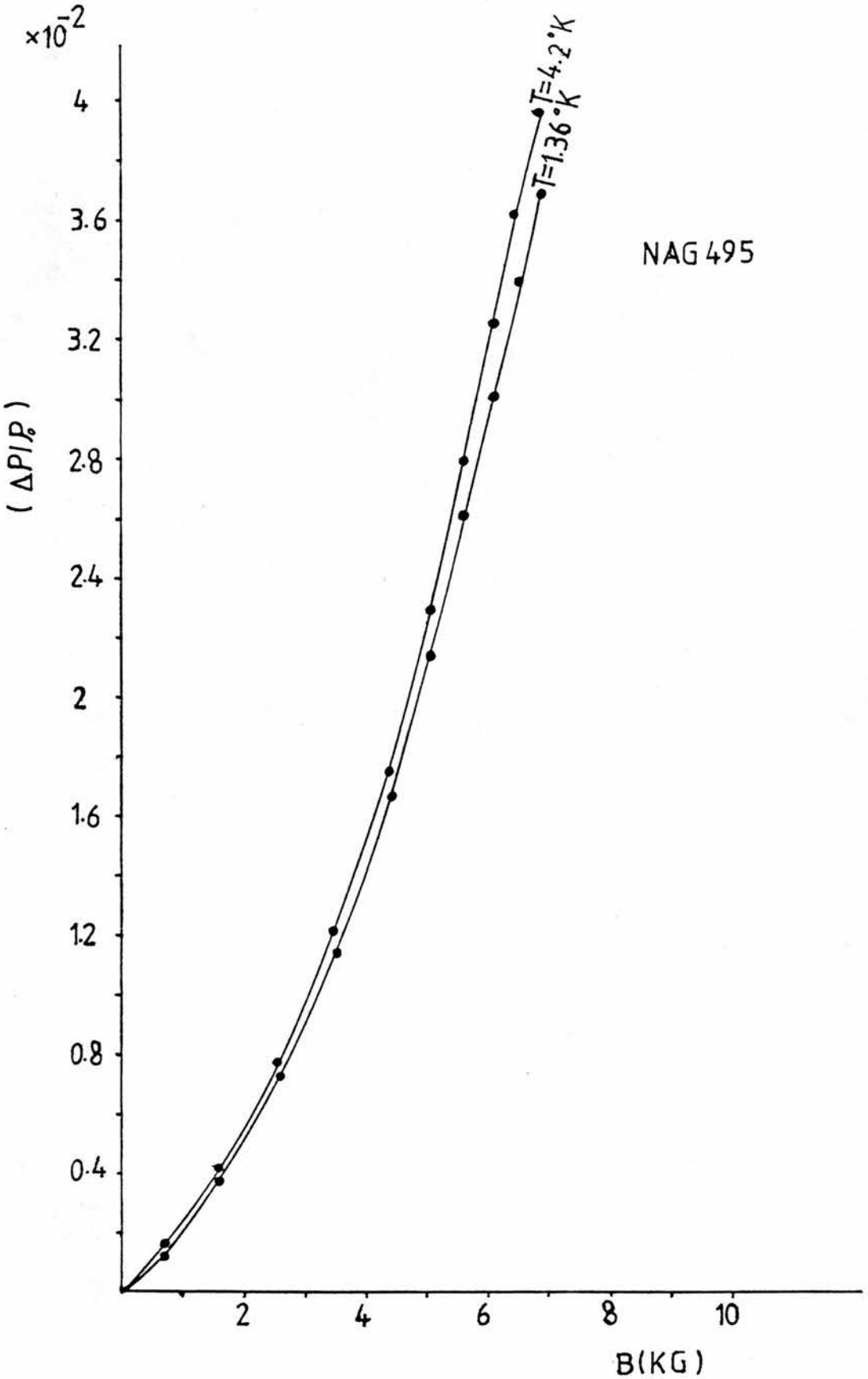

Fig·4·8

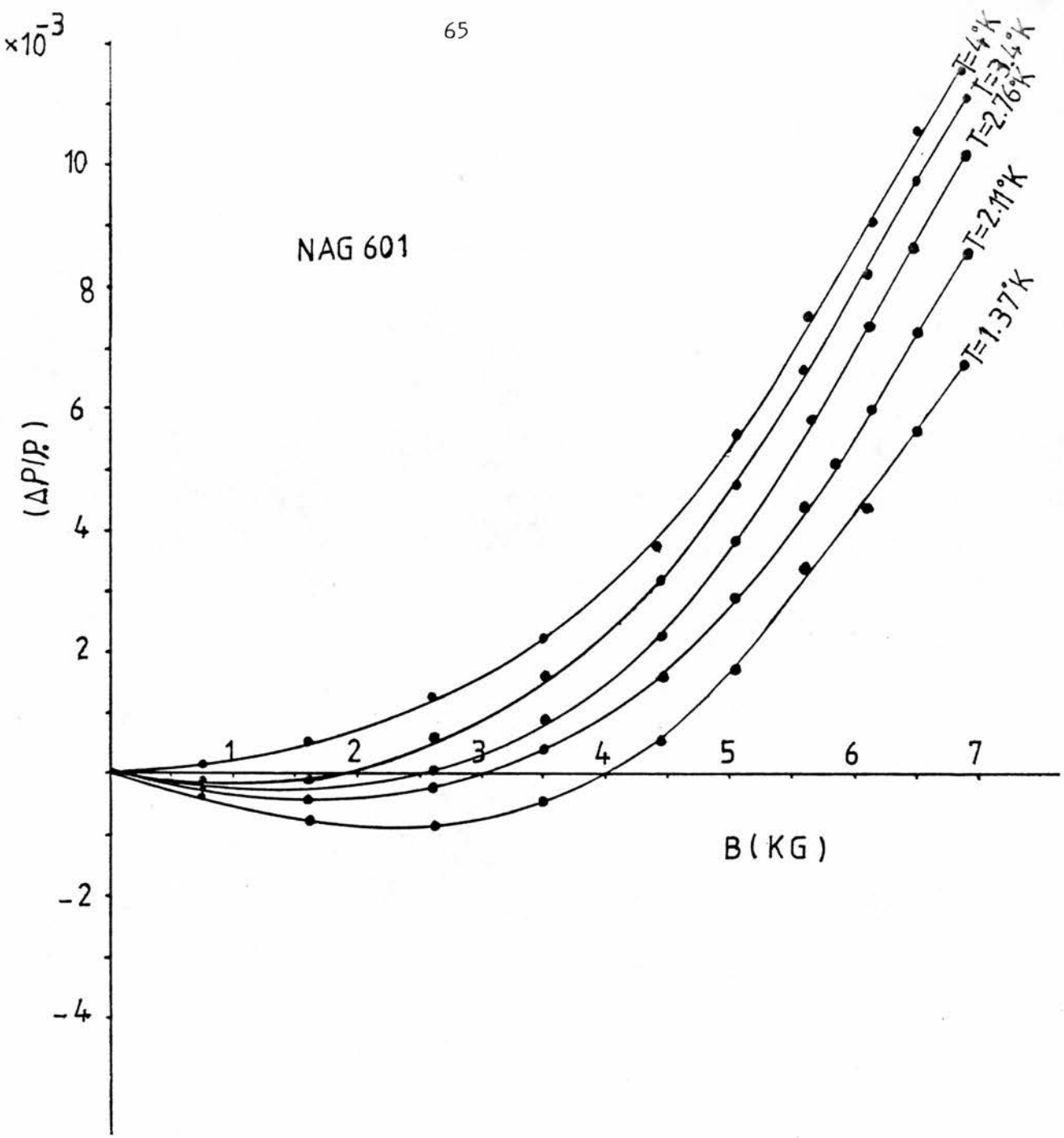
×10⁻³
10
8
6
4
2
-2
-4
(ΔP/P.)
NAG 601
1
2
3
4
5
6
7
B(KG)
T=4°K
T=3.4°K
T=2.76°K
T=2.11°K
T=1.37°K

Fig·4.9

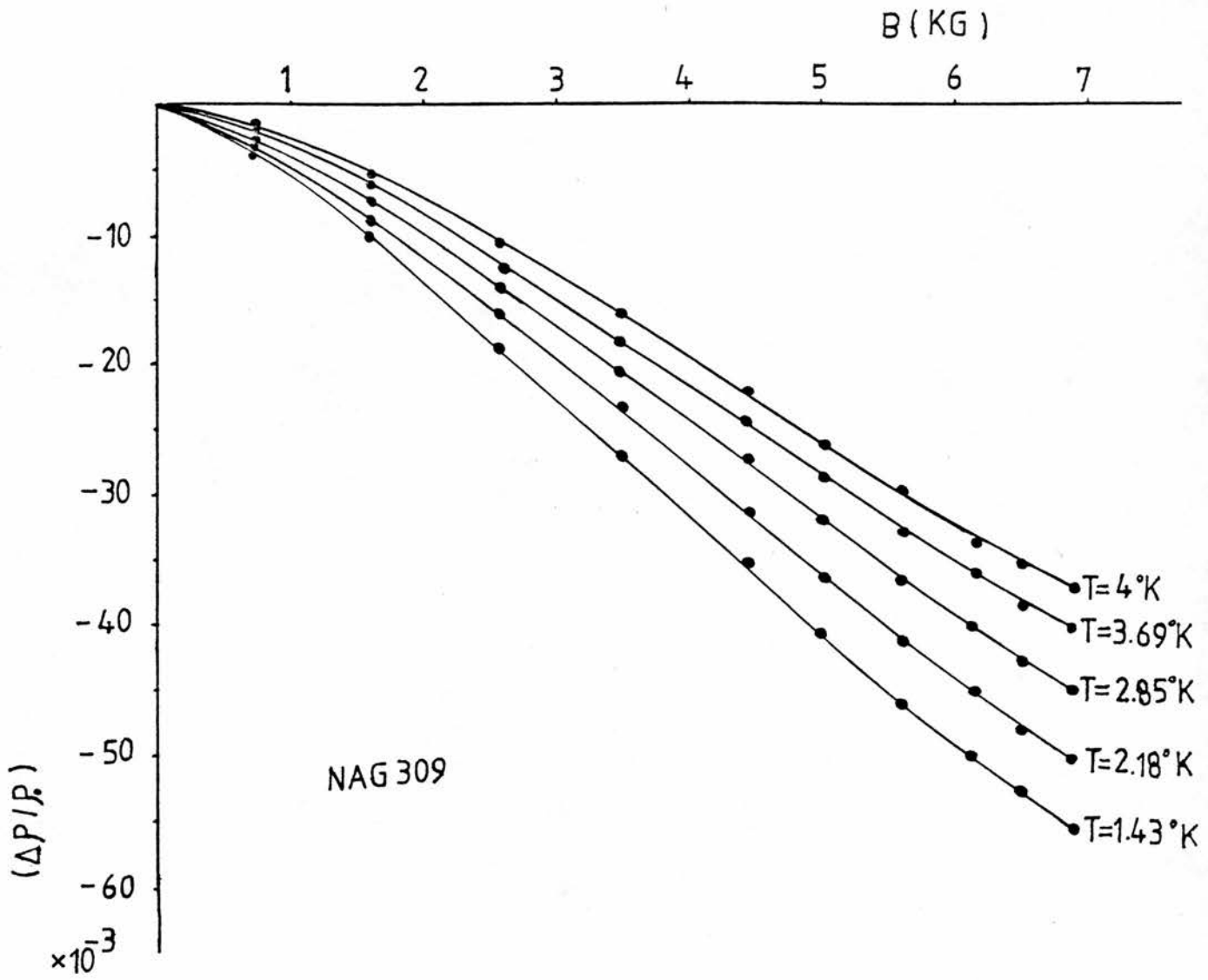
B (KG)
1
2
3
4
5
6
7
-10
-20
-30
-40
-50
-60
$\times 10^{-3}$
$(\Delta P/P_0)$
NAG 309
T= 4 °K
T=3.69°K
T= 2.85°K
T=2.18° K
T=1.43 °K

Fig·4·10

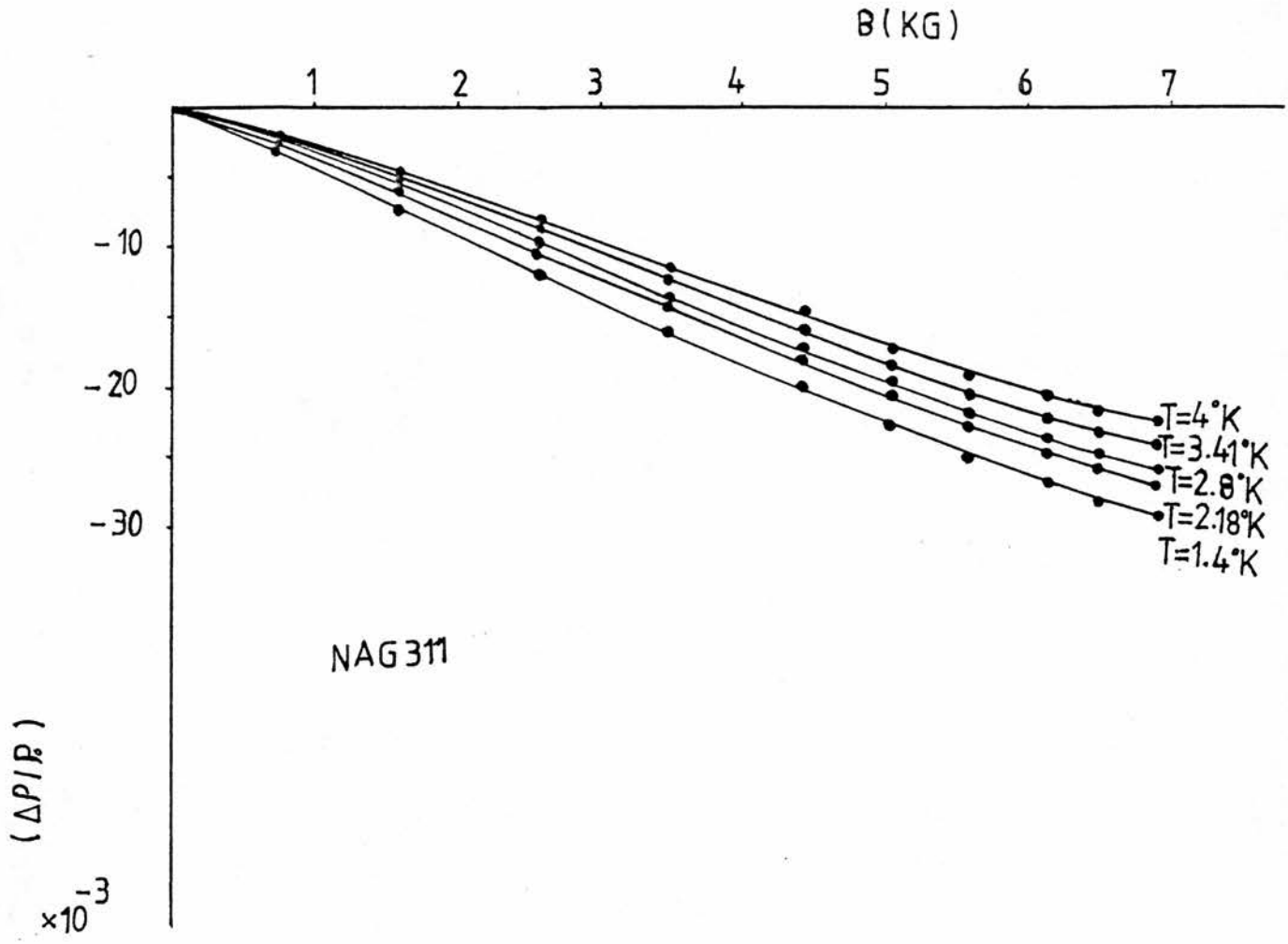

Fig·4·11

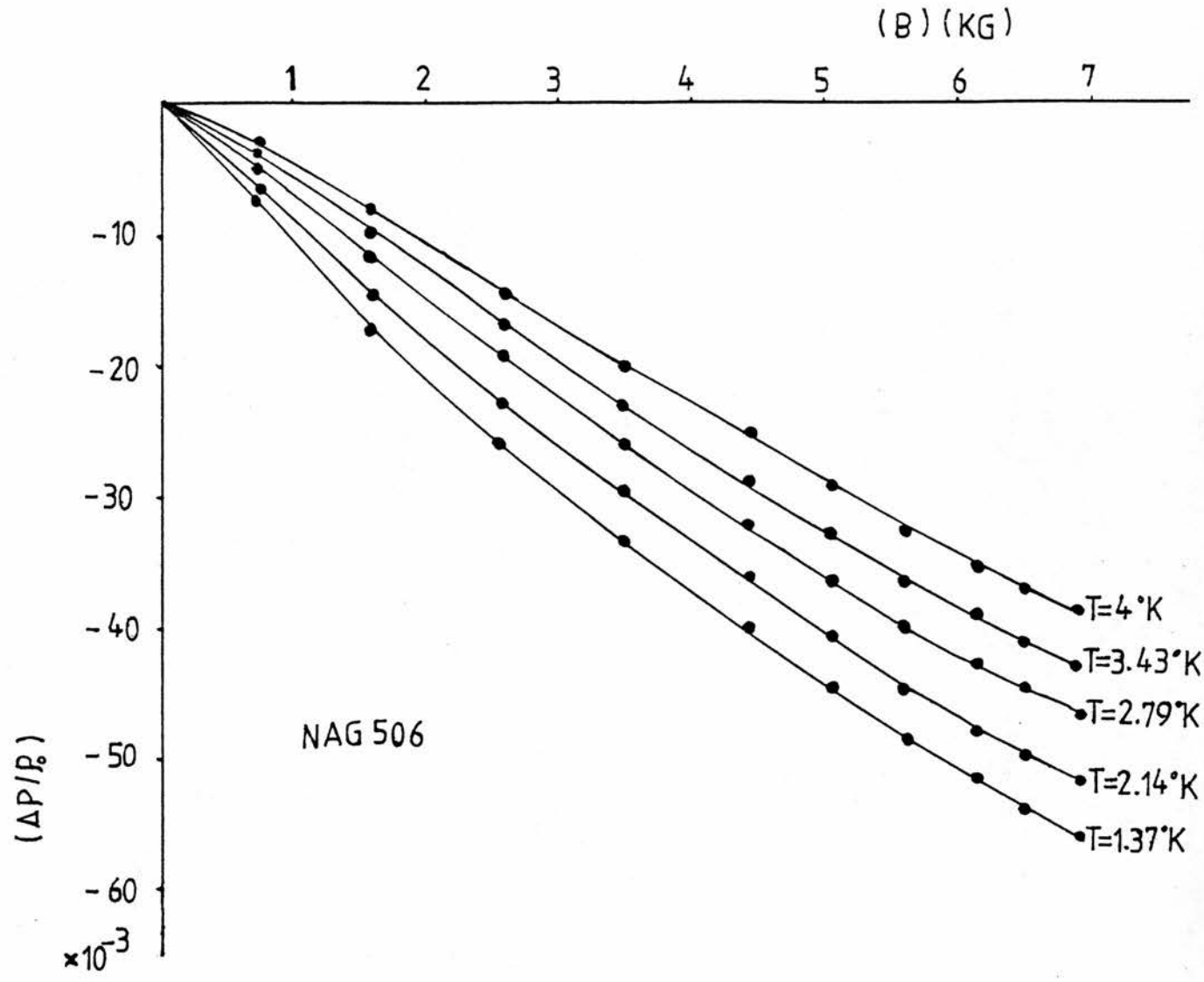
(B)(KG)
1
2
3
4
5
6
7
-10
-20
-30
-40
-50
-60
×10⁻³
(ΔP/P₀)
NAG 506
T=4°K
T=3.43°K
T=2.79°K
T=2.14°K
T=1.37°K

Fig·4·12

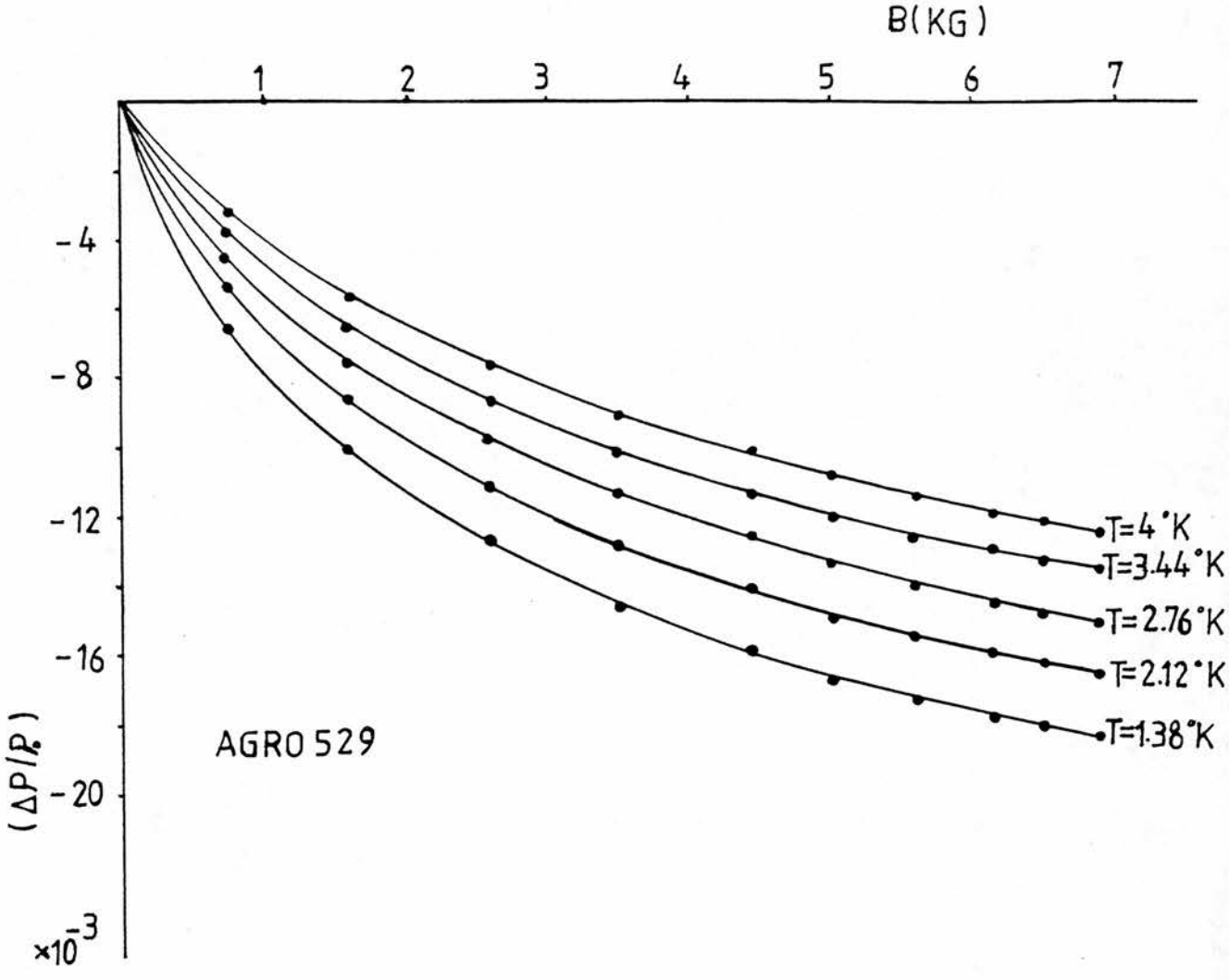
B(KG)
1
2
3
4
5
6
7
-4
-8
-12
-16
-20
(ΔP/P.)
×10⁻³
AGRO 529
T=4 °K
T=3.44 °K
T=2.76 °K
T=2.12 °K
T=1.38 °K

Fig·4·13

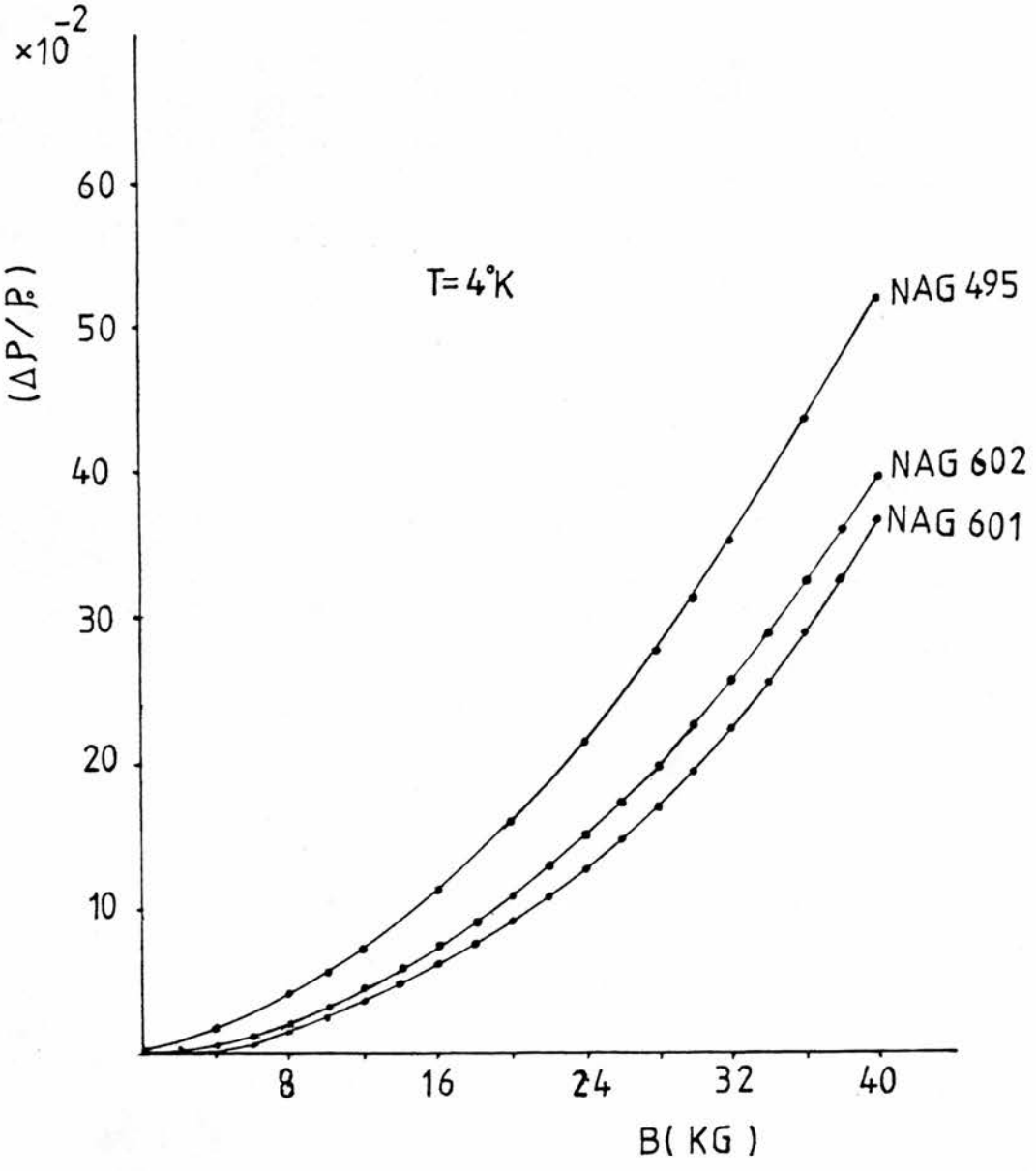
×10⁻²
60
50
40
30
20
10
(ΔP/P₀)
T= 4°K
NAG 495
NAG 602
NAG 601
8
16
24
32
40
B(KG)

Fig·4·14

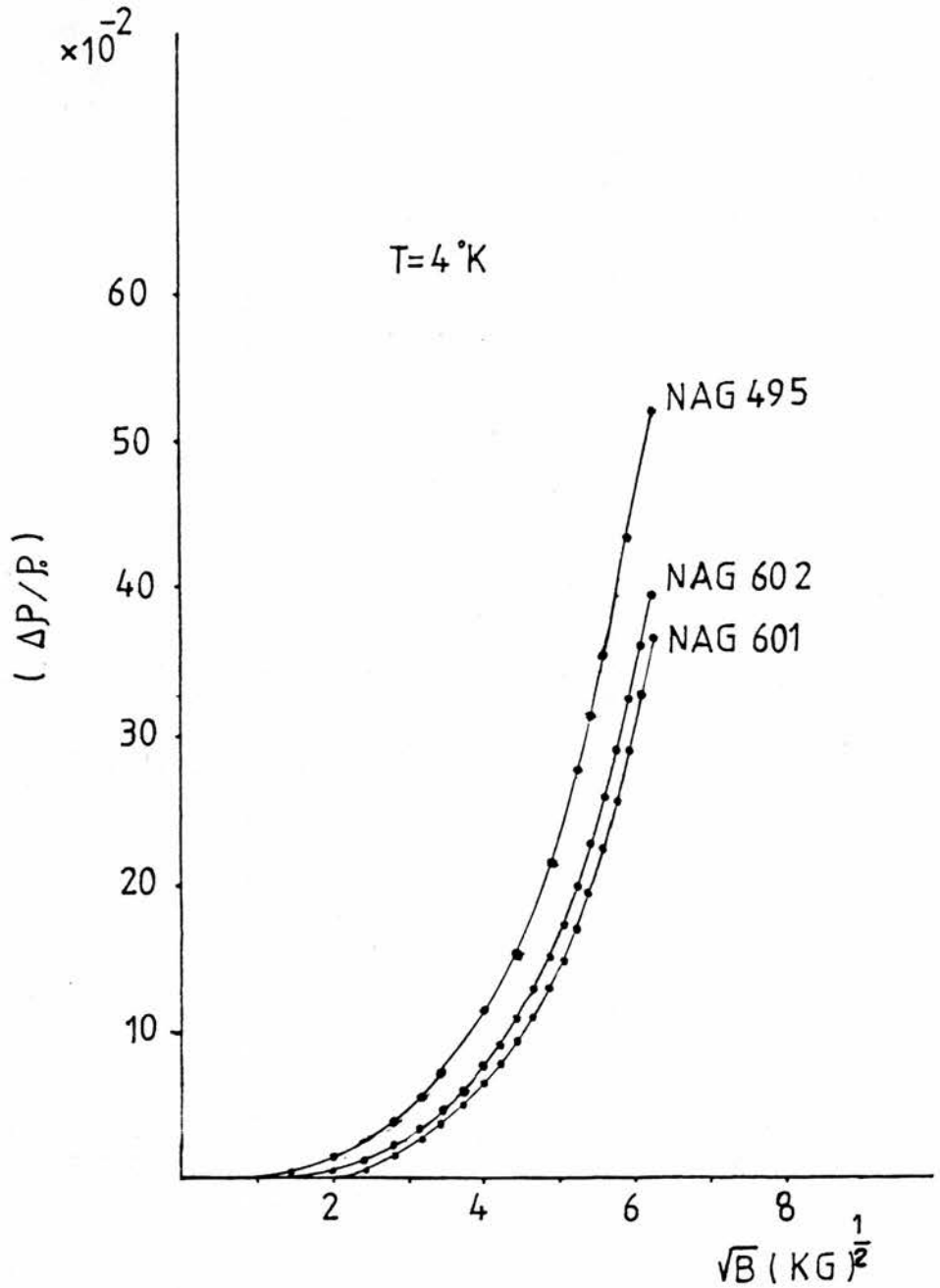

Fig·4·15

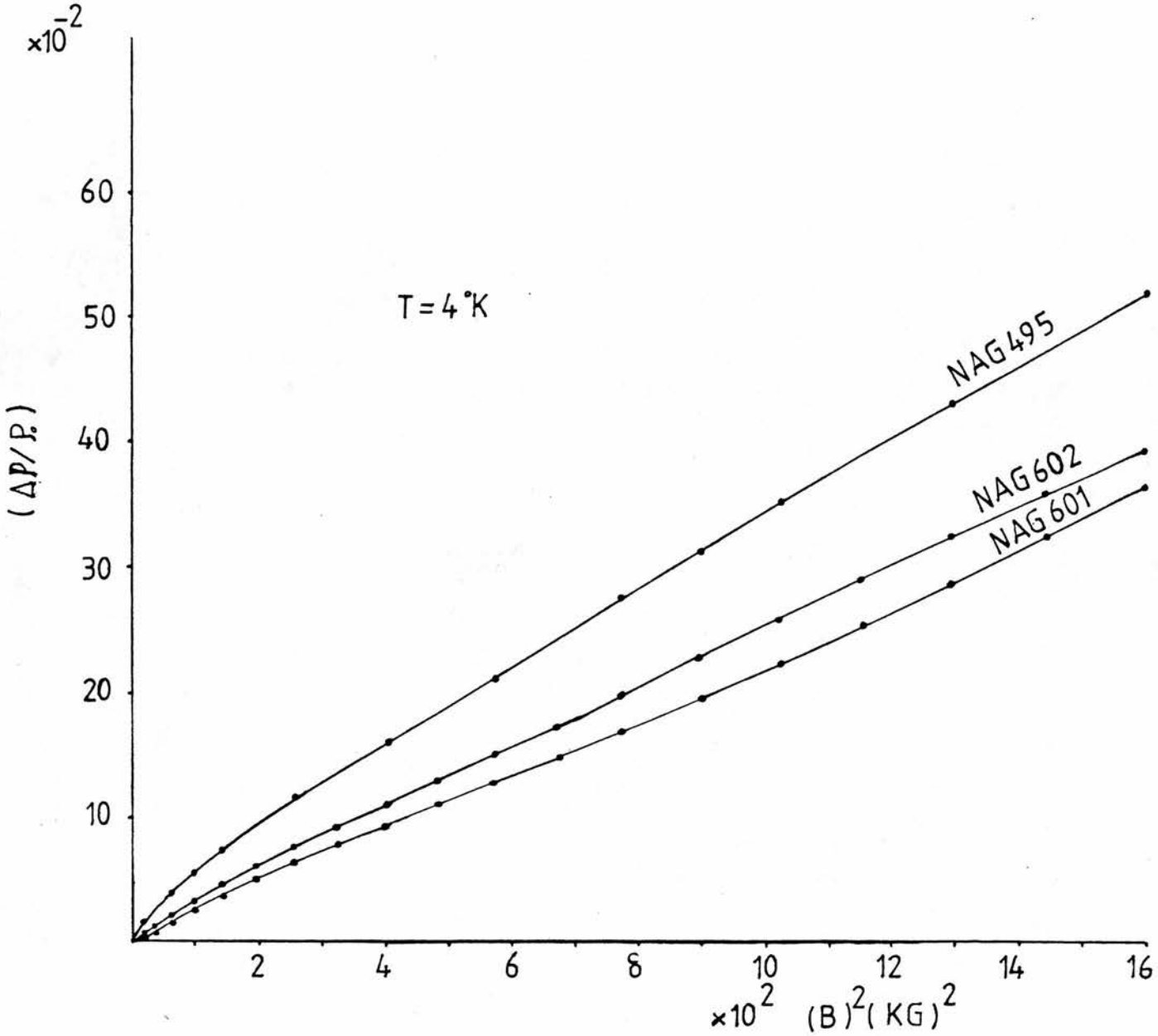
×10⁻²
60
50
40
30
20
10
(ΔP/P.)
T = 4°K
NAG495
NAG602
NAG601
2
4
6
8
10
12
14
16
×10²
(B)²(KG)²

Fig · 4·16

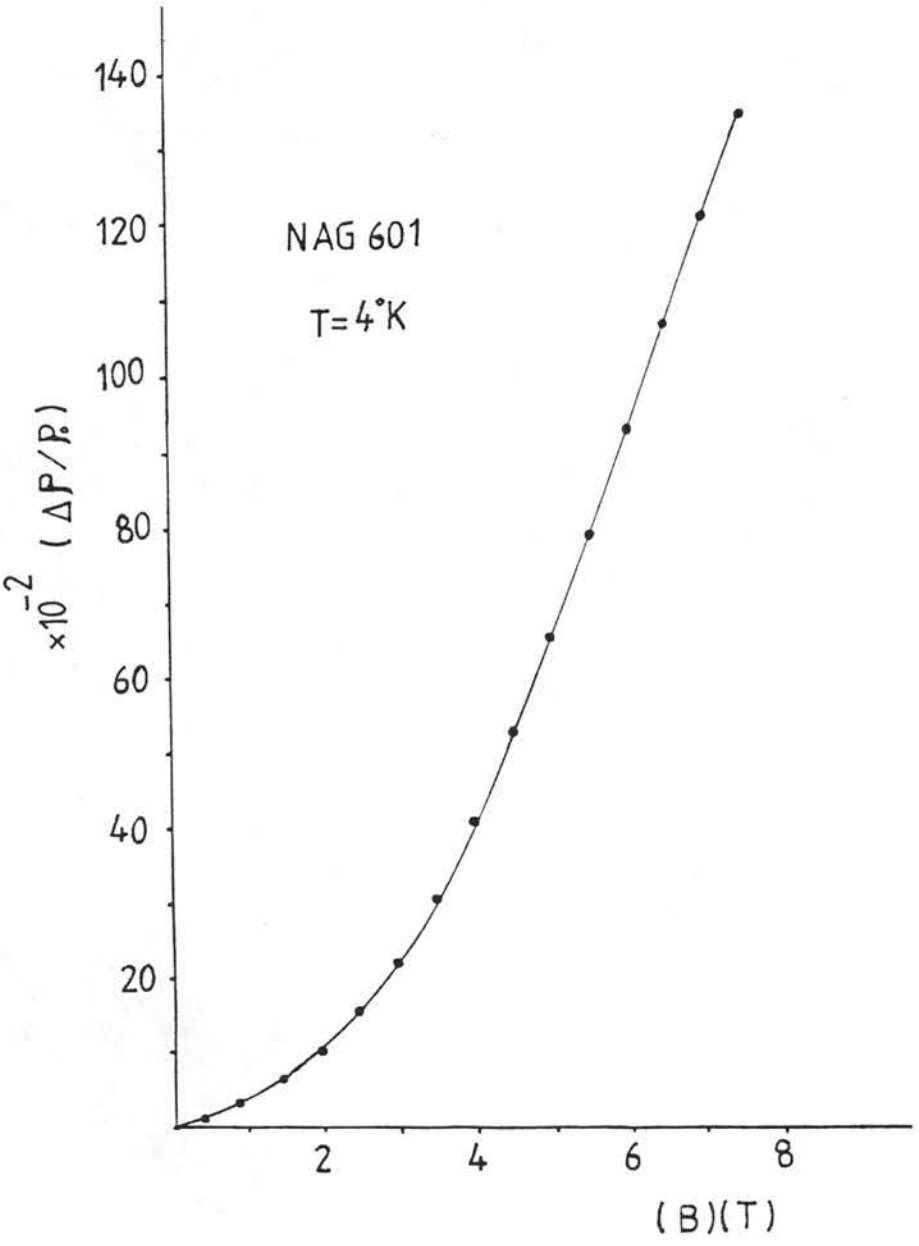

Fig·4·17

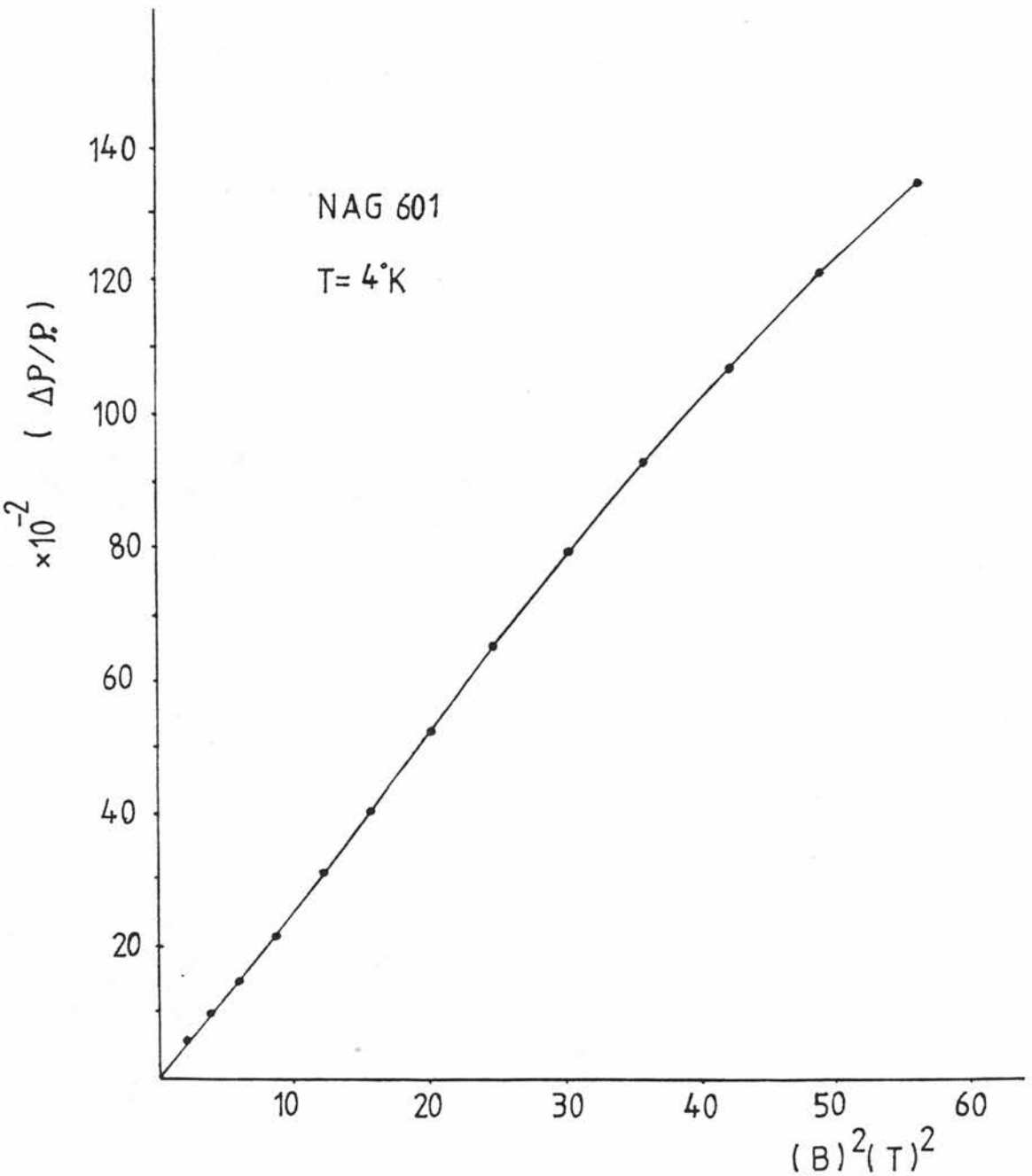
NAG 601
T= 4°K
140
120
100
80
60
40
20
10
20
30
40
50
60
$(B)^2(T)^2$
$\times 10^{-2}$ ($\Delta P/P_i$)

Fig.4.18

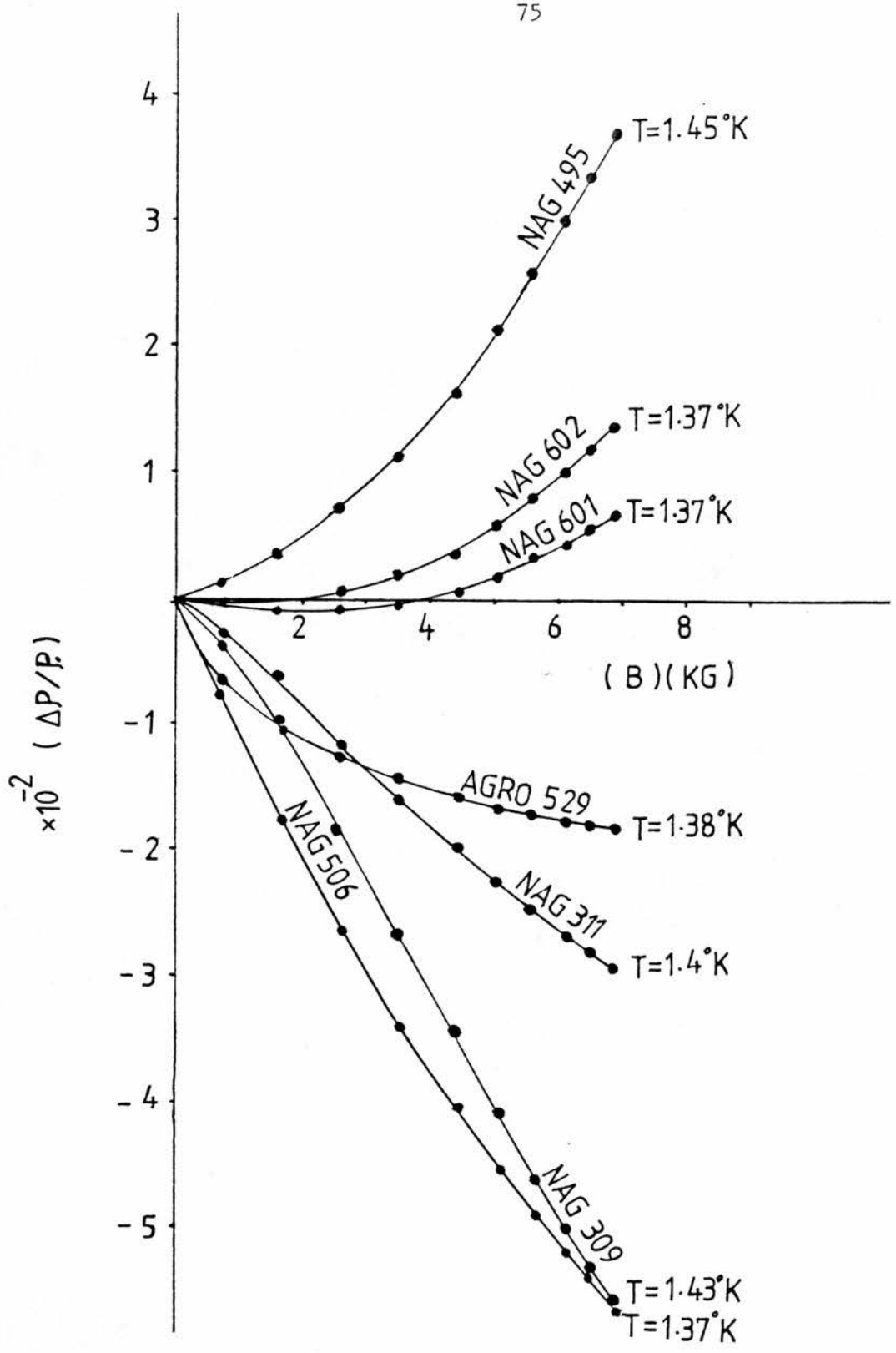
4
3
2
1
-1
-2
-3
-4
-5
2
4
6
8
(B)(KG)
$\times 10^{-2}$ ($\Delta P/P$)
NAG 495
T=1.45°K
NAG 602
T=1.37°K
NAG 601
T=1.37°K
AGRO 529
T=1.38°K
NAG 311
T=1.4°K
NAG 506
NAG 309
T=1.43°K
T=1.37°K

Fig.4.19

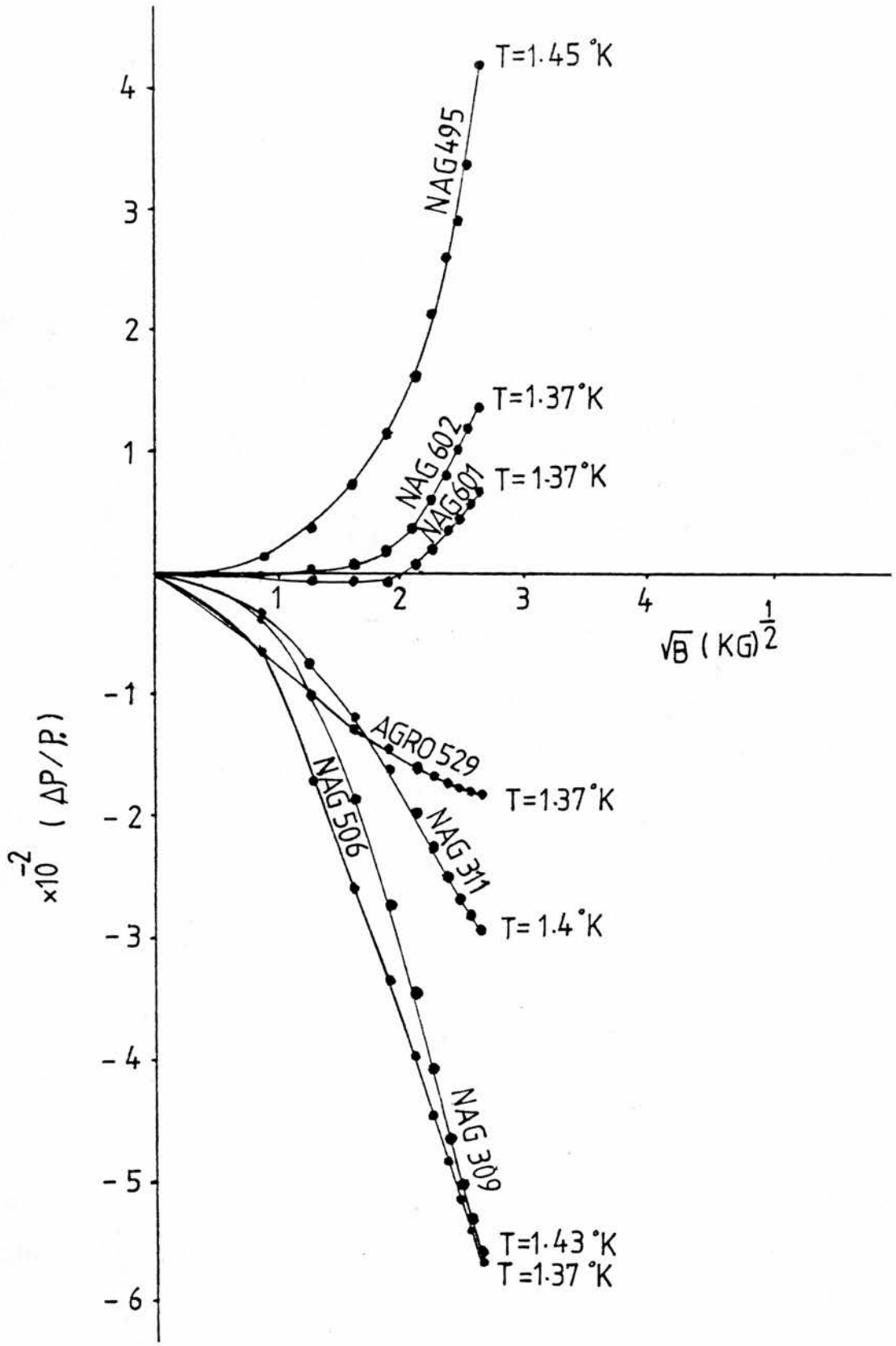
T=1·45 °K
NAG495
T=1·37°K
NAG 602
NAG601
T= 1·37°K
AGRO 529
T=1·37°K
NAG 506
NAG 311
T= 1.4°K
NAG 309
T=1·43 °K
T =1·37 °K
$\sqrt{B}$ (KG)$^{\frac{1}{2}}$
$\times 10^{-2}$ ($\Delta P/P$)

Fig·4.20

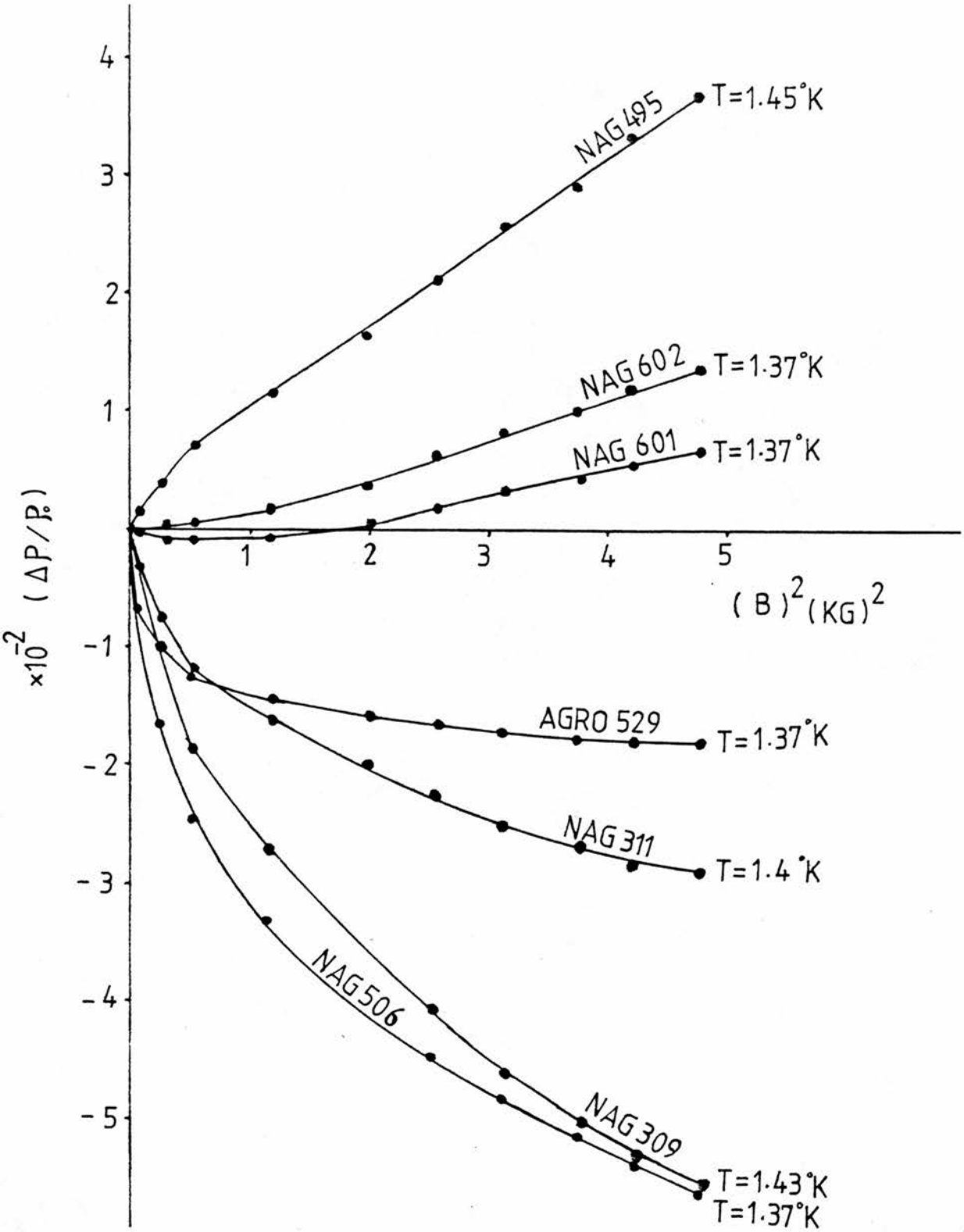
4
3
2
1
-1
-2
-3
-4
-5
1
2
3
4
5
$\times 10^{-2}$ ($\Delta P/P_o$)
(B)^2 (KG)^2
NAG 495
T=1.45°K
NAG 602
T=1.37°K
NAG 601
T=1.37°K
AGRO 529
T=1.37°K
NAG 311
T=1.4 °K
NAG 506
NAG 309
T=1.43°K
T=1.37°K

Fig·4·21

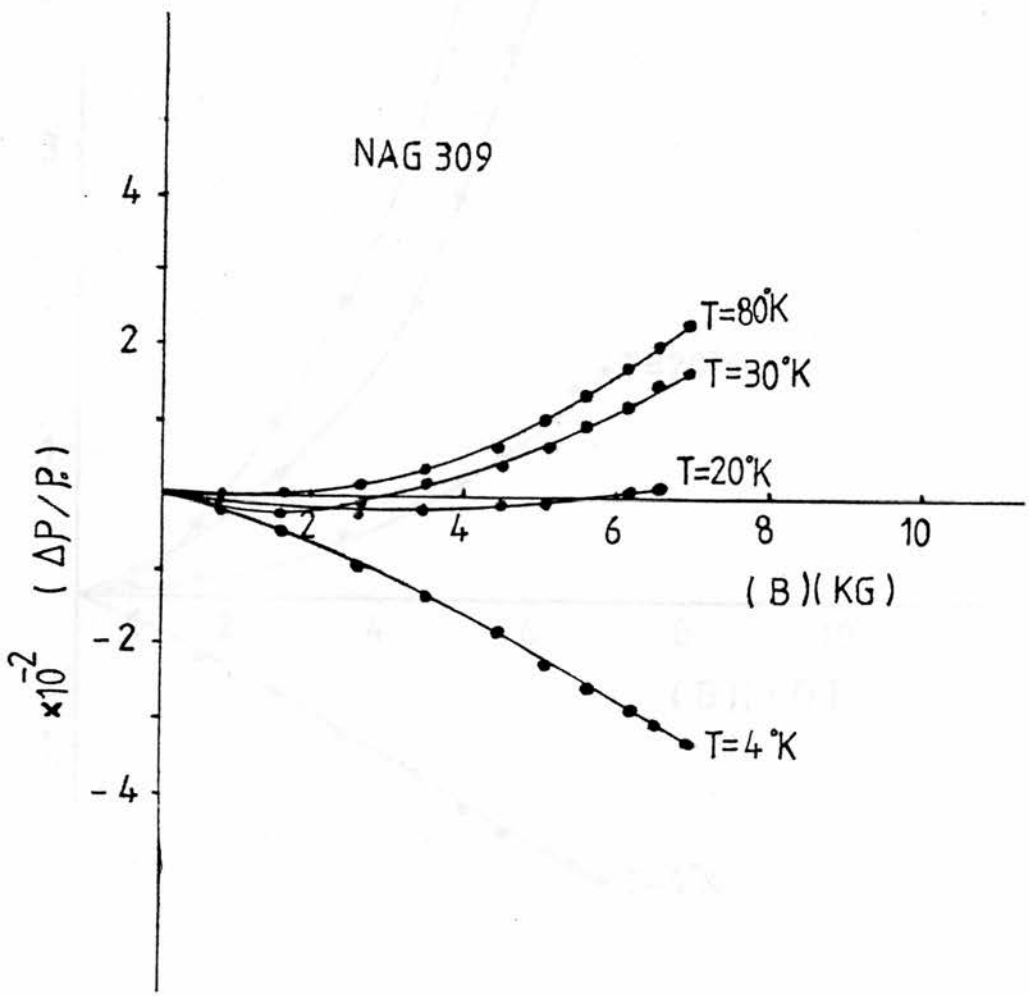
NAG 309
4
2
-2
-4
$\times 10^{-2}$ ($\Delta P / P_0$)
T=80°K
T=30°K
T=20°K
T=4°K
2
4
6
8
10
(B)(KG)

Fig·4·22

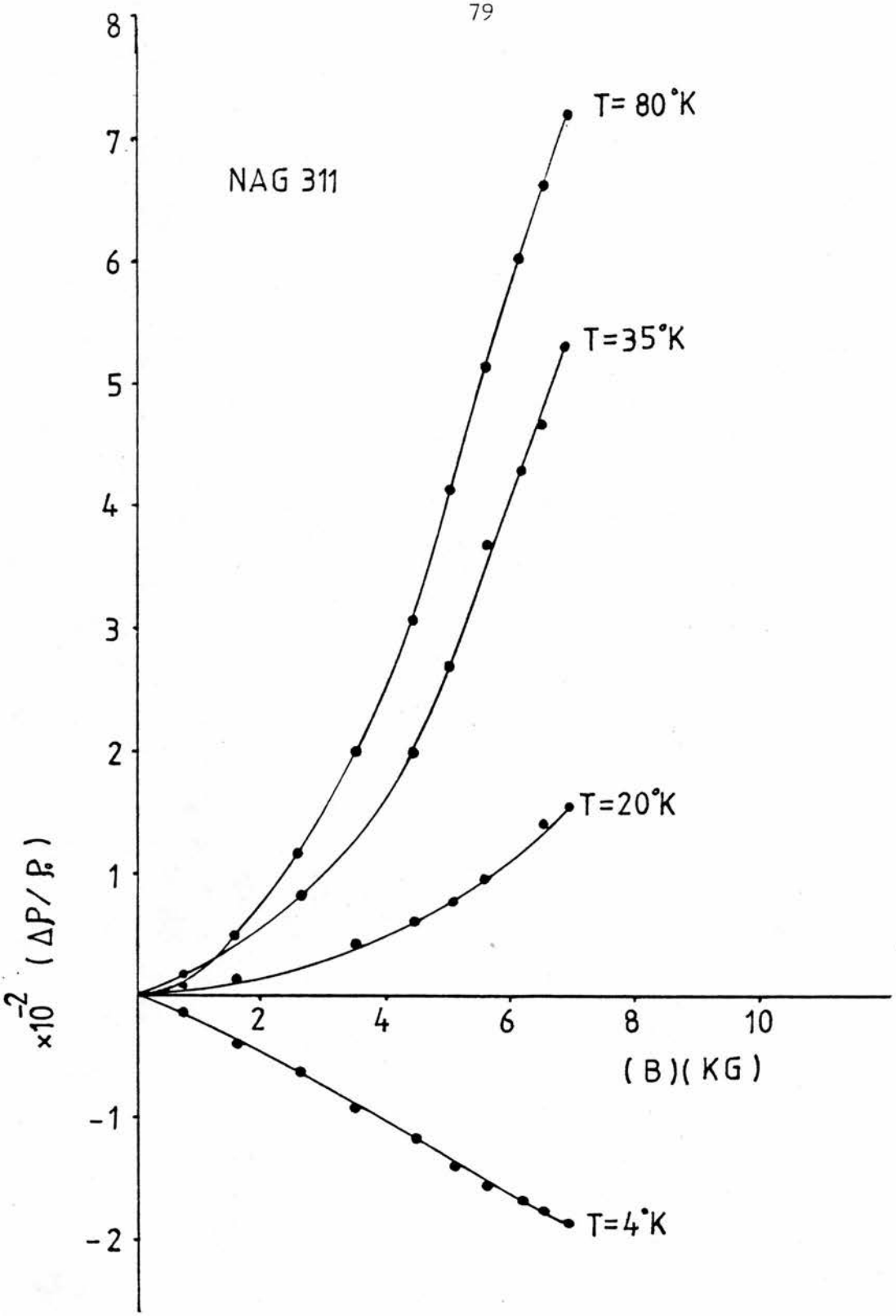
NAG 311
T= 80°K
T=35°K
T=20°K
T=4°K
8
7
6
5
4
3
2
1
-1
-2
2
4
6
8
10
(B)(KG)
$\times 10^{-2}$ (ΔP/P)

Fig·4·23

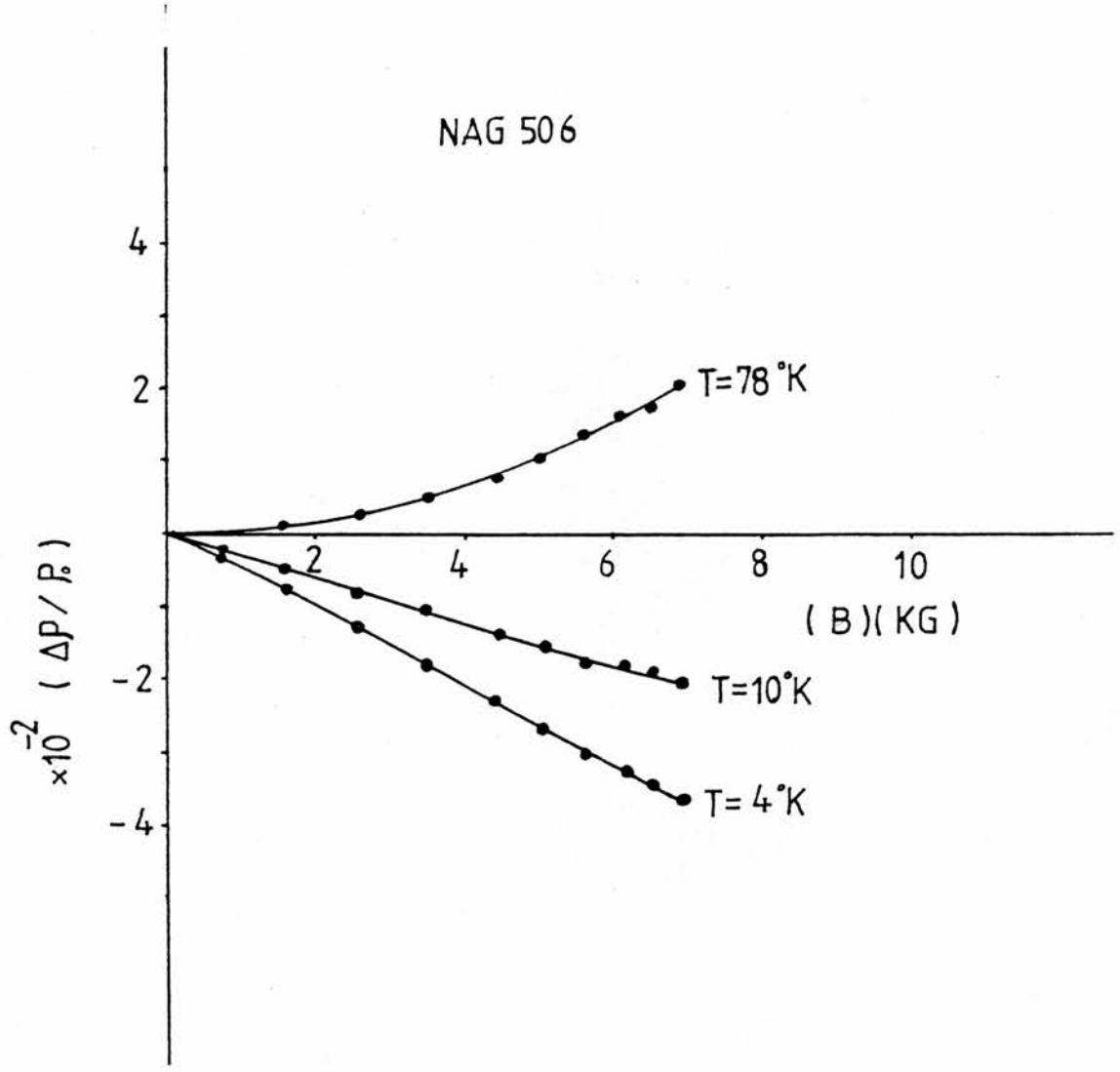

Fig·4·24

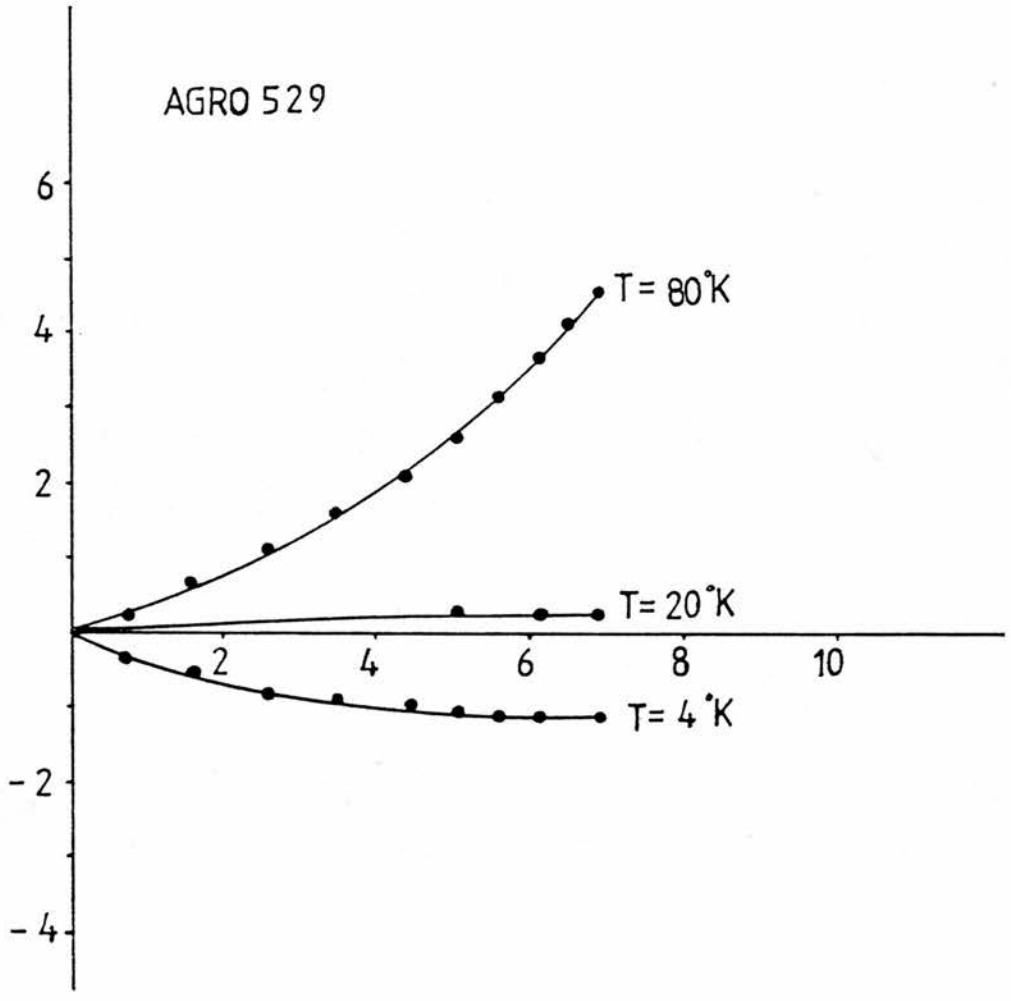

Fig·4·25

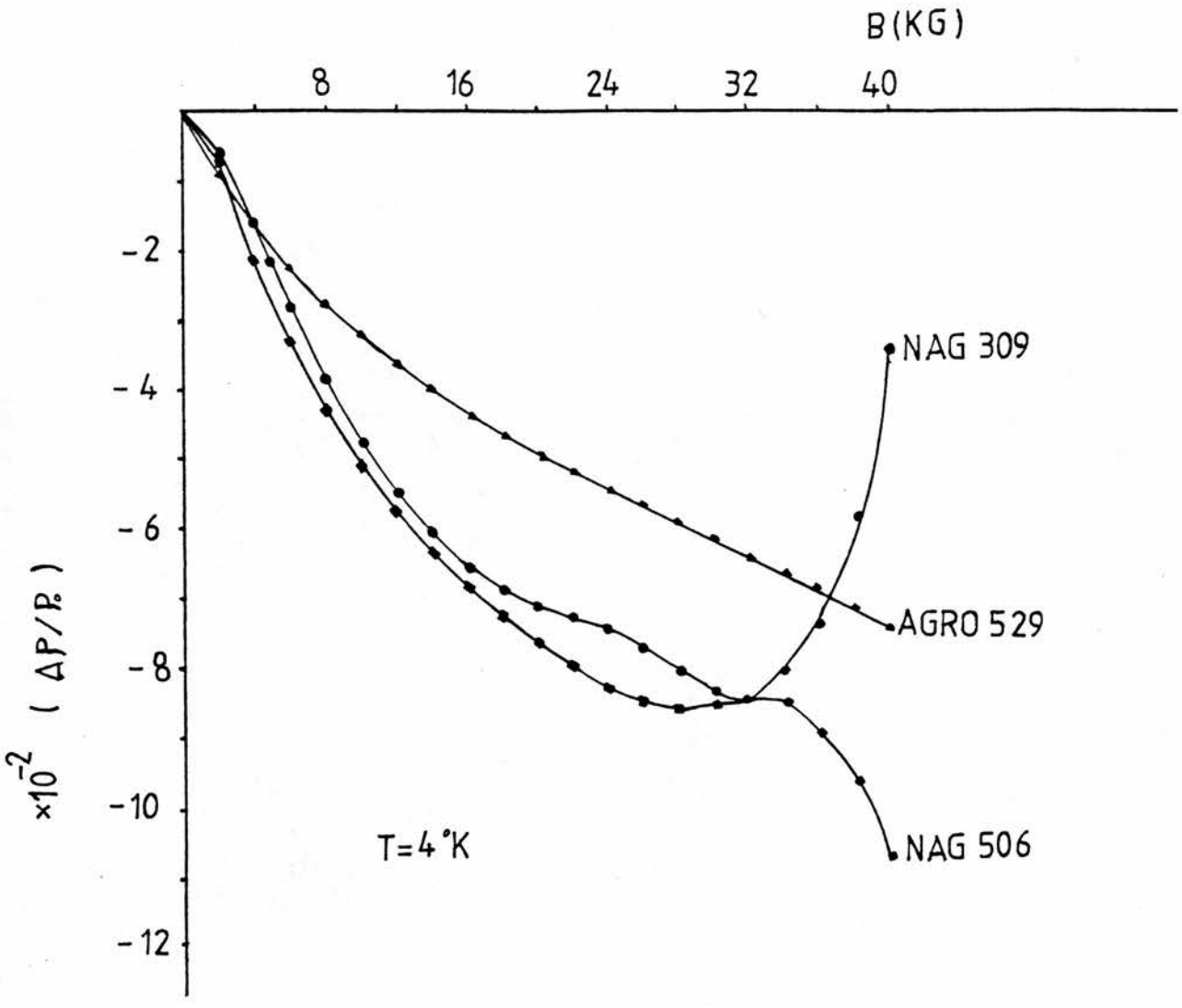
B(KG)
8
16
24
32
40
-2
-4
-6
-8
-10
-12
$\times 10^{-2}$ ($\Delta P/P_0$)
NAG 309
AGRO 529
NAG 506
T=4°K

Fig·4·26

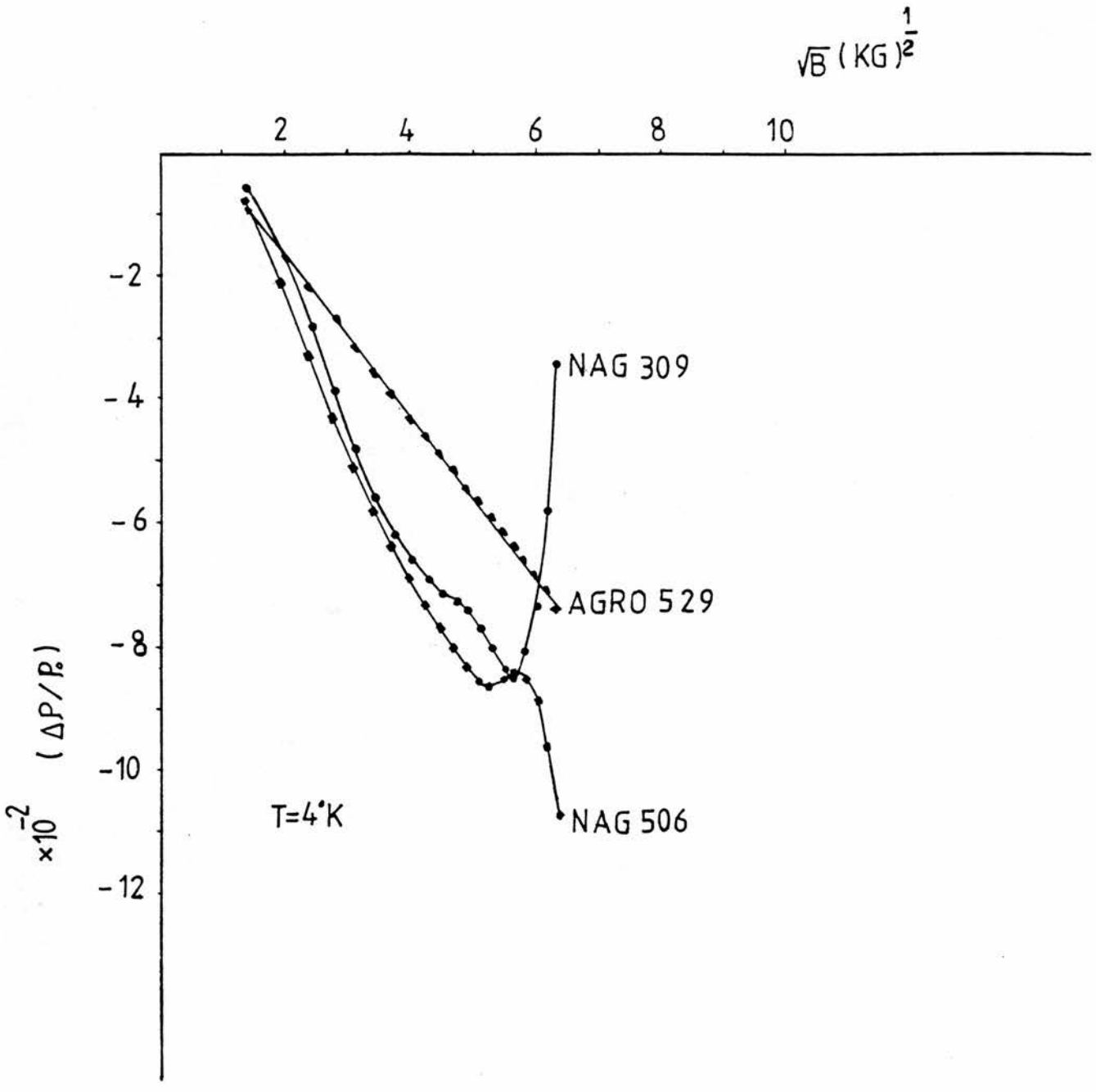

Fig·4·27

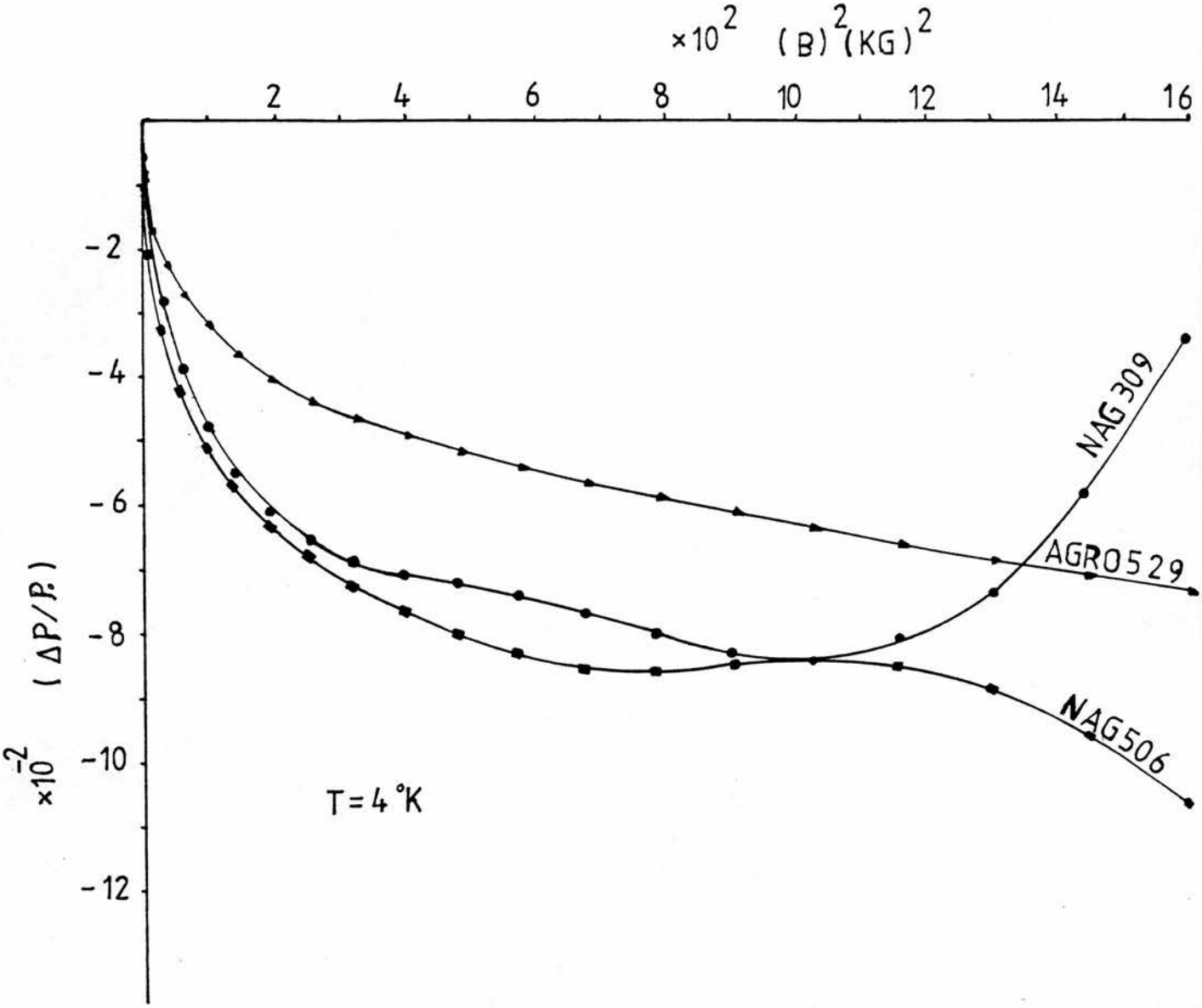
×10² (B)²(KG)²
2
4
6
8
10
12
14
16
-2
-4
-6
-8
-10
-12
×10⁻² (ΔP/P)
NAG309
AGRO529
NAG506
T = 4 °K

Fig. 4.28

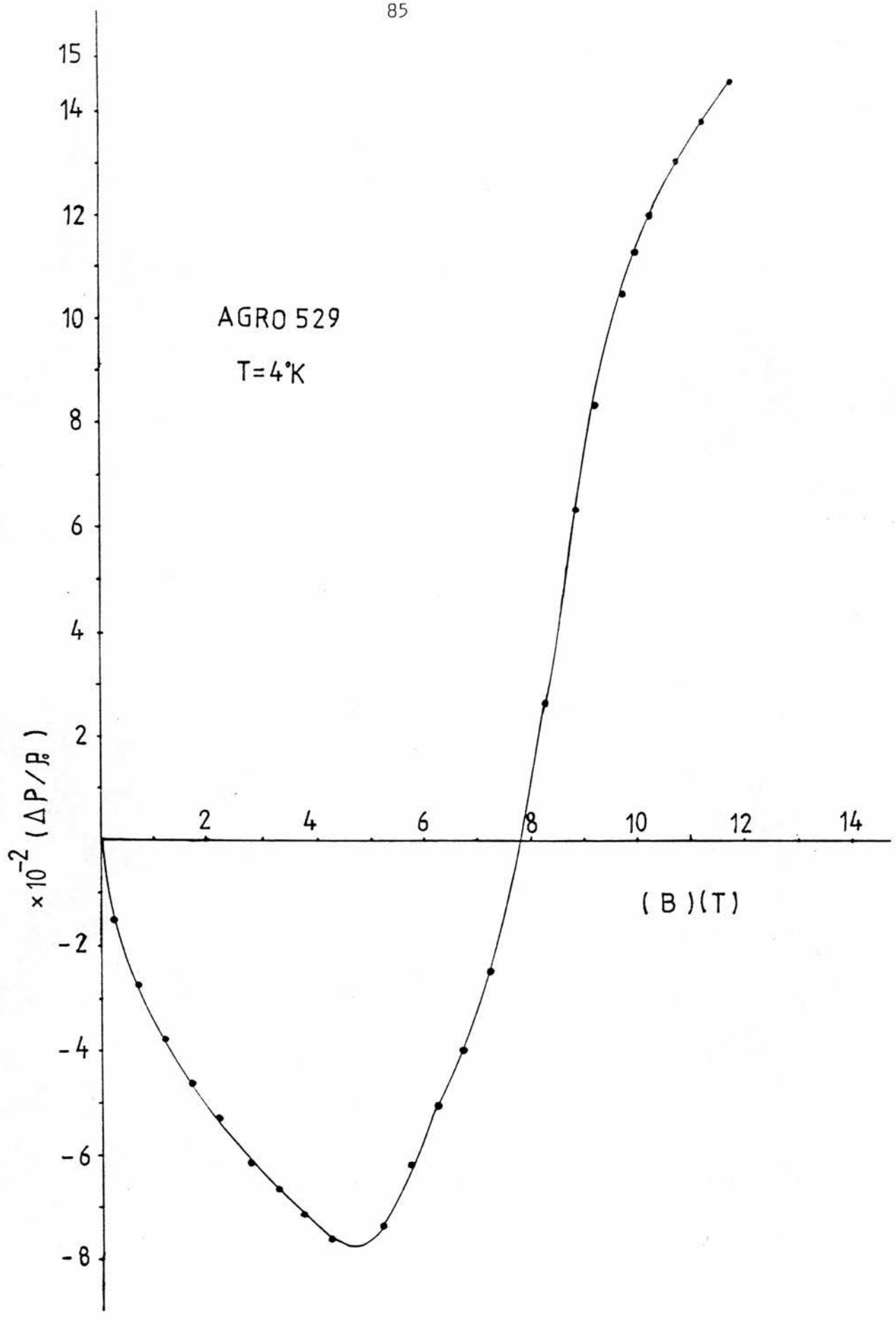
AGRO 529
T=4°K
15
14
12
10
8
6
4
2
-2
-4
-6
-8
2
4
6
8
10
12
14
(B)(T)
$\times 10^{-2}$ ($\Delta P / \rho_o$)

Fig·4·29

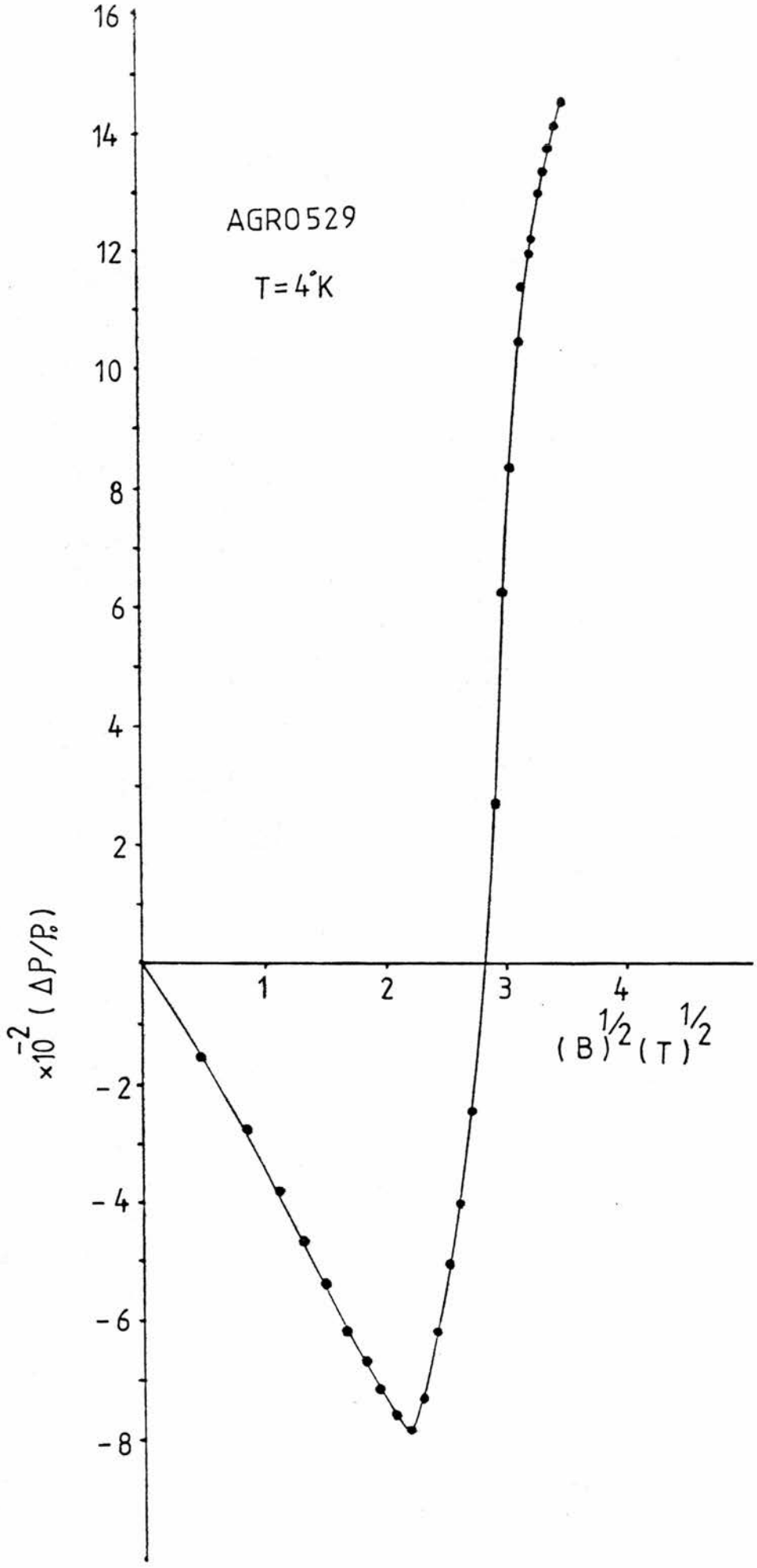
AGRO 529
T = 4°K
16
14
12
10
8
6
4
2
-2
-4
-6
-8
1
2
3
4
$(B)^{1/2}(T)^{1/2}$
$\times 10^{-2}(\Delta P/P_o)$

Fig·4·30

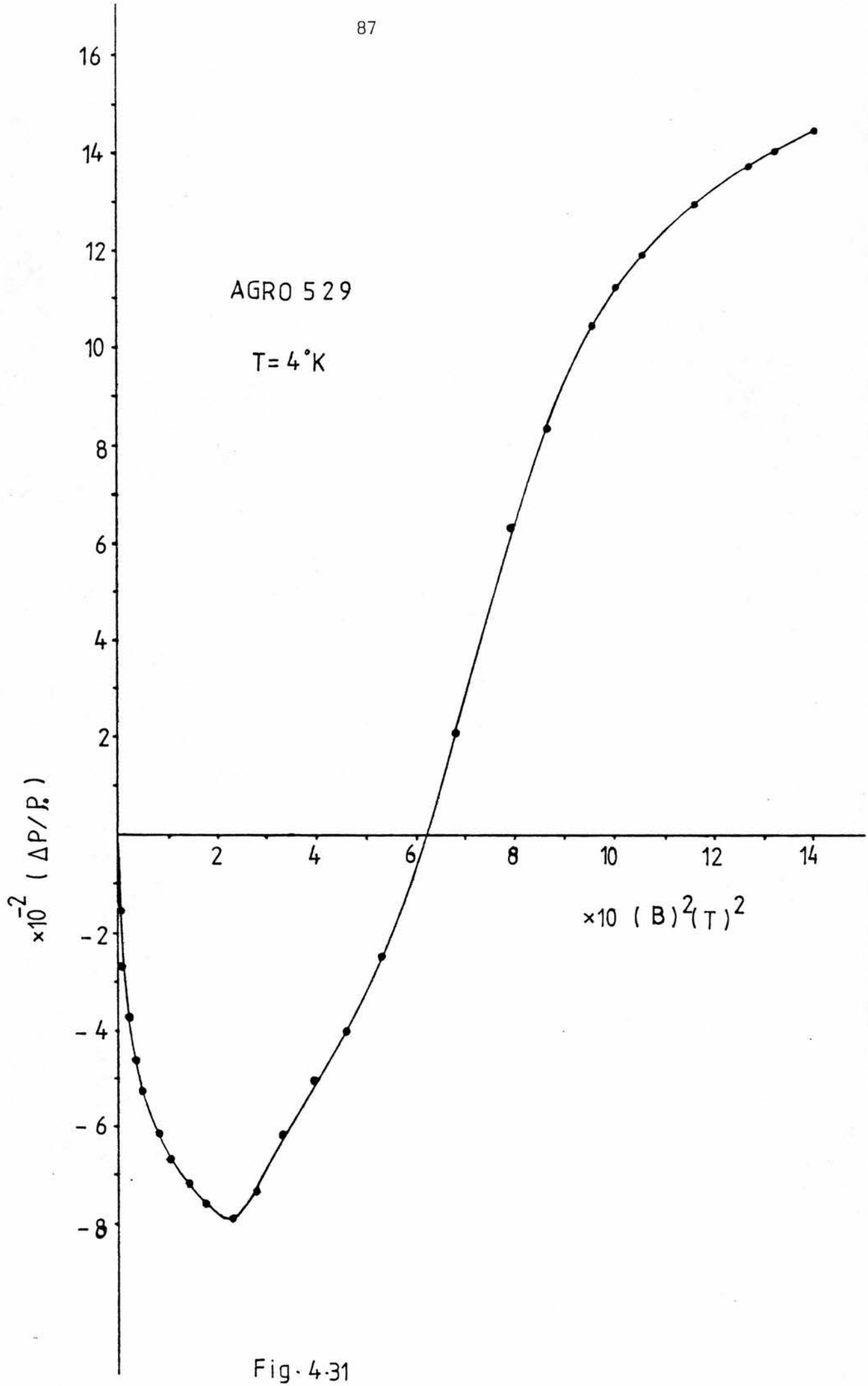

Fig. 4-31

CONCLUSION

We have used simple galvanomagnetic measurements to characterise a number of samples of indium phosphide with varying electron densities and have used low temperature measurements to estimate the compensation ratio.

For samples on the metallic side of the metal non-metal transition the conductivity is shown to agree quite well with the relation $\sigma = A\sigma_{min} (\frac{n}{n_c}) - 1)^s$. Experimentally it is found that $s = 0.7$ and $A\sigma_{min} = 1.8 \times 10^3 (\Omega m)^{-1}$ to be compared with a calculated value from Mott theory (section 4.1) of $0.32 \times 10^3 (\Omega m)^{-1}$ where $A \simeq 6.0$.

It is shown that the low temperature maxima in the Hall effect is capable of an explanation in terms of variation of the Hall factor r as the scattering mechanism varies with temperature. Thus conductivity in an impurity band may not be appropriate for samples on the metallic side of the transition.

Kawabata's recent localization theories have been used to explain the negative magnetoresistance observed at intermediate fields.

A plausible explanation of the higher field positive magnetoresistance can be given in terms of electron interaction theory in the form given by Lee and Ramakrishnan.

REFERENCES

Anderson, P W, Phys Rev 109, 1492 (1958).

Agaev , Ya, Physical Properties of A^{III} B^{V} and A^{III} B^{VI} Semiconductors,(1967).

Anderson, P W, Abrahams, E and Ramakrishnan, T V, Phys Rev Lett 43, 718 (1979).

Blood, P and Orton, J W, J Phys C: Solid State Phys Vol 7, 893 (1974).

Blakemore, J S, Solid State Physics (1969).

Busch, G and Labhart, H, Helv Phys Acta 14, 463 (1946).

Davis, E A and Compton W D, Phys Rev 140, A 2183, 94 (1965).

Economou, E N and Cohen, M H, Phys Rev B 5, 2931 (1972).

Finlayson, D M, Irvine J and Peterkin, L S, Philosophical Magazine B 39, No 3, 253-266 (1979).

Finlayson, D M and Johnson, I A, Phys Stat Sol (b), 71, 395 (1975).

Fritzsche, H and Cuevas, M, Phys Rev B 3, 4413 (1960).

Galavanov, V V, Siukaev, N V and Staroseltesva , S P, Soviet Physics - Semiconductors, Vol 2 No 7, 787 (1969).

Galavanov , V V and Siukaev, N V, Phys Stat Sol, 38, 523 (1970).

Gryaznov, O S and Ravich Yu I, Soviet Physics - Semiconductors 3, 1092 (1970).

Gor"kov, L P, Larkin, A J and Khmel"nitzkii, D E, ZhETP Letters, 30, 248 (1979).

Harris, J J and Ridley, B K, J Phys Chem Solids, Vol 33 p1455-1464 (1972).

Herring, C and Vogt, E, Phys Rev 101, 944 (1956).

Hikami, S, Larkin, A I and Nagaoka Y, Prog Theo Phys 63, 707 (1980).

Hung, C S and Gleissman, J R, Phys Rev 79, 726 (1950).

Hilsum, C et al, Semiconducting III-V Compounds, Pergamon Press (1961).

Kawabata, A, Journal of Physical Society of Japan, Vol 49 No 2, 628 (1980); Solid State Communications, Vol 34 pp 431-432 (1980).

Kovalevskaya, G G, Popov, Yu G and Siukaev, N V, Soviet Physics - Semiconductors, Vol 2 No 2,178 (1967).

Kaveh, M and Mott,N F, J Phys C : Solid State Phys 15 (1984).

Kolodziejezak, J , Phys Status Solidi, 19, 231 (1967).

Kawaguchi, Y, Kitahara,H and Kawaji, S, Solid State Communications Vol 26, 701 (1978).

Keyes, R W, J Phys Chem Solids 6, 1 (1958).

Lee, P A and Ramakrishnan, T V, Phys Rev B 26, 4009 (1982).

Ioffe, A F and Regel, A R, Prog Semiconductor 4, 237 (1960).

Mott, N F, Proc Phys Soc A, 62, 416 (1949; Adv Phys 21, 785 (1972)b; Adv Phys 21, 785 (1972)b; Metal Insulator Transition (1974).

Mott, N F and Davis E A, Electronic Processes in Non-Crystalline Materials (1971); Phil Mag 17, 1269 (1966), Phil Mag 913, 989 (1969).

Mott, N F and Twose, W D, Adv Phys 10, 107 (1961).

Miller, A and Abrahams, E, Phys Rev 120, 745 (1960).

Mansfield, R, Proc Phys Soc B, 69, 76 (1956).

Sasaki, W, J Phys Japan 21 (Suppl) 543 (1966).

Stillman, G E, Wolfe C M and Dimmock, J O, Proc 3rd Int Symp on GaAs and Related Compounds, pp 212-21 (1971).

Shipley, F M, Thesis (1952).

Straub, W D et al, Phys Rev Lett 21, 752 (1968).

Toyozawa, Y, J Phys Soc Japan, 17, 986 (1962).

Thouless, D J, J Phys C : Solid St Phys 3 1559 (1970).

van der Pauw, L T, Philips Res Rep 13, 1 (1958).

Wilson, A H, Proc Roy Soc 133, 458 (1931).

Walukiewicz, W et al, J Appl Phys, 2659 (1980).